



Title	Synthesis and Characteristic Degradation of Polymers with Cyclic Acetal Units in the Main Chain: Novel Polyaddition and Its Sequence Control
Author(s)	内藤, 理
Citation	大阪大学, 2023, 博士論文
Version Type	VoR
URL	<a href="https://doi.org/10.18910/92189">https://doi.org/10.18910/92189</a>
rights	
Note	

*The University of Osaka Institutional Knowledge Archive : OUKA*

<https://ir.library.osaka-u.ac.jp/>

The University of Osaka

**Synthesis and Characteristic Degradation of Polymers  
with Cyclic Acetal Units in the Main Chain:  
Novel Polyaddition and Its Sequence Control**

A Doctoral Thesis  
by  
**Tadashi Naito**

Submitted to  
the Graduate School of Science,  
Osaka University

February, 2023



## Acknowledgements

The thesis research was performed at the Department of Macromolecular Science, Graduate School of Science, Osaka University, under the direction of Professor Sadahito Aoshima during 2014–2017 and 2020–2023.

First of all, the author would like to express the deepest appreciation to Professor Sadahito Aoshima for his continuous encouragement throughout the author's laboratory and personal life, especially the admission for the doctoral course. The author is also deeply grateful to Professor Shokyoku Kanaoka for his kind support and insightful comments with new perspective, and Associate Professor Arihiro Kanazawa for his patient guidance, stimulating discussion, and enormous help.

The author would like to express his deep appreciation to Professor Akihito Hashidzume and Professor Hiroyasu Yamaguchi for careful reviewing of this thesis and fruitful comments.

The author would like to thank to Dr. Yasuto Todokoro and Dr. Naoya Inazumi for NMR measurements, and Dr. Akihiro Ito for mass spectroscopy. The author is also deeply grateful to Associate Professor Nathaniel A. Lynd and his wife Ms. Ayaka Lynd, and his group (The University of Texas at Austin) for providing an opportunity to study and have wonderful experiences as a visiting scholar in his group under the difficult situation associated with COVID-19 (December 2021 to February 2022).

The author is deeply indebted to Professor Yoshio Okamoto (Nagoya University; Harbin Engineering University), Professor Mitsuo Sawamoto (Kyoto University; Chubu University), Professor Eiji Yashima (Nagoya University), Professor Masami Kamigaito (Nagoya University), Professor Kotaro Satoh (Tokyo Institute of Technology), Professor Makoto Ouchi (Kyoto University), and all "ORION" members for active discussions.

The author expresses his special thanks to all members of the Aoshima's Group for useful suggestion and their friendship during the course of research. Specifically, the author is grateful to Dr. Kira B. Landenberger (Senior Lecturer/Junior Associate Professor, Kyoto University), Dr. Hayato Yoshimitsu, Dr. Mayuka Yamada, Dr. Koichiro Takii, Dr. Ryohei Saitoh, Dr. Tomoya Yoshizaki, Dr. Norifumi Yokoyama, Dr. Suzuka Matsumoto, Dr. Sensho Kigoshi, Dr. Daichi Yokota, Dr. Motoki Higuchi, Dr. Hironobu Watanabe, Dr. Keisuke Hayashi, Dr. Kazuya Maruyama, Mr. Hiroshi Oda, Ms. Chihiro Suemitsu, Ms. Natsuki Okada, Ms. Marie Kawamura, Mr. Tatsuya Suzuki, Mr. Yukinori Togo, Mr. Yoshiki Tode, Ms. Mai Hijikata, Mr. Takashi Sasahara, Ms. Tomoka Shirouchi, Ms. Yukiko Seki, Mr. Kota Fujiwara, Ms. Fumina



## *Acknowledgements*

Koga, Mr. Tsuyoshi Nishikawa, Mr. Yoshiki Tatsuno, Ms. Yurika Miyamae, Mr. Shintaro Araoka, Ms. Haruka Nishimura, Mr. Daisuke Hotta, Mr. Kazutoshi Mishima, Mr. Ryusei Kato, Ms. Maki Mimura, Mr. Masamichi Inoue, Ms. Yui Kawamura, Ms. Sae Taniguchi, Mr. Shunya Hasegawa. Mr. Yuya Asada, Mr. Yuya Kinoshita, Mr. Jun-ichi Azuma, Mr. Mikiya Umemoto, Mr. Tomoki Nara, Mr. Ryosuke Hada, Ms. Yuka Takahashi, Ms. Kana Takebayashi, Mr. Naoki Matsuo, Mr. Yuji Mishima, Mr. Masahiro Ueda, Mr. Yuto Eguchi, Ms. Aya Katto, Mr. Kyonosuke Kamigaki, Ms. Mikuri Saitoh, Mr. Akihisa Numao, Ms. Yuyu Furuki, Mr. Naoki Higashibata, Ms. Nene Maruyama, Mr. Hibiki Yamada, and Mr. Yutaka Yokawa for sharing his pleasant student life. The author is also obliged to Ms. Misato Nishiuchi, Ms. Izumi Ichimura, and Ms. Ai Yamada for their thoughtful assistance in laboratory life.

The author is grateful to the Japan Society for the Promotion of Sciences (JSPS) for JSPS Research Fellowship for Young Scientists (DC2) and a Grant-in-Aid for JSPS Fellow (21J11360) from April 2021 to March 2023.

Finally, the author expresses his heartfelt appreciation to his mother Hiroko Naito, his brother Noboru Naito, his grandmother Toshie Naito, his grandfather Teruo Naito, his wife Rina Naito, his son Michiharu Naito, and all his relatives for their continuous supports and considerable encouragement.

February 2023

内藤 理

Tadashi Naito

Department of Macromolecular Science

Graduate School of Science

Osaka University

# Contents

<b>Chapter 1</b>	General introduction .....	1
 <b>Part I Novel Polyaddition and Tandem Polymerization Using Cyclotrimerization for Synthesis of Degradable Polymers</b>		
<b>Chapter 2</b>	Polyaddition of vinyl ethers and phthalaldehydes via successive cyclotrimerization reactions: selective model reactions and synthesis of acid-degradable linear poly(cyclic acetal)s .....	16
<b>Chapter 3</b>	Tandem polymerization consisting of cyclotrimerization and the Tishchenko reaction: synthesis of acid- and alkali-degradable polymers with cyclic acetal and ester structures in the main chain .....	33
 <b>Part II Novel Sequence Periodic Polymer Synthesis Consisting of Cyclic Trimer Formation and Copolymerization with Vinyl Monomers</b>		
<b>Chapter 4</b>	Two-step degradable ABAC-type periodic poly(cyclic acetal)s synthesized by sequence-programmed monomer formation and subsequent polyaddition based on cyclotrimerization of one vinyl monomer and two aldehydes .....	57
<b>Chapter 5</b>	Alternating cationic copolymerization of vinyl ethers and sequence-programmed cyclic trimer consisting of one vinyl ether and two aldehydes for ABCC-type periodic terpolymer .....	79
<b>Chapter 6</b>	Summary.....	97
<b>List of Publications .....</b>		<b>99</b>



## Chapter 1

## General introduction

**Background***Various factors responsible for the polymer properties*

Polymer materials exhibit tunable properties, including mechanical, thermal, electrical, and chemical properties. Polymer properties are determined by various structural parameters (Figure 1). Specifically, the structural parameters of the main and side chains, monomer sequences, chain length, and topology are characteristics of macromolecules, unlike small molecules. To obtain polymers with desired properties, polymerization protocols for simultaneous control of these structural parameters are in high demand.

A polymer chain is composed of a main chain and side chains. Various functional groups can be introduced into both the main and side chains. Polymerization mechanisms can be categorized into chain-growth and step-growth polymerizations. In the case of vinyl monomers used for chain-growth polymerization, the polymerization proceeds through different mechanisms depending on the electronic or resonance contributions of substituents on the vinyl groups.<sup>1,2</sup> The resulting polymers with carbon–carbon bonds in the main chain are restricted to side chain functionalization. Unlike the case of vinyl polymerization, ring-opening polymerization of cyclic monomers permits the introduction of heteroatoms into the main chain of the polymer because the heteroatoms remain intact after the completion of the propagating reactions.<sup>3,4</sup> Step-growth polymerization permits the generation of a polymer with various functional groups in the main chain. Novel organic reactions that have never been applied into polymer chemistry are utilized for step-growth polymerizations via successive reactions, resulting in polymers with structures differing from conventional polymers.

In polymerizations of two or more monomers, differences in monomer sequences, which are another structural parameter, arise from the reaction orders of the monomers.<sup>5-8</sup> For example, block,<sup>9-14</sup> random,<sup>15-17</sup> and alternating<sup>18-20</sup> copolymers consisting of common monomer components exhibit distinct functions depending on the monomer sequences. An ultimate goal of synthetic polymer chemistry is to obtain polymers with defined monomer sequences comparable to natural macromolecules such as proteins and DNA.<sup>21,22</sup> Monomer sequences of natural macromolecules are completely defined, which contributes to the complicated and highly specific functions in living creatures. However, sequence-regulated polymerization using more than two kinds of monomers is usually challenging to be achieved. Novel polymerization systems allowing precise sequence control have been studied enthusiastically.

Control of the chain lengths and topologies of polymers has become feasible and is accompanied by the development of living polymerization.<sup>23-40</sup> Polymer molecular weights (MWs) are controlled by living polymerizations with suitable monomer/initiator ratios. Various shapes, such as graft, macrocyclic, and star structures, can be synthesized using suitable monomers and initiators.<sup>41,42</sup> For example, graft copolymers can form micelles with smaller aggregation numbers than linear block copolymers. This characteristic aggregation behavior permits precise control of the wettability on the surface.<sup>43,44</sup>

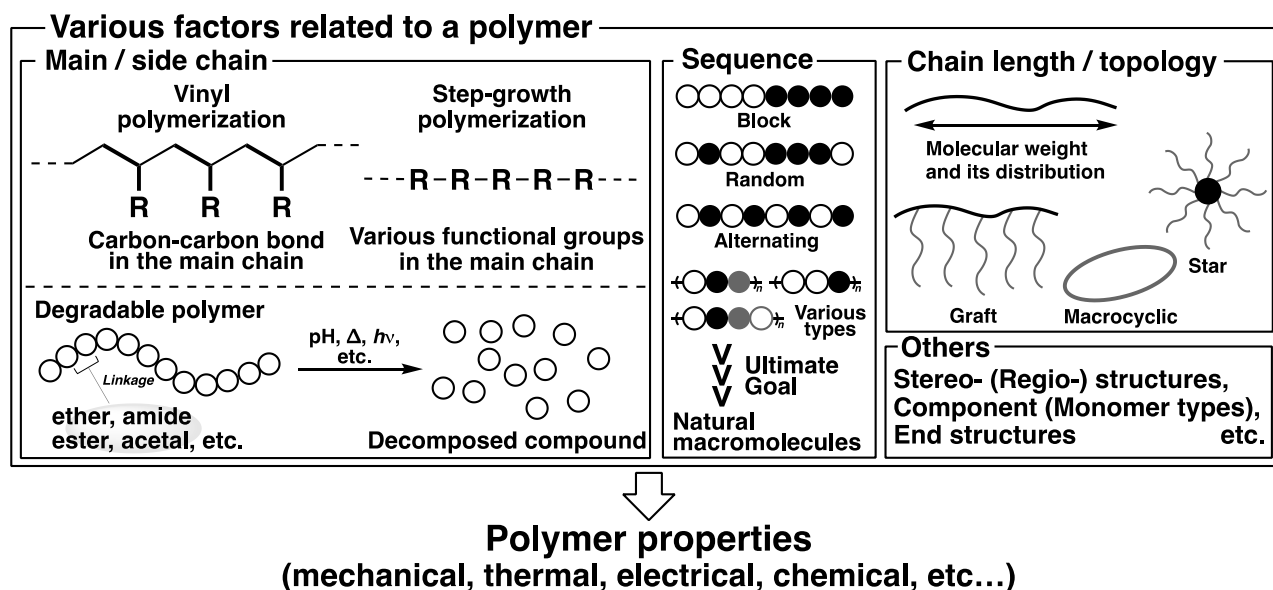


**Figure 1.** Various factors responsible for polymer properties.

### Polymerization procedure

In chain-growth polymerization (non-living polymerization), successive reactions of active species, which are generated from initiator molecules, continuously occur with monomer molecules until aborted by chain transfer or termination reactions; hence, relatively high-MW polymers are generated in the early stages of the polymerization (Figure 2 upper). A newly generated active species or another initiator molecule subsequently undergoes propagation until side reactions abort it. Therefore, the MWs of polymers obtained by non-living chain-growth polymerization are generally uncontrolled. To achieve control of the MWs and primary structures of polymers, various living polymerization systems have been devised in recent decades. Living polymerizations are free from side reactions and allow for quantitative initiation and even propagation of all propagating chains. A representative strategy for living polymerization is to construct an appropriate active-dormant equilibrium to keep the concentration of active species very low. For example, in 1984, Higashimura and coworkers reported the living cationic polymerization of isobutyl vinyl ether (IBVE) with an  $\text{HI}/\text{I}_2$  initiating system.<sup>31</sup> Living polymerization proceeds via the reversible cleavage of carbon–iodine bonds. Subsequently, living cationic polymerizations via dormant-active equilibria were achieved with various initiating systems, such as a weak Lewis acid generating a nucleophilic counteranion, a strong Lewis acid/weak Lewis base combination, and a Lewis acid/tetraalkylammonium salt combination.<sup>33–37,45,46</sup>

To synthesize a linear polymer via step-growth polymerization, a bifunctional monomer must be used, unlike the case of chain-growth polymerization (Figure 2 lower). Polymerization starts from a reaction of two monomers to yield a dimer with two unreacted functional groups, which can subsequently react with a monomer, an oligomer, or a polymer. These reactions occur successively until deactivation of the functional groups. The successive reactions between monomer–monomer, monomer–oligomer (polymer), and oligomer (polymer)–oligomer (polymer) occur statistically; hence, the MW and MWD are usually uncontrollable in step-growth polymerizations.<sup>47</sup> A polymer with a high MW is produced at the later stages because monomer–monomer reactions preferentially occur in the early stage of polymerization. A characteristic of step-growth polymerization is that polymers with various functional groups in the main chain can be generated by applying

diverse organic reactions for bond formation. Polyesters, polyamides, and polyurethanes, which are essential materials used in our daily lives, are generally produced via step-growth polymerizations.<sup>48,49</sup> Recent developments in step-growth polymerization include chain-growth condensation polymerization (CGCP) and multicomponent reaction-based sequence-regulated polymerization. CGCP compensates for the drawbacks of conventional step-growth condensation polymerizations, such as uncontrolled MW and broad MWD. CGCP has been achieved by activating polymer end groups in the following two ways:<sup>50,51</sup> (i) reactivity enhancement of polymer end groups by resonance or inductive effects from substituents<sup>52,53</sup> and (ii) intramolecular catalyst transfer through transmetalation and reductive elimination.<sup>54,55</sup> On the other hand, various multicomponent reactions have been reported<sup>56,57</sup> and gradually applied to polymer chemistry since the first multicomponent reaction was reported in 1850 by Strecker (amino acid syntheses via a three-component reaction involving amines, aldehydes, and cyanides).<sup>58–70</sup> For example, multi-component polymerization (Passerini polymerization) has been used to produce ABCB-type sequence-regulated polymers.<sup>63</sup> Various other multicomponent reactions are also applied to step-growth polymerization, which allows for precise monomer sequences and main-chain functionalization that are inaccessible with chain-growth polymerization.<sup>67–70</sup>

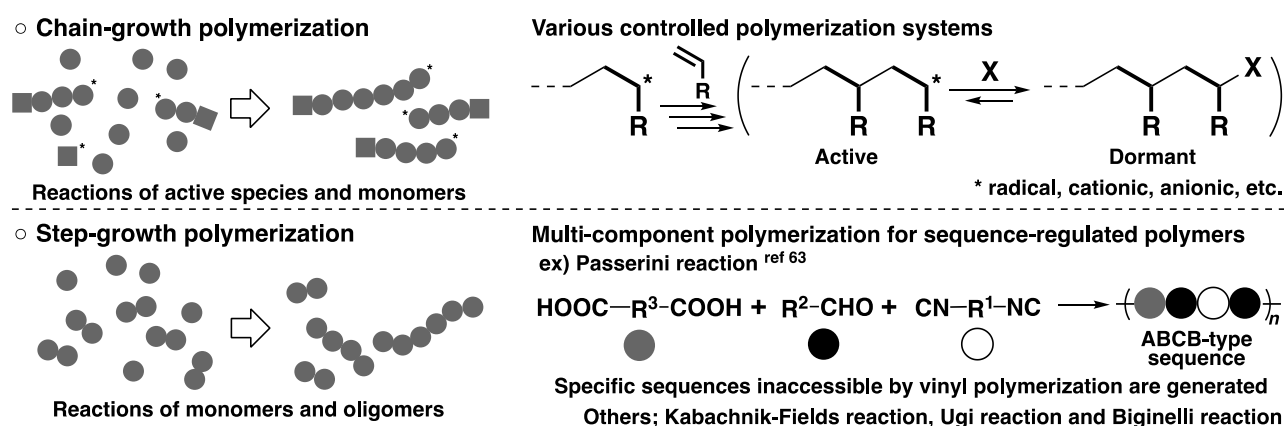


**Figure 2.** The differences between chain-growth and step-growth polymerizations.

### Tandem polymerization

Tandem polymerization is a powerful tool for the syntheses of polymers with complicated structures via two or more simultaneously occurring reactions (Figure 3). Polymers produced with multiple reactions are obtained via a single-step operation in tandem polymerization, which is in contrast to conventional methodologies employing multiple steps consisting of polymerizations and isolations. Tandem polymerizations are classified as either orthogonal<sup>71–74</sup> or non-orthogonal<sup>75–79</sup> type. For example, Grubbs and coworkers devised an orthogonal tandem polymerization consisting of atom transfer radical polymerization and ring-opening metathesis polymerization (ROMP) in the presence of a dual functional initiator, resulted in a block copolymer of methyl methacrylate (MMA) and 1,5-cyclooctadiene.<sup>72</sup> On the other hand, Kamigaito and coworkers synthesized a random poly(MA-co-VEs) by non-orthogonal-type, interconvertible radical and cationic copolymerization via reversible activation of a common dormant species.<sup>75,76</sup> This type of polymers cannot be generated by multi-step cationic and radical polymerizations. As seen in this example, non-orthogonal tandem polymerization effectively yields polymers inaccessible to conventional polymerization systems.

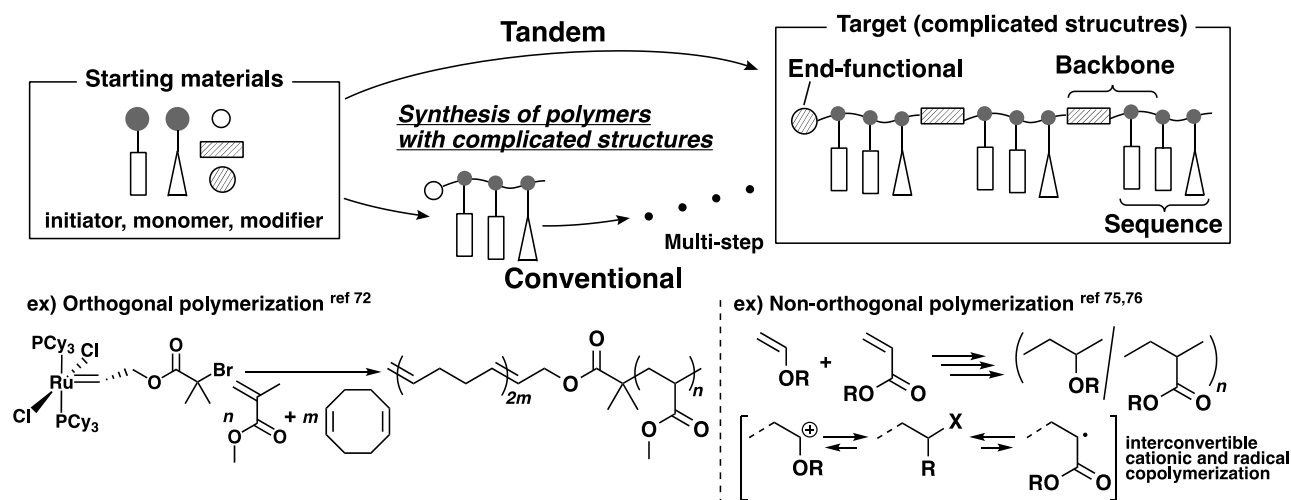
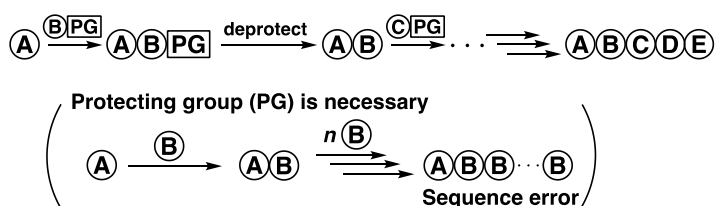


**Figure 3.** Advantages of tandem polymerization.

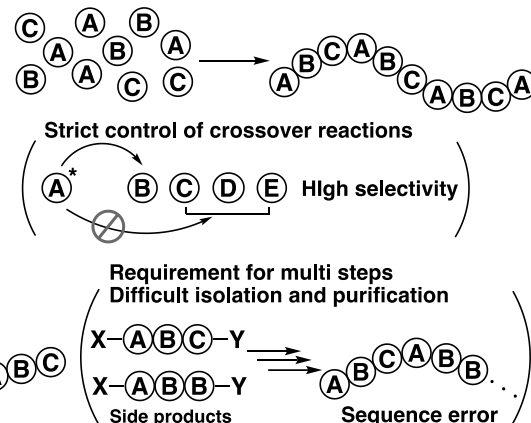
### Sequence-regulated polymers

The polymerization protocols used to control monomer sequences are roughly divided into the following three categories: iterative method, direct polymerization, and sequence-programmed monomer strategy (Figure 4). The iterative method employs step-by-step monomer addition.<sup>80–83</sup> In general, the use of protecting groups allows for the suppression of sequence errors derived from successive reactions and other side reactions. Although the iterative method is the most reliable strategy, considerable time and effort are required due to the multiple steps, including deprotection and purification. Strategies for simplifying the isolation and purification steps have been investigated, as exemplified by the Merrifield peptide synthesis.<sup>84</sup> Direct copolymerization is the most practical method because the sequence-regulated polymer is obtained *via* a single-step operation.<sup>85–87</sup> However, successful reports are very limited because the propagating species derived from each monomer must undergo a highly selective crossover reaction to a specific monomer. For example, Hsieh and Saegusa independently reported ABC-type sequence-regulated terpolymerization by adding a third monomer into alternating copolymerization systems.<sup>85,86</sup> In the sequence-programmed monomer strategy, a reactive oligomer containing a periodic monomer sequences is synthesized and subsequently polymerized to yield polymers with periodic sequences.<sup>88–94</sup> Although the preparations of such monomers require multiple steps consisting of iterative reactions, isolations, and purifications, a high-MW polymer with the desired monomer sequences can be obtained. For example, Kamigaito and coworkers reported that various sequence-regulated polymers were synthesized by radical polyaddition of sequence-programmed oligomers prepared in an iterative radical addition reaction.<sup>90–92</sup> The obtained polymers have periodic sequences inaccessible to conventional radical polymerizations. In addition, simultaneous control of both monomer sequences and stereostructures was attained by ROMP using sequence-regulated cyclic oligomers.<sup>93,94</sup>

## i) Iterative polymerization



## ii) Direct copolymerization



## iii) Polymerization using sequence-programmed monomer

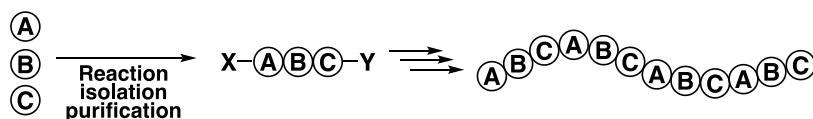


**Figure 4.** Various polymerization systems for sequence-regulated polymers.

### Organic reactions and polymerizations of aldehydes

The carbonyl group in an aldehyde is polarized because of the two lone electron pairs and the electronegativity of the oxygen atom; hence, aldehydes exhibit high reactivity toward various organic compounds.<sup>95</sup> For example, the Prins reaction is an acid-mediated reaction of aldehydes and alkenes.<sup>96–98</sup> The generally accepted reaction mechanism is described in Figure 5. After acid-promoted activation of the aldehyde, the reaction of the activated aldehyde and an alkene produces a carbocation, which can give 1,3-diols, allylic alcohols, and 1,3-dioxanes depending on the reaction conditions. In industry, the Prins reaction has been applied in syntheses of fragrance and flavor ingredients, such as isoprenol, indolarome, and nopol.<sup>99,100</sup>

The use of a novel organic reaction in polymer chemistry potentially leads to a novel polymerization system. The extremely high selectivities of organic reactions are important in generating a high-MW polymer. For example, the application of a Cu-catalyzed azide-alkyne cycloaddition (CuAAC) in polymer chemistry was achieved in the mid-2000s.<sup>101–104</sup> After this breakthrough, many scientists utilized this reaction as a bond-forming reaction, a cross-linking reaction, and a monomer synthesis.<sup>105–112</sup> On the other hand, limited applications of the Prins reaction in polymer chemistry have been reported.<sup>113,114</sup>

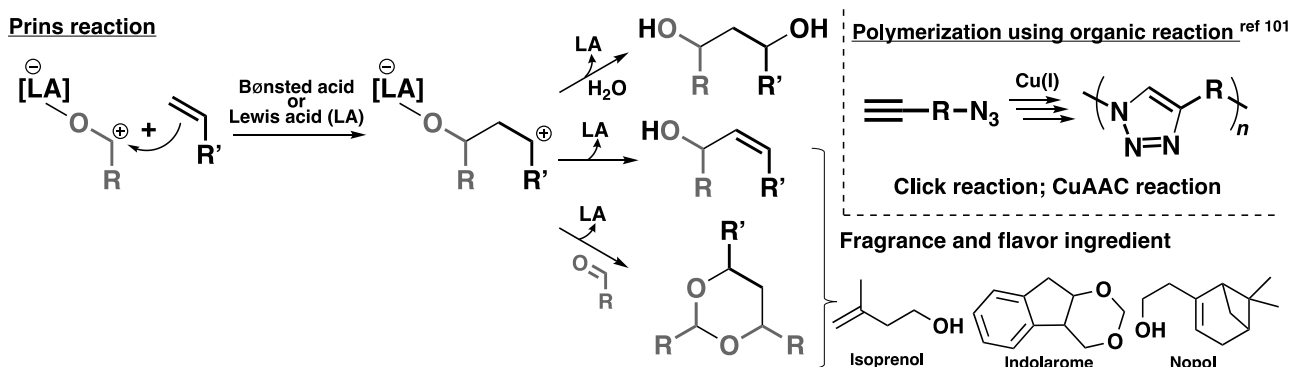


**Figure 5.** The mechanism of the Prins reaction and an example of the polymerization using an organic reaction.



### Cationic copolymerization of vinyl ethers and conjugated aldehydes

Addition polymerizations of aldehydes with appropriate structures are sometimes feasible, although harsh conditions are required because of obstacles resulting from the generation of trioxane-type side products and depolymerization derived from the extremely low ceiling temperature. In particular, aromatic aldehydes do not undergo cationic homopolymerization,<sup>115</sup> except for special types such as *o*-phthalaldehyde (OPA).<sup>116</sup> In contrast, cationic copolymerizations of VEs or styrenes with conjugated aldehydes, such as aromatic aldehydes and plant-derived aldehydes, have been developed via the elaborate design of the initiating systems.<sup>117–121</sup> In these copolymerizations, the Lewis acid catalysts are responsible for the copolymerization behavior (Figure 6). Specifically, the alternating living cationic copolymerization proceeds with  $\text{GaCl}_3$ , whereas  $\text{EtAlCl}_2$  facilitates a highly selective cyclotrimerization involving one VE and two aldehyde molecules. Various degradable polymers, such as dual stimuli-responsive polymers,<sup>122,123</sup> polymers with degradable bonds introduced into specific positions,<sup>124</sup> and 2:(1+1)-type sequence-defined polymers,<sup>125</sup> were synthesized via copolymerizations of VEs and aldehydes.

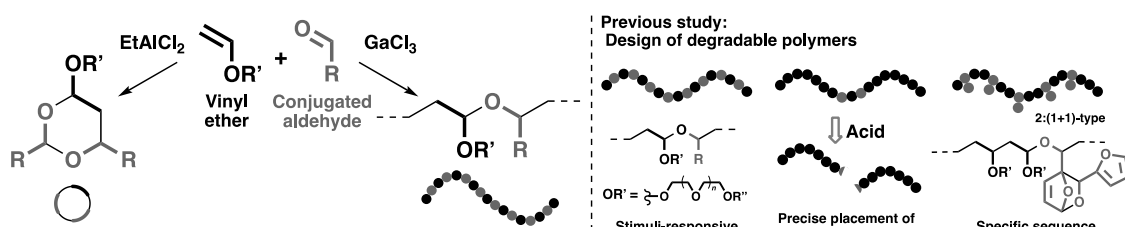


**Figure 6.** Controlled alternating copolymerization and cyclotrimerization of VE and aldehyde.

Kunitake and coworkers homopolymerized OPA by cationic, anionic, and coordination mechanisms, which, unlike conjugated monoaldehydes, yielded high-MW polymers.<sup>116,126</sup> The polymers obtained from cationic polymerization had cyclic structures.<sup>127,128</sup> Furthermore, Aoshima and coworkers reported that OPA underwent cationic copolymerizations with various alkyl VEs and even with bulky  $\beta,\beta$ -disubstituted VEs (Figure 7 upper).<sup>129–131</sup> In contrast, isophthalaldehyde and terephthalaldehyde, which contain two aldehyde moieties at the *meta*- and *para*-positions, act as bifunctional monomers to undergo cross-linking,<sup>124</sup> polyaddition,<sup>132–135</sup> and polycondensation<sup>136</sup> reactions (Figure 7 lower).

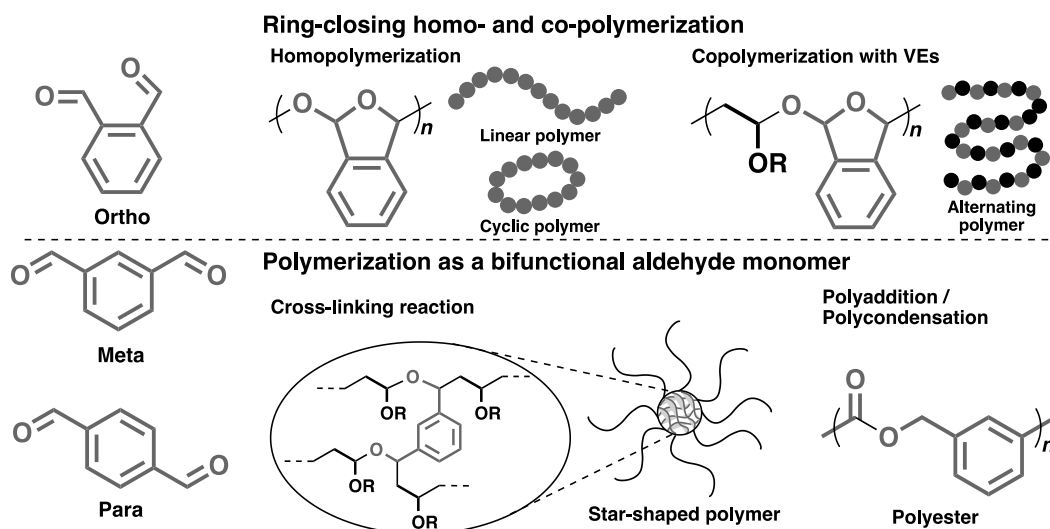


**Figure 7.** Various (co)polymerization systems using phthalaldehyde derivatives.

## Objective and Outline of This Thesis

The development of a polymerization protocol based on the cyclic acetal formation would potentially lead to polymers with periodic monomer sequences and/or specific units in the main chain, because the cyclotrimerization forms an ABA-type sequence-programmed cyclic acetal exhibiting both rigidity and reactivity toward acids. This thesis aims to construct a novel polymerization system utilizing the cyclotrimerization of one vinyl monomer and two aldehyde molecules. Initially, appropriate reaction conditions were investigated for the selective cyclotrimerization reactions. Based on the results, poly(cyclic acetal)s were synthesized with successive cyclotrimerization reactions. In addition, a tandem polymerization consisting of cyclotrimerization and the Tishchenko reaction was devised to yield polymers with cyclic acetal and ester moieties in the main chain. On the other hand, two types of sequence-programmed monomers were synthesized by cyclotrimerization. Sequence-programmed monomers were employed to synthesize polymers with periodic monomer sequences based on successive cyclotrimerization and concurrent cationic vinyl addition and ring-opening copolymerization.

This thesis consists of two parts. Part I (Chapters 2 and 3) describes successive cyclotrimerizations for polymers with specific structures in the main chain. In Part II (Chapters 4 and 5), ABAC- and ABCC-type periodic polymers are described, and these were synthesized by copolymerization of two different types of sequence-programmed monomers prepared by cyclotrimerizations (Figure 8).

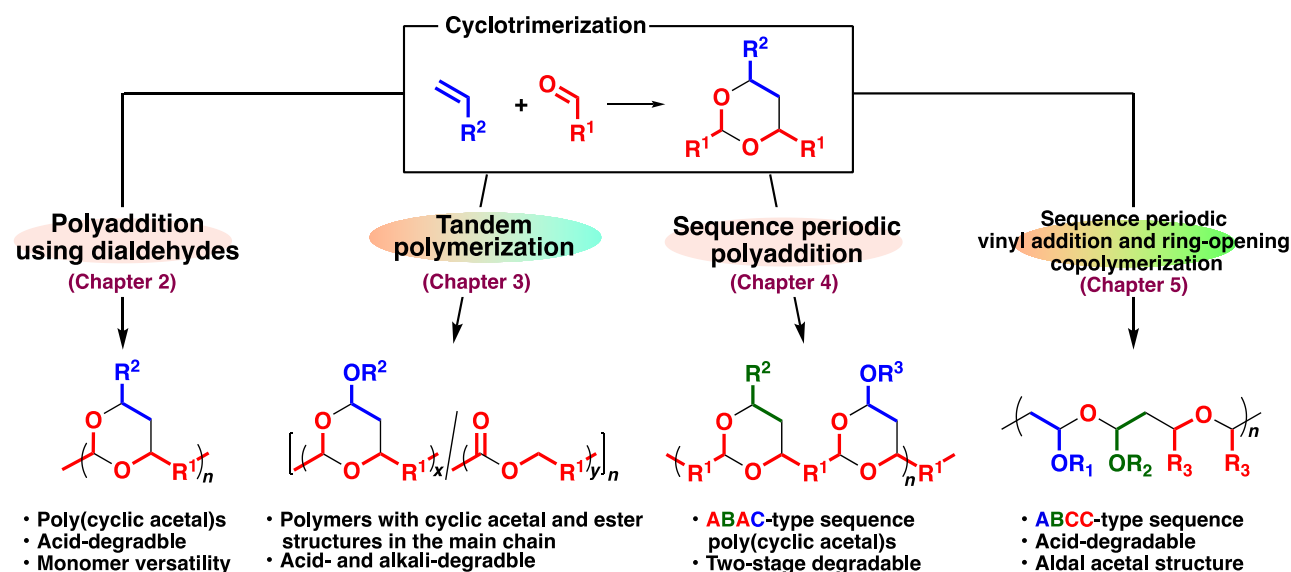


**Figure 8.** Objective and outline of this thesis.

In Chapter 2, a polyaddition via the cyclotrimerization of one VE and two conjugated aldehydes successfully proceeds under the optimized conditions based on the model reactions, yielding a polymer with cyclic acetal structures in the main chain (Figure 9). The use of less reactive or non-polymerizable vinyl monomers and the choice of adequate Lewis acid catalysts are demonstrated to be critical factors for efficient successive reactions. In addition, the obtained polymer exhibits selective acid-degradability and high glass-transition temperatures based on the acid-lability and rigidity of the cyclic acetal structures.

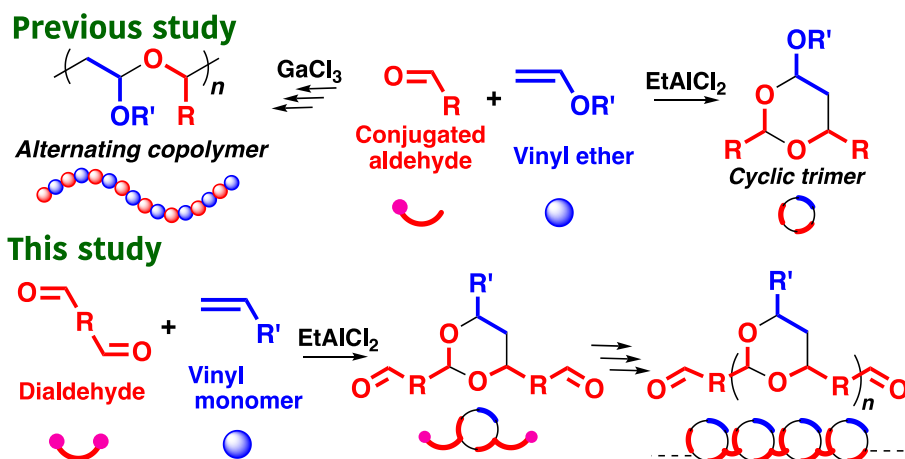


**Figure 9.** Polyaddition via cyclotrimerization of vinyl monomers and dialdehydes.

Chapter 3 describes a novel tandem polymerization system consisting of cyclotrimerization and the Tishchenko reaction of VEs and dialdehydes using a catalyst mixture of  $\text{EtAlCl}_2$  and  $\text{Al}(\text{O}i\text{Pr})_3$  (Figure 10). The obtained polymers with cyclic acetal and ester structures in the main chain can be hydrolyzed under acidic and alkali conditions. The initial molar ratio of the catalyst mixture is highly responsible for the composition ratios of cyclic acetal and ester structures, which are generated by cyclotrimerization and the Tishchenko reaction, respectively. Moreover, the author employs transesterification reaction for three-component tandem polymerization with dicarboxylic acid ester as the third component, which results in a polymer with cyclic acetal and two different ester structures in the main chain.

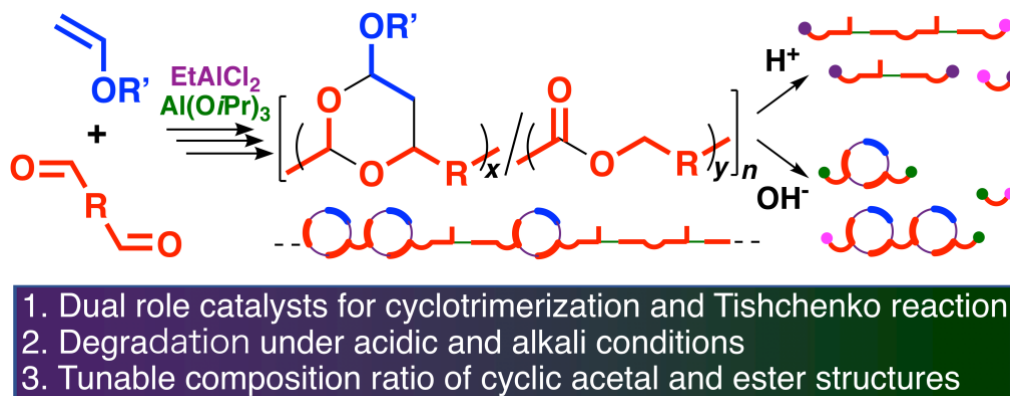


**Figure 10.** Tandem polymerization consisting of cyclotrimerization and the Tishchenko reaction.

In Chapter 4, ABAC-type periodic poly(cyclic acetal)s are generated via the sequence-programmed monomer synthesis and subsequent polyaddition reaction based on cyclotrimerizations (Figure 11). The use of 1,1-diphenylethylene (DPE) is important for synthesizing the cyclic trimer in high yield because the successive cyclotrimerization and other side reactions are suppressed due to the steric hindrance of DPE. The obtained ABA-type sequence-programmed cyclic trimer undergoes successive cyclotrimerization with VEs. The obtained ABAC-type periodic polymers have two different kinds of cyclic acetal structures as well as two phenyl rings and vinyl monomer-derived side chains that are alternately arranged. Such polymers exhibit two-step degradability under acidic conditions.

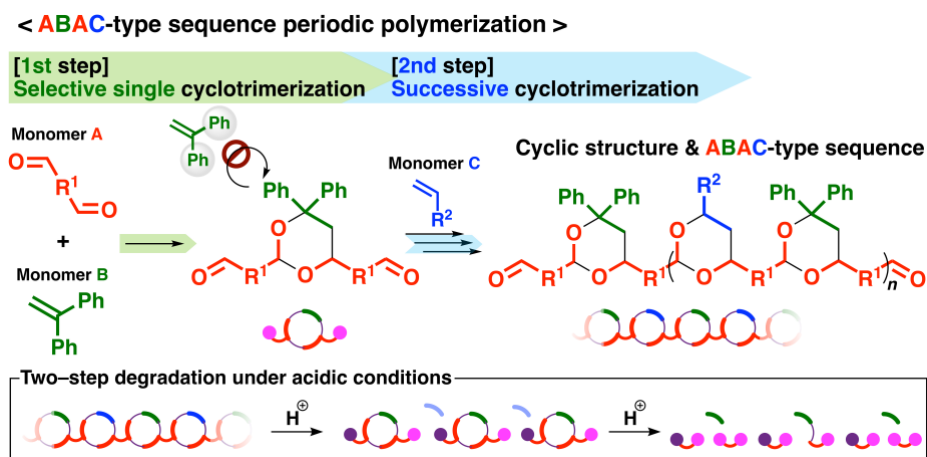


**Figure 11.** Synthesis of ABAC-type sequence periodic polymers via successive cyclotrimerization of sequence-programmed cyclic trimer and vinyl monomers.

In Chapter 5, the author investigates concurrent cationic vinyl addition and ring-opening copolymerization of VEs and the sequence-programmed cyclic trimers prepared from cyclotrimerization. Vinyl monomer and aldehyde units incorporated into cyclic trimers affect the occurrence of crossover reactions with VEs. Alternating-like cationic copolymerization is demonstrated to proceed when 2-nonenal-containing cyclic trimers are used under the optimized conditions. The structural analysis of the acid methanolysis product of the obtained polymer indicates that ABCC-type periodic sequences are mainly generated (Figure 12).

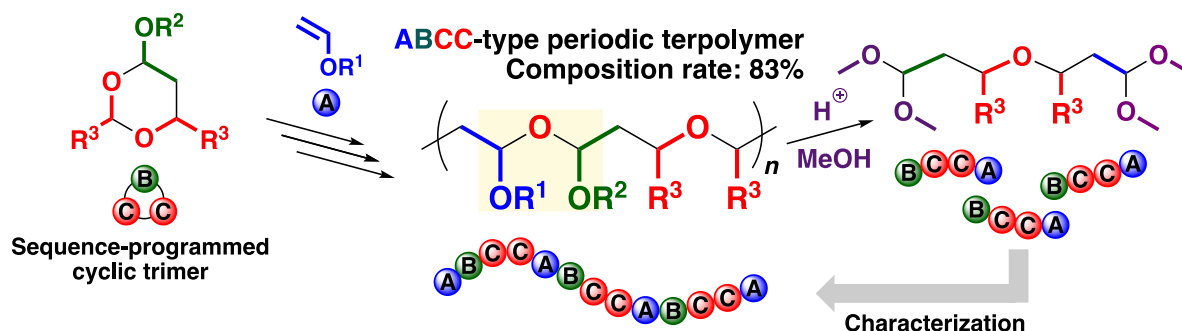


**Figure 12.** Concurrent cationic vinyl addition and ring-opening copolymerization of sequence-programmed cyclic trimer and vinyl ethers.

## References

1. Grubbs, R. B.; Grubbs, R. H. *Macromolecules* **2017**, *50*, 6979–6997.
2. Leonard, J. In *Polymer Handbook 4th Edition*; Brandrup, J.; Immergut, E. H.; Grulke, E. A. Eds.; Wiley, New York, 1999.
3. Olsén, P.; Odelius, K.; Albertsson, A.-C. *Biomacromolecules* **2016**, *17*, 699–709.
4. De Hoe, G. X.; Şucu, T.; Shaver, M. P. *Acc. Chem. Res.* **2022**, *55*, 1514–1523.
5. Lutz, J.-F. *Polym. Chem.* **2010**, *1*, 55–62.
6. Badi, N.; Lutz, J.-F. *Chem. Soc. Rev.* **2009**, *38*, 3383–3390.
7. Ouchi, M.; Sawamoto, M. *Polym. J.* **2018**, *50*, 83–94.
8. Kamigaito, M. *Polym. J.* **2022**, *53*, 239–248.
9. Swarc, M.; Levy, M.; Milkovich, R. *J. Am. Chem. Soc.* **1956**, *78*, 2656–2657.

8. Kamigaito, M. *Polym. J.* **2022**, *53*, 239–248.
9. Swarc, M.; Levy, M.; Milkovich, R. *J. Am. Chem. Soc.* **1956**, *78*, 2656–2657.
10. Bates, F. S.; Fredrickson, G. H. *Phys. Today* **1999**, *52*, 32–38.
11. Kataoka, K.; Harada, A.; Nagasaki, Y. *Adv. Drug. Deliv. Rev.* **2001**, *47*, 113–131.
12. Riess, G. *Prog. Polym. Sci.* **2003**, *28*, 1107–1170.
13. Kang, S.; Park, M. J. *ACS Macro Lett.* **2020**, *9*, 1527–1541.
14. Lequeieu, J.; Magenau, A. J. D. *Polym. Chem.* **2021**, *12*, 12–28.
15. Li, L.; Raghupathi, K.; Song, C.; Prasad, P.; Thayumanavan, S. *Chem. Commun.* **2014**, *50*, 13417–13432.
16. Tsitsilianis, C.; Gotzamanis, G.; Iatridi, Z. *Eur. Polym. J.* **2011**, *47*, 497–510.
17. Terashima, T. *Polym. J.* **2014**, *46*, 664–673.
18. Bianchini, C.; Meli, A. *Coord. Chem. Rev.* **2002**, *225*, 35–66.
19. Longo, J. M.; Sanford, M. J.; Coates, G. W. *Chem. Rev.* **2016**, *116*, 15167–15197.
20. Nishimori, K.; Ouchi, M. *Chem. Commun.* **2020**, *56*, 3473–3483.
21. Lutz, J.-F.; Lehn, J.-M.; Meijer, E. W.; Matyjaszewski, K. *Nat. Rev. Mater.* **2016**, *1*, 16024.
22. Anfinsen, C. B. *Science* **1973**, *181*, 223–230.
23. Otsu, T. *J. Polym. Sci. Part A: Polym. Chem.* **2000**, *38*, 2121–2136.
24. Coessens, V.; Pintauer, T.; Matyjaszewski, K. *Prog. Polym. Sci.* **2001**, *26*, 337–377.
25. Lorandi, F.; Fantin, M.; Matyjaszewski, K. *J. Am. Chem. Soc.* **2022**, *144*, 15413–15430.
26. Kamigaito, M.; Ando, T.; Sawamoto, M. *Chem. Rev.* **2001**, *101*, 3689–3745.
27. Ouchi, M.; Terashima, T.; Sawamoto, M. *Chem. Rev.* **2009**, *109*, 4963–5050.
28. Yamago, S. *Chem. Rev.* **2009**, *109*, 5051–5068.
29. Hawker, C. J.; Bosman, A. W.; Harth, E. *Chem. Rev.* **2001**, *101*, 3661–3688.
30. Moad, G.; Rizzardo, E.; Thang, S. H. *Aust. J. Chem.* **2005**, *58*, 379–410.
31. Miyamoto, M.; Sawamoto, M.; Higashimura, T. *Macromolecules* **1984**, *17*, 265–268.
32. Faust, R.; Kennedy, J. P. *Polym. Bull.* **1986**, *15*, 273–280.
33. Kennedy, J. P. *J. Polym. Sci., Part A: Polym. Chem.* **1999**, *37*, 2285–2293.
34. Puskas, J. E.; Kaszas, G. *Prog. Polym. Sci.* **2000**, *25*, 403–452.
35. Aoshima, S.; Yoshida, T.; Kanazawa, A.; Kanaoka, S. *J. Polym. Sci., Part A: Polym. Chem.* **2007**, *45*, 1801–1813.
36. Aoshima, S.; Kanaoka, S. *Chem. Rev.* **2009**, *109*, 5245–5287.
37. Kanazawa, A.; Kanaoka, S.; Aoshima, S. *Chem. Lett.* **2010**, *39*, 1232–1237.
38. Szwarc, M. *Nature* **1956**, *178*, 1168–1169.
39. Hadjichristidis, N.; Pitsikalis, M.; Pispas, S.; Iatrou, H. *Chem. Rev.* **2001**, *101*, 3747–3792.
40. Bak, I. G.; Chae, C.-C.; Lee, J.-S. *Macromolecules* **2022**, *55*, 1923–1945.
41. Zheng, Y.; Li, S.; Weng, Z.; Gao, C. *Chem. Soc. Rev.* **2015**, *44*, 4091–4130.
42. Qiu, L. Y.; Bae, Y. H. *Pharm. Res.* **2006**, *23*, 1–30.
43. Pispas, S.; Hadjichristidis, N.; Mays, J. W. *Macromolecules* **1996**, *29*, 7378–7385.
44. Pitsikalis, M.; Woodward, J.; Mays, J. W.; Hadjichristidis, N. *Macromolecules* **1997**, *30*, 5384–5389.
45. Sawamoto, M. *Prog. Polym. Sci.* **1991**, *16*, 111–172.
46. Kamigaito, M.; Sawamoto, M. *Macromolecules* **2020**, *53*, 6749–6753.

47. Bossion, A. K.; Heifferon, V.; Meabe, L.; Zivic, N.; Taton, D.; Hedrick, J. L.; Long, T. E.; Sardon, H. *Prog. Polym. Sci.* **2019**, *90*, 164–210.
48. Weinland, D. H.; Van Putten, R.-J.; Gruter, G.-J. M. *Eur. Polym. J.* **2022**, *164*, 110964.
49. Sardon, H.; Pascual, A.; Mecerreyes, D.; Taton, D.; Cramail, H.; Hedrick, J. L. *Macromolecules* **2015**, *48*, 3153–3165.
50. Yokozawa, T.; Yokoyama, A. *Chem. Rev.* **2009**, *109*, 5595–5619.
51. Yokozawa, T.; Ohta, Y. *Chem. Rev.* **2016**, *116*, 1950–1968.
52. Yokozawa, T.; Shimura, H. *J. Polym. Sci., Part A: Polym. Chem.* **1999**, *37*, 2607–2618.
53. Yokozawa, T.; Asai, T.; Sugi, R.; Ishigooka, S.; Hiraoka, S. *J. Am. Chem. Soc.* **2000**, *122*, 8313–8314.
54. Yokoyama, A.; Miyakoshi, R.; Yokozawa, T. *Macromolecules* **2004**, *37*, 1169–1171.
55. Sheina, E. E.; Liu, J.; Iovu, M. C.; Laird, D. W.; McCullough, R. D. *Macromolecules* **2004**, *37*, 3526–3528.
56. Dömling, A.; Wang, W.; Wang, K. *Chem. Rev.* **2012**, *112*, 3083–3135.
57. Zarganes-Tzitzikas, T.; Chandgude, A. L.; Dömling, A. *Chem. Rec.* **2015**, *15*, 981–996.
58. Strecker, A. *Ann. Chem. Pharm.* **1850**, *75*, 27–45.
59. Wang, J.; Liu, X.; Feng, X. *Chem. Rev.* **2011**, *111*, 6947–6983.
60. Kakuchi, R. *Angew. Chem. Int. Ed.* **2014**, *53*, 46–48.
61. Zhang, Z.; You, Y.; Hong, C. *Macromol. Rapid Commun.* **2018**, *39*, 1800362.
62. Kreye, O.; Tóth, T.; Meier, M. A. R. *J. Am. Chem. Soc.* **2011**, *133*, 1790–1792.
63. Deng, X.-X.; Li, L.; Li, Z.-L.; Lv, A.; Du, F.-S.; Li, Z.-C. *ACS Macro Lett.* **2012**, *1*, 1300–1303.
64. Tuten, B. T.; Bui, A. H.; Wiedbrauk, S.; Truong, V. X.; Raston, C. L.; Barner-Kowollik, C. *Chem. Commun.* **2021**, *57*, 8328–8331.
65. Alkan, B.; Daglar, O.; Luleburgaz, S.; Gungor, B.; Gunay, U. S.; Hizal, G.; Tunca, U.; Durmaz, H. *Polym. Chem.* **2022**, *13*, 258–266.
66. Yang, L.; Zhang, Z.; Cheng, B.; You, Y.; Wu, D.; Hong, C. *Sci. China Chem.* **2015**, *58*, 1734–1740.
67. Yang, B.; Zhao, Y.; Wei, Y.; Fu, C.; Tao, L. *Polym. Chem.* **2015**, *6*, 8233–8239.
68. Xue, H.; Zhao, Y.; Wu, H.; Wang, Z.; Yang, B.; Wei, Y.; Wang, Z.; Tao, L. *J. Am. Chem. Soc.* **2016**, *138*, 8690–8693.
69. Zhang, Y.; Zhao, Y.; Yang, B.; Zhu, C.; Wei, Y.; Tao, L. *Polym. Chem.* **2014**, *5*, 1857–1862.
70. Moldenhauer, F.; Kakuchi, R.; Theato, P. *ACS Macro Lett.* **2016**, *5*, 10–13.
71. (a) Mecerreyes, D.; Moineau, G.; Dubois, P.; Jérôme, R.; Hedrick, J. L.; Hawker, C. J.; Malmström, E. E.; Trollsas, M. *Angew. Chem. Int. Ed.* **1998**, *37*, 1274–1276. (b) Mecerreyes, D.; Atthoff, B.; Boduch, K. A.; Trollsas, M.; Hedrick, J. L. *Macromolecules* **1999**, *32*, 5175–5182.
72. Bielawski, C. W.; Louie, J.; Grubbs, R. H. *J. Am. Chem. Soc.* **2000**, *122*, 12872–12873.
73. Ogura, Y.; Terashima, T.; Sawamoto, M. *ACS Macro Lett.* **2013**, *2*, 985–989.
74. Sample, C. S.; Kellstedt, E. A.; Hillmyer, M. A. *ACS Macro Lett.* **2022**, *11*, 608–614.
75. Aoshima, H.; Uchiyama, M.; Satoh, K.; Kamigaito, M. *Angew. Chem. Int. Ed.* **2014**, *53*, 10932–10936.
76. Satoh, K.; Hashimoto, H.; Kumagai, S.; Aoshima, H.; Uchiyama, M.; Ishibashi, R.; Fujiki, Y.; Kamigaito, M. *Polym. Chem.* **2017**, *8*, 5002–5011.
77. Lee, H.-K.; Bang, K.-T.; Hess, A.; Grubbs, R. H.; Choi, T.-L. *J. Am. Chem. Soc.* **2015**, *137*, 9262–9265.
78. Kanazawa, A.; Kanaoka, S.; Aoshima, S. *J. Am. Chem. Soc.* **2013**, *135*, 9330–9333.

80. Scolleder, S. C.; Schneider, R. V.; Wetzel, K. S.; Boukis, A. C.; Meier, M. A. R. *Macromol. Rapid Commun.* **2017**, *38*, 160711.
81. Xu, J. *Macromolecules* **2019**, *52*, 9068–9093.
82. Wang, X.; Zhang, X.; Ding, S. *Polym. Chem.* **2021**, *12*, 2668–2688.
83. Sharma, A.; Kumar, A.; de la Torre, B. G.; Albericio, F. *Chem. Rev.* **2022**, *122*, 13516–13546.
84. Merrifield, R. B. *J. Am. Chem. Soc.* **1963**, *85*, 2149–2154.
85. Hsieh, H. L. *J. Macromol. Sci., Part A- Chem.* **1973**, *7*, 1525–1535.
86. Saegusa, T.; Kobayashi, S.; Kimura, Y. *Macromolecules* **1977**, *10*, 68–72.
87. Mimura, M.; Kanazawa, A.; Aoshima, S. *Macromolecules* **2019**, *52*, 7572–7583.
88. Cho, I. *Prog. Polym. Sci.* **2000**, *25*, 1043–1087.
89. Zhang, J.; Matta, M. E.; Hillmyer, M. A. *ACS Macro Lett.* **2012**, *1*, 1383–1387.
90. Satoh, K.; Mizutani, M.; Kamigaito, M. *Chem. Commun.* **2007**, 1260–1262.
91. Satoh, K.; Ozawa, S.; Mizutani, M.; Nagai, K.; Kamigaito, M. *Nat. Commun.* **2010**, *1*, 6.
92. Satoh, K.; Ishizuka, K.; Hamada, T.; Handa, M.; Abe, T.; Ozawa, S.; Miyajima, M.; Kamigaito, M. *Macromolecules* **2019**, *52*, 3327–3341.
93. Miyajima, M.; Satoh, K.; Horibe, T.; Ishihara, K.; Kamigaito, M. *J. Am. Chem. Soc.* **2020**, *142*, 18955–18962.
94. Miyajima, M.; Satoh, K.; Kamigaito, M. *Polym. Chem.* **2021**, *12*, 423–431.
95. Vollhardt, K. P. C.; Schore, N. E. *Organic Chemistry: Structure and function*, 8th Edition, W. H. Feeman and Co., New York, 2019.
96. Arundale, E.; Mikeska, L. A. *Chem. Rev.* **1952**, *51*, 505–555.
97. Sabitha, G.; Reddy, K. B.; Bhikshapathi, M.; Yadav, J. S. *Tetrahedron Lett.* **2006**, *47*, 2807–2810.
98. Hirai, K.; Takeda, R.; Hutchison, J. A.; Uji-i, H. *Angew. Chem. Int. Ed.* **2020**, *59*, 5332–5335.
99. Itoh, H.; Maeda, H.; Yamada, S.; Hori, Y.; Mino, T.; Sakamoto, M. *RSC Adv.* **2014**, *4*, 61619–61623.
100. Dono, F.; Akeroyd, N.; Schiet, F.; Narula, A. *Angew. Chem. Int. Ed.* **2019**, *58*, 7174–7179.
101. Díaz, D. D.; Punna, S.; Holzer, P.; McPherson, A. K.; Sharpless, K. B.; Fokin, V. V.; Finn, M. G. *J. Polym. Sci., Part A: Polym. Chem.* **2004**, *42*, 4392–4403.
102. Binder, W. H.; Kluger, C. *Macromolecules* **2004**, *37*, 9321–9330.
103. Helms, B.; Mynar, J. L.; Hawker, C. J.; Fréchet, J. M. J. *J. Am. Chem. Soc.* **2004**, *126*, 15020–15021.
104. Tsarevsky, N. V.; Bernaerts, K. V.; Dufour, B.; Du Prez, F. E.; Matyjaszewski, K. *Macromolecules* **2004**, *37*, 9308–9313.
105. Delaittre, G.; Guimard, N. K.; Barner-Kowollik, C. *Acc. Chem. Res.* **2015**, *48*, 1296–1307.
106. Espeel, P.; Du Prez, F. E. *Macromolecules* **2015**, *48*, 2–14.
107. Martens, S.; Holloway, J. O.; Du Prez, F. E. *Macromol. Rapid Commun.* **2017**, *38*, 1700469.
108. Hashidzume, A.; Nakamura, T.; Sato, T. *Polymer* **2013**, *54*, 3448–3451.
109. Yamasaki, S.; Kamon, Y.; Xu, L.; Hashidzume, A. *Polymers* **2021**, *13*, 1627.
110. Okuno, K.; Arisawa, T.; Kamon, Y.; Hashidzume, A.; Winnik, F. M. *Langmuir* **2022**, *38*, 5156–5165.
111. Mohapatra, H.; Ayarza, J.; Sanders, E. C.; Scheuermann, A. M.; Griffin, P. J.; Esser-Kahn, A. P. *Angew. Chem. Int. Ed.* **2018**, *57*, 11208–11212.
112. Mueller, J. O.; Voll, D.; Schmidt, F. G.; Delaittre, G.; Barner-Kowollik, C. *Chem. Commun.* **2014**, *50*, 15681–15684.

112. Mueller, J. O.; Voll, D.; Schmidt, F. G.; Delaittre, G.; Barner-Kowollik, C. *Chem. Commun.* **2014**, 50, 15681–15684.
113. Inagi, S.; Doi, Y.; Kishi, Y.; Fuchigami, T. *Chem. Commun.* **2009**, 2932–2934.
114. Inagi, S.; Takei, N.; Fuchigami, T. *Polym. Chem.* **2013**, 4, 1221–1227.
115. Aso, C.; Tagami, S.; Kunitake, T. *Kobunshi Kagaku* **1966**, 23, 63–68.
116. Aso, C.; Tagami, S.; Kunitake, T. *J. Polym. Sci., Part A-1: Polym. Chem.* **1969**, 7, 497–511.
117. Ishido, Y.; Aburaki, R.; Kanaoka, S.; Aoshima, S. *J. Polym. Sci., Part A: Polym. Chem.* **2010**, 48, 1838–1843.
118. Ishido, Y.; Aburaki, R.; Kanaoka, S.; Aoshima, S. *Macromolecules* **2010**, 43, 3141–3144.
119. Ishido, Y.; Kanazawa, A.; Kanaoka, S.; Aoshima, S. *Macromolecules* **2012**, 45, 4060–4068.
120. Ishido, Y.; Kanazawa, A.; Kanaoka, S.; Aoshima, S. *J. Polym. Sci., Part A: Polym. Chem.* **2014**, 52, 1334–1343.
121. Nara, T.; Kanazawa, A.; Aoshima, S. *Macromolecules* **2022**, 55, 6852–6859.
122. Aoshima, S.; Oda, Y.; Matsumoto, S.; Shinke, Y.; Kanazawa, A.; Kanaoka, S. *ACS Macro Lett.* **2014**, 3, 80–85.
123. Matsumoto, S.; Kanazawa, A.; Kanaoka, S. *Polym. Chem.* **2019**, 10, 4134–4141.
124. Kawamura, M.; Kanazawa, A.; Kanaoka, S.; Aoshima, S. *Polym. Chem.* **2015**, 6, 4102–4108.
125. Matsumoto, S.; Kanazawa, A.; Aoshima, S. *J. Am. Chem. Soc.* **2017**, 139, 7713–7716.
126. Aso, C.; Tagami, S. *Macromolecules* **1969**, 2, 414–419.
127. Kaitz, J. A.; Diesendruck, C. E.; Moore, J. S. *J. Am. Chem. Soc.* **2013**, 135, 12755–12761.
128. Kaitz, J. A.; Diesendruck, C. E.; Moore, J. S. *Macromolecules* **2013**, 46, 8121–8128.
129. Hayashi, K.; Kanazawa, A.; Aoshima, S. *Polym. Chem.* **2019**, 10, 3712–3717.
130. Hayashi, K.; Kanazawa, A.; Aoshima, S. *Macromolecules* **2022**, 55, 1365–1375.
131. Hayashi, K.; Kanazawa, A.; Aoshima, S. *Macromolecules* **2022**, 55, 3276–3286.
132. Sweeny, W. *J. Appl. Polym. Sci.* **1963**, 7, 1983–1989.
133. Yamaguchi, I.; Kimishima, T.; Osakada, K.; Yamamoto, T. *J. Polym. Sci., Part A: Polym. Chem.* **1997**, 35, 1265–1273.
134. Onozawa, S.; Sakakura, T.; Tanaka, M.; Shiro, M. *Tetrahedron* **1996**, 52, 4291–4302.
135. Karmel, I. S. R.; Fridman, N.; Tamm, M.; Eisen, M. S. *Organometallics* **2015**, 34, 2933–2942.
136. Yokozawa, T.; Nakamura, F. *Makromol. Chem. Rapid Commun.* **1993**, 14, 167–172.



## **Part I**

# **Novel Polyaddition and Tandem Polymerization Using Cyclotrimerization for Synthesis of Degradable Polymers**

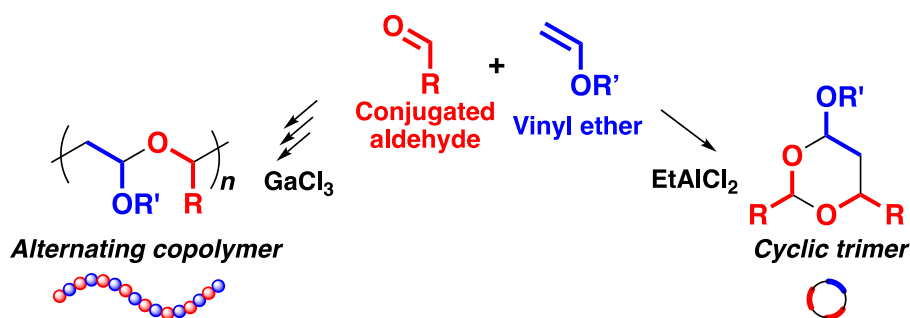


## Polyaddition of vinyl ethers and phthalaldehydes via successive cyclotrimerization reactions: selective model reactions and synthesis of acid-degradable linear poly(cyclic acetal)s

### Introduction

Polymers with functional groups in the main chain are of diverse interest because of their properties that are not exerted by vinyl monomer-derived polymers with carbon-carbon bonds in the main chain. A variety of general-purpose but highly functional polymers, such as polyesters, polyamides, and polyurethanes, are industrially produced via step-growth polymerization reactions, such as polyadditions and polycondensations. Recent studies have demonstrated that click reactions,<sup>1</sup> such as azide-alkyne cycloadditions, thiol-ene additions, and Diels-Alder reactions, are also effective for the synthesis of polymers via step-growth polymerization.<sup>2-8</sup> Moreover, multicomponent reactions, such as the Ugi reaction and Kabachnik-Fields reaction, have been recently employed for polymerizations to introduce new types of structures into the main chain.<sup>9-13</sup> Extremely high efficiency and selectivity are important prerequisites to yield high-MW polymers via multicomponent reactions.

In the previous study in the Aoshima's laboratory on the cationic alternating copolymerization of vinyl ethers (VEs) and conjugated aldehydes, a cyclic trimer consisting of one VE and two aldehyde units was generated with high selectivity under optimized conditions (Scheme 1).<sup>14-16</sup> The alternating copolymerization preferentially proceeded in a controlled manner without generating cyclic trimers when  $\text{GaCl}_3$  was used as a Lewis acid catalyst in a nonpolar solvent such as toluene at  $-78^\circ\text{C}$ . However, the cyclic trimer was obtained as a byproduct using an inappropriate catalyst or solvent at higher temperatures. The substituents at the *para*-position of the conjugated aldehydes influenced the yield of the byproduct. A cyclic trimer was exclusively yielded in the reaction of isobutyl VE (IBVE) and benzaldehyde (BzA) using  $\text{EtAlCl}_2$  as a catalyst in toluene.

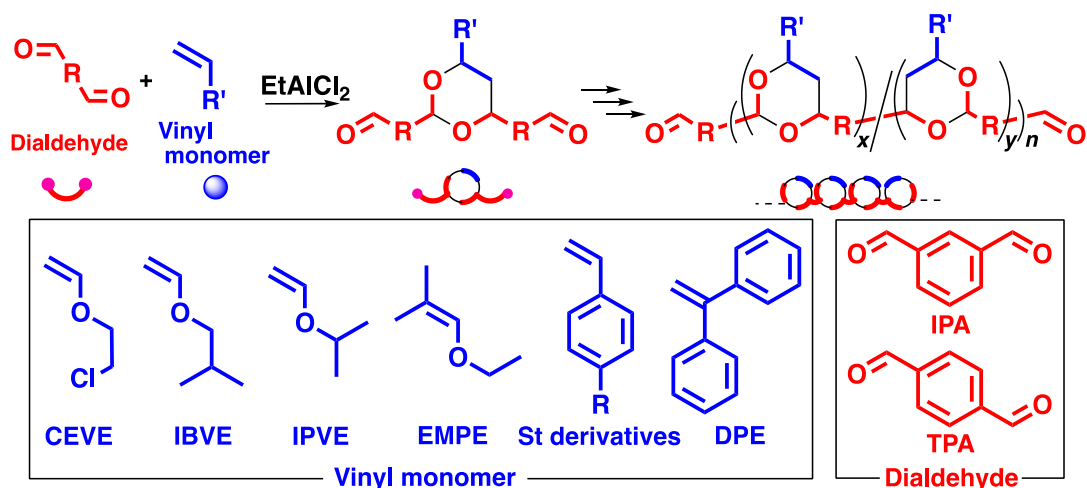


**Scheme 1.** The difference in the obtained products between two Lewis acids.

The selective cyclotrimerization reaction of vinyl compounds and conjugated aldehydes, known as the Prins cyclization,<sup>17</sup> is highly attractive as a bond-forming reaction for step-growth polymerization. Specifically, the use of dialdehydes instead of monoaldehydes for the reaction with VEs is expected to yield a cyclic trimer with two unreacted aldehyde moieties. Thus, the remaining reactive sites of the cyclic trimer will undergo subsequent cyclotrimerization with a VE molecule and an aldehyde moiety of the dialdehyde monomer or another cyclic trimer. Successive cyclotrimerization reactions among the monomers and generated cyclic trimers are expected to generate linear polymers with cyclic acetal structures in the main chain in a step-

growth manner. Due to acid lability of acetal moieties, obtained polymers are most likely degraded under acidic conditions. Moreover, various functional groups are potentially introduced into the side chains with the use of appropriate vinyl compounds. Additionally, the obtained poly(cyclic acetal)s are expected to have high glass transition temperatures ( $T_g$ s) and acid degradability. The rigid but degradable structure is highly attractive for use as functional materials. To the best of the author's knowledge, however, synthesis of polymers via cyclotrimerization of dialdehyde and vinyl monomer has not been reported although there have been many examples of the synthesis of polyacetals via methods such as acetalization of dialdehydes and polyols or transacetalization of diacetals.<sup>18</sup>

In this chapter, the polyaddition reactions of VEs with isophthalaldehyde (IPA) or terephthalaldehyde (TPA) via cyclotrimerization were examined to synthesize polymers with cyclic acetal structures in the main chain (Scheme 2). The appropriate conditions for selective cyclotrimerization were first investigated with a model reaction using a monofunctional aldehyde. The polyaddition reaction was subsequently conducted under the established conditions. Various VEs and conjugated dialdehydes were also polymerized via cyclotrimerization. Moreover, reactions using styrene (St) derivatives instead of VEs were examined for the polyaddition with IPA via cyclotrimerization.



**Scheme 2.** Polyaddition via cyclotrimerization of vinyl monomers and dialdehydes (compounds shown in squares are monomers used in this study).

## Experimental Section

### Materials

2-Chloroethyl VE (CEVE; TCI, >97.0%) was washed with a 10% aqueous sodium hydroxide solution and then water and was distilled twice under reduced pressure over calcium hydride. IBVE (TCI, >99.0%) and isopropyl VE (IPVE; Wako, >97.0%) were washed with a 10% aqueous sodium hydroxide solution and then water and were distilled twice over calcium hydride. *p*-Methoxystyrene (pMOS; Wako, >97.0%), *p*-methylstyrene (pMeSt; TCI, >96.0%), St (Wako, >99.0%), 1,1-diphenylethylene (DPE; TCI, >98.0%), and BzA (Wako, >98.0%) were distilled twice over calcium hydride under reduced pressure. IPA (TCI, >98%) and TPA (Nacalai Tesque, >98%) were recrystallized from heptane and dichloromethane/hexane, respectively; vacuum dried for more than 3 h; and then dried by azeotropy with toluene. Ethyl 2-methyl-1-propenyl ether (EMPE) was prepared from isobutyraldehyde diethyl acetal (TCI, >95.0%) according to a previous report<sup>19</sup> and then distilled twice over Na

before use. Tetrahydrofuran (THF; Wako, >99.5%) was distilled over calcium hydride and then lithium aluminum hydride. Ethyl acetate was distilled twice over calcium hydride. Commercially available  $\text{EtAlCl}_2$  (Wako, 1.0 M solution in hexane) and  $\text{SnCl}_4$  (Aldrich, 1.0 M solution in dichloromethane) were used without further purification. For  $\text{GaCl}_3$ , a stock solution in hexane was prepared from anhydrous  $\text{GaCl}_3$  (Aldrich, >99.999%). For  $\text{InCl}_3$ , a stock solution in ethyl acetate was prepared from anhydrous  $\text{InCl}_3$  (Strem, 99.999%). Dichloromethane (Wako, 99.0%) was dried by passage through solvent purification columns (Glass Counter). Hydrochloric acid (Nacalai Tesque) and 1,2-dimethoxyethane (Nacalai Tesque) for acid hydrolysis were used as received. All the chemicals except for dichloromethane, hydrochloric acid, and 1,2-dimethoxyethane were stored in brown ampules.

### Polymerization procedure

The following describes a typical polymerization procedure. A glass tube equipped with a three-way stopcock was dried using a heat gun (Ishizaki; PJ-206A; blow temperature of  $\sim 450^\circ\text{C}$ ) under dry nitrogen. Dichloromethane, THF, CEVE, and IPA were added successively into the tube using dry syringes. The polymerization was started by the addition of a prechilled  $\text{EtAlCl}_2$  solution (500 mM) in dichloromethane/hexane. After 4 h, the reaction was terminated with methanol containing a small amount of an aqueous ammonia solution. The quenched mixture was diluted with dichloromethane and washed with water. The volatiles were then removed under reduced pressure at  $50^\circ\text{C}$  to yield the polymer. The monomer conversion was determined by proton nuclear magnetic resonance ( $^1\text{H}$  NMR) analysis (for IPA and TPA) and gas chromatography (column packing material: PEG-20M-Uniport HP for CEVE, IBVE, IPVE, and EMPE; GL Sciences Inc.) using hexane as an internal standard. Specifically, the conversion of IPA was calculated based on the integral ratios of the peaks at 3.5–4.3, 5.6–6.4, and 10 ppm in the  $^1\text{H}$  NMR spectrum and the CEVE conversion determined by gas chromatography in the case of the polymerization of CEVE and IPA. The conversion of the formyl group was calculated from the integral ratios of the peaks at 5.6–6.4 and 10 ppm in the  $^1\text{H}$  NMR spectrum and the conversion of IPA.

### Acid hydrolysis

The acid hydrolysis of the polymers was conducted with 0.5 M aq. HCl in 1,2-dimethoxyethane at  $60^\circ\text{C}$  for 4 h. The quenched mixture was diluted with dichloromethane and successively washed with an aqueous sodium hydroxide solution and water. The volatiles were removed under atmospheric pressure at room temperature for several days or under reduced pressure for several hours.

### Characterization

The molecular weight distribution (MWD) of the polymers was measured by gel permeation chromatography (GPC) in chloroform at  $40^\circ\text{C}$  with polystyrene gel columns [TSKgel GMH<sub>HR</sub>-M  $\times$  2 (exclusive limit molecular weight =  $4 \times 10^6$ ; bead size = 5  $\mu\text{m}$ ; column size = 7.8 mm I.D.  $\times$  300 mm); flow rate = 1.0 mL min<sup>-1</sup>] connected to a Tosoh DP-8020 pump, a CO-8020 column oven, a UV-8020 ultraviolet detector, and an RI-8020 refractive-index detector. The weight-average molecular weight ( $M_w$ ) and the polydispersity ratio (weight-average molecular weight/number-average molecular weight [ $M_w/M_n$ ]) were calculated from the chromatograms with respect to 16 polystyrene standards (Tosoh;  $M_n = 577\text{--}1.09 \times 10^6$ ,  $M_w/M_n \leq 1.1$ ). NMR spectra were recorded using a JEOL JNM-ECA 500 (500.16 MHz for  $^1\text{H}$  and 125.77 MHz

for  $^{13}\text{C}$ ) spectrometer. Matrix-assisted laser desorption/ionization time-of-flight mass spectrometry (MALDI-TOF-MS) spectra were recorded using a Shimadzu/Kratos AXIMA-CFR spectrometer (linear mode; voltage: 20 kV; pressure  $< 1.9 \times 10^{-3}$  Pa) with dithranol as a matrix and sodium trifluoroacetate as an ion source. Electrospray ionization mass spectrometry (ESI-MS) spectra were recorded using an LTQ Orbitrap XL spectrometer (Thermo Scientific). Differential scanning calorimetry (DSC) was conducted with an EXSTAR-6000 calorimeter (Seiko Instruments Inc.). Thermal gravimetric analysis (TGA) was conducted with an STA 6000 apparatus (PerkinElmer Co.)

## Results and Discussion

### Cyclotrimerization of BzA and VEs in dichloromethane using Lewis acids

To achieve an efficient polyaddition reaction, the cyclotrimerization of one VE and two aldehyde units must proceed with high selectivity in a suitable solvent for polymerizations (dichloromethane). Thus, a model reaction was first conducted using BzA, a conjugated monoaldehyde, and various VEs in conjunction with a Lewis acid catalyst in the presence of THF in dichloromethane at 0 °C (Table 1). Among several VEs examined, CEVE underwent highly selective cyclotrimerization with BzA when  $\text{EtAlCl}_2$  was used as a catalyst (entry 1 in Table 1).

**Table 1.** Cyclotrimerization of BzA and various VEs using Lewis acid catalysts<sup>a</sup>

entry	catalyst	vinyl monomer	time	conv (%) <sup>b</sup>		cyclic trimer/ byproduct <sup>c</sup>
				vinyl monomer	BzA	
1	$\text{EtAlCl}_2$	CEVE	1 h	46	>99	>99/~0
2		IBVE	1 h	96	>99	35/65 <sup>d</sup>
3		IPVE	3 min	>99	>99	44/56 <sup>d</sup>
4	$\text{GaCl}_3$	CEVE	3 min	>99	95	53/47
5	$\text{InCl}_3$	CEVE	4 h	25	2	3/97
6	$\text{SnCl}_4$	CEVE	3 min	5	2	17/83
7	$\text{EtAlCl}_2$	pMeSt	1 h	14	0	0/100
8	$\text{GaCl}_3$	pMeSt	4 h	85	27	4/96
9		St	4 h	31	8	13/87
10		DPE	72 h	15	28	85/15
11		DPE (−78 °C)	24 h	36	73	>99/~0

<sup>a</sup>  $[\text{BzA}]_0 = 0.50$  (entries 1–6, 9, and 10), 0.20 (entries 7 and 8), or 0.40 (entry 11) M,  $[\text{vinyl monomer}]_0 = 0.50$  (entries 1–6, 9, and 10), 0.20 (entries 7 and 8), or 0.40 (entry 11) M,  $[\text{Lewis acid}]_0 = 50$  (entries 1–3 and 7), 2.0 (entries 4 and 6), 5.0 (entries 5, 8, 9, and 10), or 10 (entry 11) mM,  $[\text{THF}] = 1.0$  (entries 1–3) or 0 (entries 4–11) M, in dichloromethane at 0 (entries 1–10) or −78 (entry 11) °C. <sup>b</sup> Determined by gas chromatography and  $^1\text{H}$  NMR analysis of products. <sup>c</sup> Estimated by  $^1\text{H}$  NMR analysis of the obtained products. <sup>d</sup> The ratio of a cyclic trimer consisting of one VE and two BzA, a cyclic trimer consisting of two VE and two BzA, and other byproducts were 35/<27/>38 (entry 2) and 44/<9/>47 (entry 3). See Figures S2 and S3 for the detail.

The GPC curve of the product (Figure 1A) showed a unimodal peak with a very narrow MWD in the low-MW region. Moreover,  $^1\text{H}$  NMR (Figure 2A) and ESI-MS (Figure 1B) analyses revealed that a cyclic trimer consisting of one CEVE and two BzA units was exclusively produced. The product was composed of diastereomers as confirmed by the appearance of four singlet peaks at 5.7–6.3 ppm (peaks 2; 6.29, 6.25, 5.74, and 5.73 ppm), although all the signals could not be assigned to the diastereomers.<sup>20</sup> Unlike the case of CEVE, the reactions using IBVE or IPVE as a VE monomer generated byproducts, such as a VE homopolymer and a cyclic trimer consisting of two VE units and one aldehyde unit (entries 2 and 3 in Table 1), which was indicated by  $^1\text{H}$  NMR and ESI-MS (Figure S1–S3) analyses. These undesired reactions likely occurred due to the higher reactivity of the two VEs than that of CEVE.

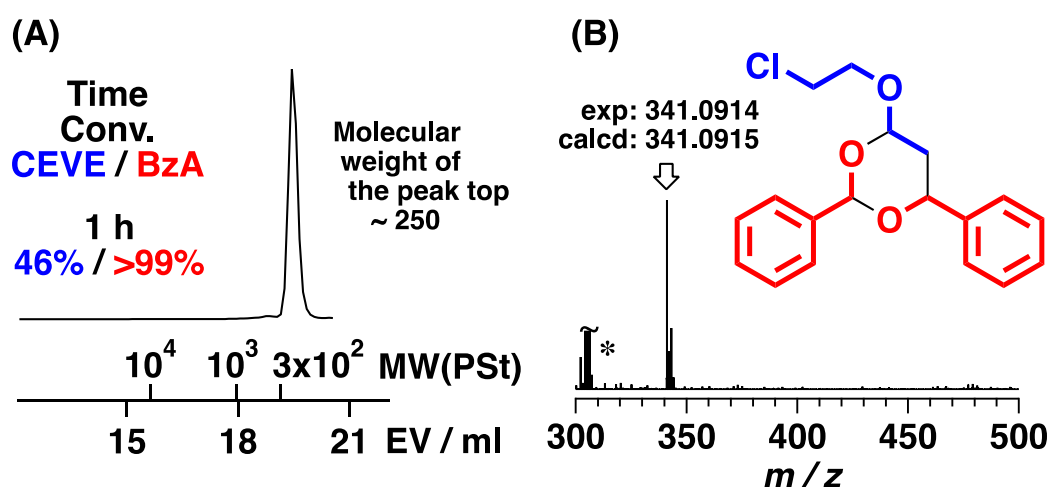


**Figure 1.** (A) MWD curve and (B) ESI-MS spectrum of the product obtained by the cyclotrimerization of CEVE and BzA ( $[\text{CEVE}]_0 = 0.50$  M,  $[\text{BzA}]_0 = 0.50$  M,  $[\text{EtAlCl}_2]_0 = 50$  mM,  $[\text{THF}] = 1.0$  M, in dichloromethane at 0 °C; entry 1 in Table 1; \* Contamination. The same signal was detected when solvents were analyzed).

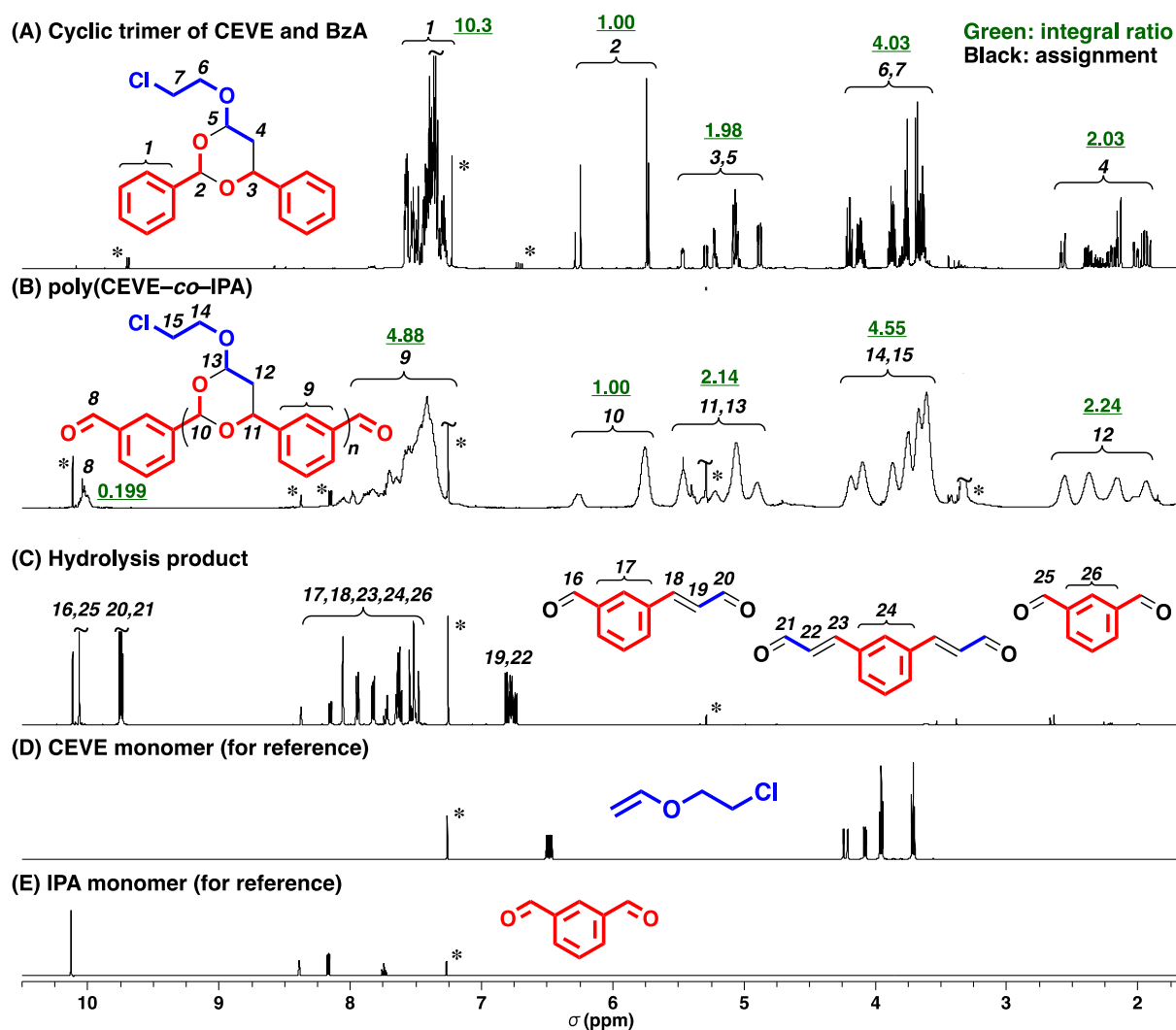
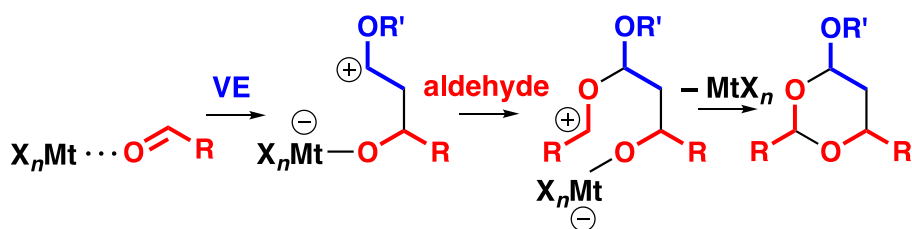


**Figure 2.**  $^1\text{H}$  NMR spectra of (A) the product obtained in the model reaction using CEVE and BzA (entry 1 in Table 1), (B) the product obtained by polyaddition of CEVE and IPA (entry 1 in Table 2), (C) its hydrolysis product, (D) CEVE monomer, and (E) IPA monomer (in  $\text{CDCl}_3$  at 30  $^\circ\text{C}$ ; \* solvents, residual monomer, or byproducts; number written in green: integral ratio). The assignments of the hydrolysis products are partly based on references 22 and 23.

An appropriate Lewis acid catalyst was also very important for the selective cyclotrimerization reaction. When  $\text{GaCl}_3$ ,  $\text{InCl}_3$ , or  $\text{SnCl}_4$  was used instead of  $\text{EtAlCl}_2$ , VE homopolymerization preferentially occurred, resulting in a decreased selectivity (entries 4-6). The first step of the cyclotrimerization reaction appears to be the coordination of the Lewis acid catalyst to the carbonyl oxygen of the aldehyde (Scheme 3). The generated carbocation reacts with a VE molecule and subsequently with an aldehyde, producing a carbocation that reacts with the oxygen atom coordinated by the Lewis acid catalyst to yield a cyclic trimer. Therefore,  $\text{EtAlCl}_2$ , which is a Lewis acid catalyst that exerts both a strong affinity for carbonyl groups and a low activity in cationic polymerization,<sup>21</sup> was chosen for the selective cyclotrimerization reaction.





**Scheme 3.** Postulated mechanism of cyclotrimerization.

### Polyaddition via the cyclotrimerization of CEVE and IPA

Based on the results of the model reaction, the polyaddition of CEVE and IPA, which contains two aldehyde units at the *meta* positions, was conducted using EtAlCl<sub>2</sub> as a Lewis acid catalyst in the presence of THF in dichloromethane at 0 °C. As shown in Figure 3A, both monomers were smoothly consumed to reach nearly quantitative conversion in 4 h, which resulted in the generation of a polymer with a unimodal MWD ( $M_w = 2.2 \times 10^3$ ,  $M_w/M_n = 1.77$ ; entry 1 in Table 2). Additionally, the MWD peaks of the products shifted to the high-MW region as the monomer conversion increased (Figure 3C). The upward increase in the  $M_w$  values in the latter stages of the polymerization (Figure 3B) suggests that the polymerization reaction proceeded by a step-growth mechanism. Theoretically, the MW potentially increases when the monomer conversion is increased. In addition, the conversion of the formyl group in IPA was lower than the IPA conversion but higher than the half of the IPA conversion, which indicates that monomer–monomer, monomer–oligomer (polymer), and oligomer (polymer)–oligomer (polymer) reactions occurred statistically. This is because both the conversion values will agree when chain-growth propagation occurs, while the conversion of the formyl group will be the half of the IPA conversion in ideal step-growth propagation.

**Table 2.** Polyaddition of various VEs and dialdehydes<sup>a</sup>

entry	VE	dialdehyde	time	conv (%) <sup>b</sup>		$M_w \times 10^{-3}$ <sup>c</sup>	$M_w/M_n$ <sup>c</sup>	cyclic trimerization/ side reaction <sup>d</sup>
				VE	dialdehyde			
1	CEVE	IPA	4 h	96	95	2.2	1.77	90/10
2		TPA	4 h	90	85	3.6	2.39	87/13
3	IBVE	IPA	1 h	>99	95	1.7	2.09	63/37
4	IPVE	IPA	15 min	>99	84	1.0	1.75	42/58
5	EMPE	IPA	4 h	>99	>99	3.1	2.21	95/5

<sup>a</sup> [VE]<sub>0</sub> = 0.50 M, [dialdehyde]<sub>0</sub> = 0.50 M, [EtAlCl<sub>2</sub>]<sub>0</sub> = 50 mM, [THF] = 1.0 M (entries 1–4) or [ethyl acetate] = 1.0 M (entry 5), in dichloromethane at 0 °C. <sup>b</sup> Determined by gas chromatography and <sup>1</sup>H NMR analysis of products. <sup>c</sup> Determined by GPC (polystyrene standards). <sup>d</sup> Determined by <sup>1</sup>H NMR analysis.

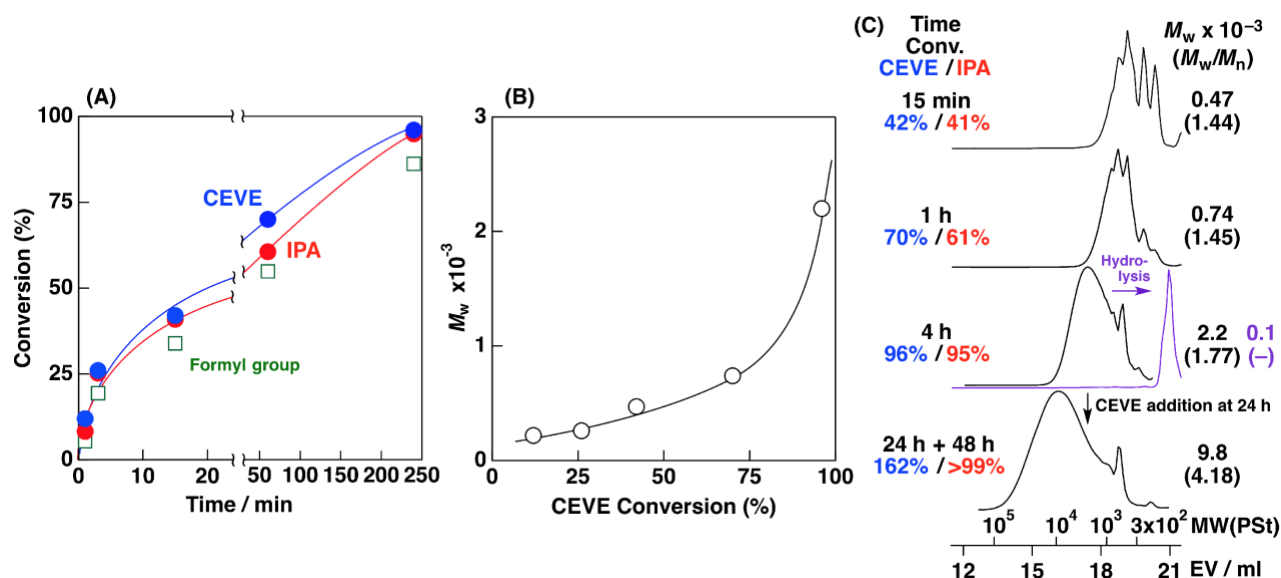


**Figure 3.** (A) Time–conversion curves of polyaddition of CEVE and IPA, (B)  $M_w$  values, and (C) MWD curves of the obtained products ( $[IPA]_0 = 0.50$  M,  $[CEVE]_0 = 0.50$  M,  $[CEVE]_{added} = 0.25$  M for the bottom curve in (C),  $[EtAlCl_2]_0 = 50$  mM,  $[THF] = 1.0$  M, in dichloromethane at 0 °C; entry 1 in Table 2).

The  $^1H$  NMR spectrum of the obtained polymer (Figure 2B) exhibited peaks assigned to cyclic acetal structures, which indicated that the polyaddition reaction successfully proceeded via the successive cyclotrimerization. The peaks were assigned by comparing the spectra of the polymer of CEVE and IPA and the model cyclic trimer of CEVE and BzA. For example, the peaks at 5.7 and 6.3 ppm were assigned to the protons of cyclic acetal structures. These acetal peaks appeared at different positions because the products were composed of a mixture of diastereomers. The integral ratios of all the peaks supported that a polymer with cyclic acetal structures in the main chain was obtained. Additionally, the number-average degree of polymerization was determined to be 10 from the peak integral ratio of the methine protons of the cyclic acetal structures (peak 10) and the aldehyde protons (peak 8) at the polymer chain ends. This value was consistent with the MW estimated from GPC using polystyrene calibration. It should be noted here that the  $^1H$  NMR spectra indicates the signals due to the remaining aldehyde moiety at the polymer chain ends. Indeed, MWD curves of the products shifted to the high-MW region when the subsequent polyaddition proceeded by the sequential addition of a fresh supply of CEVE monomer at the later stages of the polymerization (the bottom curve in Figure 3C)

MALDI-TOF-MS analysis of the product also confirmed that the polymerization occurred via the cyclotrimerization reactions (Figure 4). A single series of peaks were mainly observed at constant intervals of  $m/z = 240$ , which corresponds to the mass value of CEVE and IPA units. Furthermore, the  $m/z$  values of the series are consistent with the mass values of the structures with an  $\alpha$ - and  $\omega$ -ends derived from an  $O=CH-C_6H_5$  moieties.

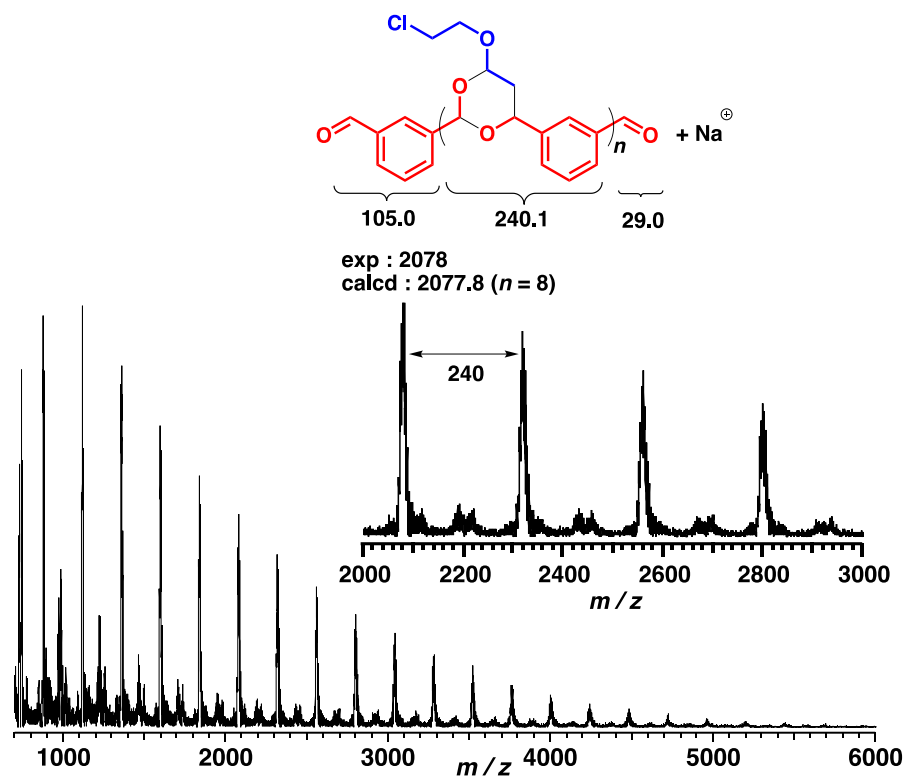
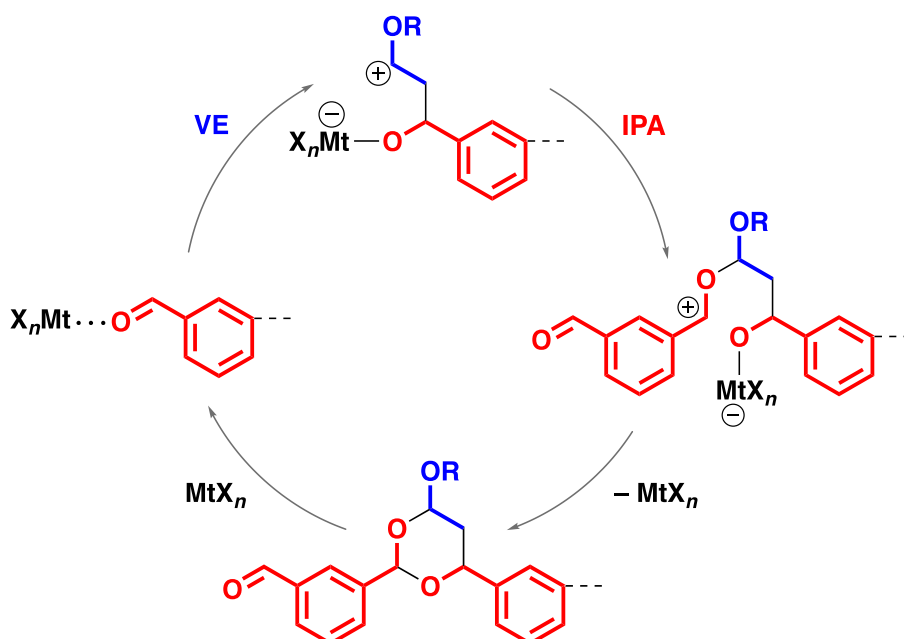


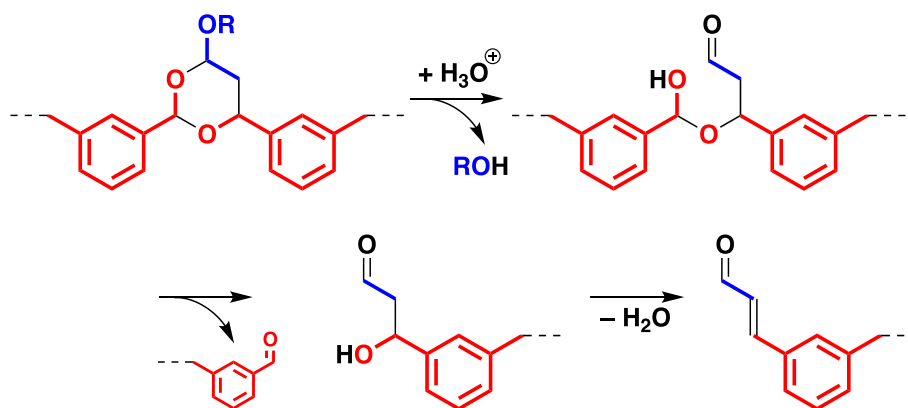
**Figure 4.** MALDI-TOF-MS spectrum of the polymer obtained by polyaddition via cyclotrimerization of CEVE and IPA {polymerization conditions:  $[\text{CEVE}]_0 = 0.50 \text{ M}$ ,  $[\text{IPA}]_0 = 0.50 \text{ M}$ ,  $[\text{EtAlCl}_2]_0 = 50 \text{ mM}$ ,  $[\text{THF}] = 1.0 \text{ M}$ , in dichloromethane at  $0^\circ\text{C}$ ;  $M_w(\text{GPC}) = 1.8 \times 10^3$ }.

The polymerization mechanisms are explained as follows. First, the cyclotrimerization of one VE and two IPA molecules starts through the coordination of the Lewis acid catalyst to the carbonyl oxygen in a manner similar to the model reaction demonstrated above (Scheme 3). Unlike the cyclic trimer obtained using BzA, however, the cyclic trimer consisting of one VE and two IPA units has two remaining aldehyde moieties. Thus, the cyclotrimerization subsequently occurs through the aldehyde moiety of the cyclic trimer, a VE, and the aldehyde moiety of either an IPA monomer, another cyclic trimer, or a poly(cyclic trimer). As an example, the reaction through an IPA monomer, a VE monomer, and the aldehyde moiety at the chain end of a poly(cyclic trimer) is shown in Scheme 4. Such cyclotrimerization reactions continuously occur to produce a polymer with cyclic acetal structures in the main chain until all VE monomers are consumed. The formation of a thermodynamically stable six-membered cyclic acetal structure is likely the driving force of the cyclotrimerization. Indeed, the polyaddition proceeded at a relative high temperature ( $0^\circ\text{C}$ ) unlike the case of the cationic alternating copolymerization of VEs and conjugate aldehydes. The latter polymerization must be conducted at a low temperature, such as  $-78^\circ\text{C}$ , due to the low ceiling temperature associated with the stability of the linear acetal structures in the main chain.



**Scheme 4.** Plausible reaction mechanism for the polyaddition of CEVE and IPA using a Lewis acid catalyst.

The polymer of CEVE and IPA is susceptible to acid due to the acid lability of the acetal structures in the main chain, while this polymer is stable under neutral or basic conditions. Indeed, the polymer was hydrolyzed under acidic conditions because of the degradation of the cyclic acetal structures (Scheme 5). After hydrolysis, the MWD curve clearly shifted to the low-MW region (the purple curve in Figure 3C). The  $^1\text{H}$  NMR spectrum of the hydrolysis product (Figure 2C) contained sharp peaks assigned to the structures of IPA and conjugated dialdehydes that have two extra carbon atoms between the benzene ring and the aldehyde moiety.<sup>22,23</sup> Decomposition products derived from CEVE moieties were most likely removed during the purification procedure.



**Scheme 5.** One possible pathway of acid hydrolysis reaction of the polymer.

#### Polyaddition via the cyclotrimerization of various VEs and dialdehydes

The polyaddition behavior was significantly affected by the reactivity of the VEs. A highly reactive VE was unsuitable for the efficient polyaddition via exclusive cyclotrimerization in dichloromethane. When IBVE or IPVE, which are more reactive than CEVE, were used for the polymerization with IPA, both cyclotrimerization and VE homopolymerization occurred to yield complicated mixtures (entries 3 and 4 in

Table 2; Figure S2 and S3). Additionally, the cyclotrimerization of two VE monomers and one IPA monomer occurred in an analogous manner to the model reaction, which generated a cyclic acetal structure with one aldehyde moiety. This undesired structure functioned not as a monomer but as a terminator in the polyaddition because no aldehyde moieties remained after the cyclic acetal structure with one aldehyde moiety had been consumed via cyclotrimerization.

VE monomers with low reactivities were indispensable for polyaddition reactions to occur without undesired reactions, such as homopolymerization of the VEs. Notably, EMPE, which is a  $\beta,\beta$ -dimethyl VE that does not homopolymerize<sup>24,25</sup> nor copolymerize with aromatic aldehydes,<sup>16</sup> was found to undergo the polyaddition with IPA via cyclotrimerization. Both EMPE and IPA were smoothly consumed, yielding a polymer with cyclic acetal structures in the main chain, under conditions similar to those for the polyaddition using CEVE (entry 5 in Table 2; Figure 5). The formation of a six-membered cyclic acetal structure with two aldehyde moieties likely compensated for the steric repulsion derived from the dimethyl groups. To the best of the author's knowledge, this is the first example of a polymerization using EMPE as a monomer.

TPA, the *para*-disubstituted counterpart of IPA, was also successfully polymerized with CEVE via cyclotrimerization. The polyaddition using TPA generated a polymer with cyclic acetal structures in the main chain (entry 2 in Table 2) under conditions similar to those for IPA. Polyaddition of TPA with EMPE also proceeded successfully, which yielded a product similar to that obtained by the polymerization of IPA and EMPE.

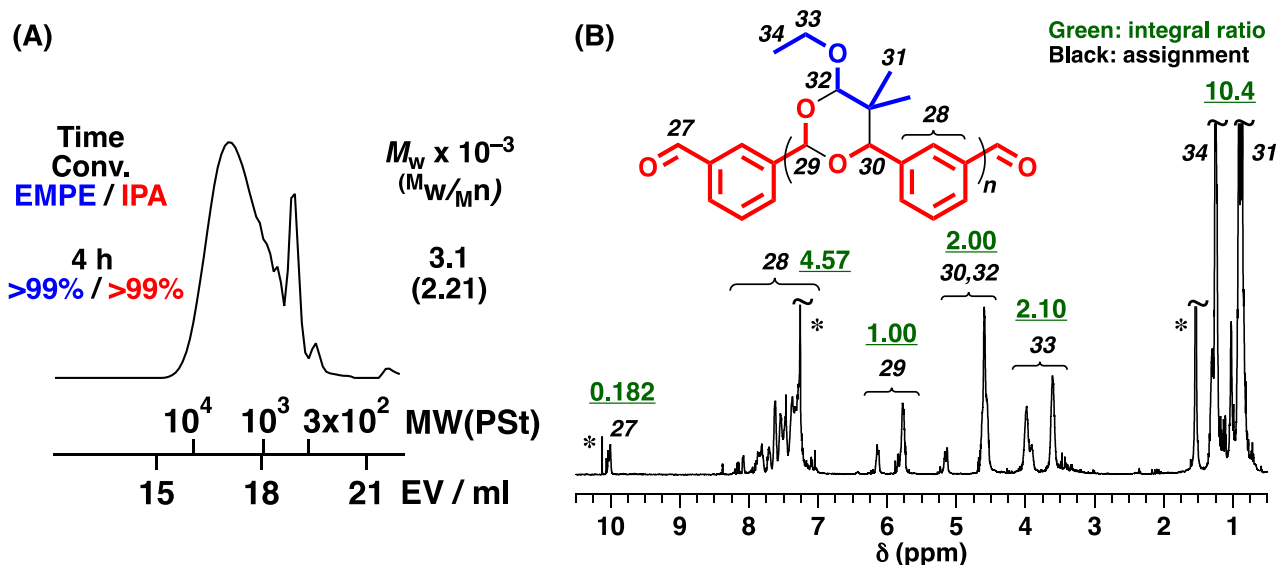


**Figure 5.** (A) MWD curve and (B)  $^1\text{H}$  NMR spectrum (in  $\text{CDCl}_3$  at 30 °C) of the product obtained by the polyaddition of EMPE and IPA (entry 5 in Table 2;  $[\text{EMPE}]_0 = 0.50$  M,  $[\text{IPA}]_0 = 0.50$  M,  $[\text{EtAlCl}_2]_0 = 50$  mM,  $[\text{ethyl acetate}] = 1.0$  M, in dichloromethane at 0 °C; \* solvent, residual monomer, or water; number written in green: integral ratio).

### Cyclotrimerization of *St* derivatives and BzA

*St* derivatives can undergo cyclotrimerizations with conjugated aldehydes in a manner similar to VEs. To explore the polyaddition reactions using *St* derivatives, model reactions were conducted using BzA and various *St* derivatives. pMOS, a highly reactive *St* derivative in cationic polymerization because of the large electron-donating ability of the *p*-methoxy group, was first employed for the reaction with BzA. However, only a homopolymer of pMOS was obtained from the reactions using various Lewis acid catalysts in dichloromethane, as confirmed by  $^1\text{H}$  NMR analysis. For pMeSt, which is less reactive than pMOS, no cyclic trimers were obtained using  $\text{EtAlCl}_2$  (entry 7 in Table 1), the most suitable Lewis acid catalyst for the cyclotrimerization of VEs and BzA. In contrast, the reaction using  $\text{GaCl}_3$  produced a mixture composed of a pMeSt homopolymer and a cyclic trimer of one pMeSt and two BzA units (entry 8 in Table 1). Moreover, *St*, which has a lower reactivity than pMeSt, underwent cyclotrimerization in a higher ratio (entry 9 in Table 1).

The above results indicate that less reactive *St* derivatives are efficient for the cyclotrimerization with conjugated aldehydes. In fact, DPE, which is not homopolymerized by any polymerization mechanisms, was demonstrated to be highly efficient for the selective cyclotrimerization. The product obtained from the reaction with BzA at 0 °C exhibited a unimodal, very sharp peak in the low-MW region on the MWD curve (entry 10 in Table 1). However,  $^1\text{H}$  NMR analysis suggested that 1,1,3,5,5-pentaphenylpenta-1,4-diene was partly generated as a byproduct. This compound was reported to be generated from DPE and BzA under acidic conditions.<sup>26,27</sup> Importantly, this side reaction was suppressed when the reaction of DPE and BzA was conducted at -78 °C (entry 11 in Table 1).  $^1\text{H}$  NMR and ESI-MS analyses (Figure 6B and C) suggested that a cyclic trimer consisting of one DPE and two BzA units was generated quantitatively (cyclotrimerization/side reaction = 100/0).

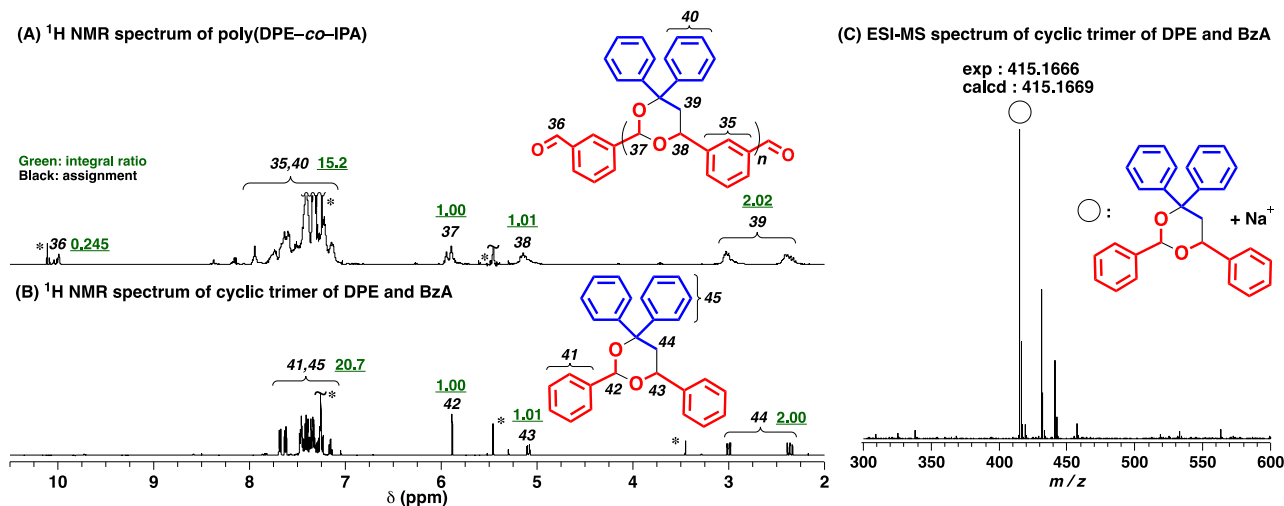


**Figure 6.**  $^1\text{H}$  NMR spectra of the products obtained by (A) polyaddition of DPE and IPA (entry 3 in Table 3) and (B) the model reaction using DPE and BzA (entry 11 in Table 1) and (C) ESI-MS spectrum of cyclic trimer of DPE and BzA (in  $\text{CDCl}_3$  at 30 °C; \* solvents, residual monomer, etc.; number written in green: integral ratio).

Polyaddition via the cyclotrimerization of DPE and IPA

Based on the model reactions demonstrated above, the polyaddition of DPE and IPA was conducted using  $\text{GaCl}_3$  as a Lewis acid catalyst in dichloromethane. At 0 °C, only oligomers were obtained (entry 1 in Table 3) because a similar side reaction to that in the cyclotrimerization of DPE and BzA occurred and/or the reaction likely had a relatively low ceiling temperature derived from the steric repulsion of DPE. Thus, the polymerization was carried out at a lower temperature (entries 2 and 3). As a result, the reaction at –78 °C successfully proceeded via cyclotrimerization and produced a polymer (entry 3 in Table 3;  $M_w = 2.3 \times 10^3$ ,  $M_w/M_n = 1.65$ ). The MWD peaks of the products shifted to the higher-MW region as the monomer conversion increased (Figure 7A). The  $^1\text{H}$  NMR spectrum of the obtained polymer (Figure 6A) contained peaks assigned to polymers with cyclic acetal structures in the main chain, which was also supported by the comparison with the spectrum of a cyclic trimer of DPE and BzA (Figure 6B). The degree of polymerization was calculated to be approximately 8 from peaks 36 and 37. TPA was also employed for the copolymerization with DPE instead of IPA. The copolymerization proceeded via cyclotrimerization (entry 4 in Table 3), which afforded a polymer with an  $M_w$  value as high as  $9.1 \times 10^3$  (Figure 7B).

**Table 3.** Polyaddition via cyclotrimerization of DPE and IPA using  $\text{GaCl}_3$ <sup>a</sup>

entry	DPE (M)	dialdehydes (M)	temp. (°C)	time (h)	conv (%) <sup>b</sup>		$M_w \times 10^{-3}$ <sup>c</sup>	$M_w/M_n$ <sup>c</sup>
					DPE	IPA		
1	0.40	IPA	0	96	49	86	0.4	1.05
2	0.40	IPA	–30	24	77	>99	1.3	1.43
3	0.40	IPA	–78	72	50	>99	2.3	1.65
4	0.40	TPA	–78	96	46	99	9.1	2.47

<sup>a</sup>  $[\text{GaCl}_3]_0 = 5.0$  (entries 1–3) or 10 (entry 4) mM, in dichloromethane. <sup>b</sup> Determined by  $^1\text{H}$  NMR analysis of products. <sup>c</sup> Determined by GPC (polystyrene standards).

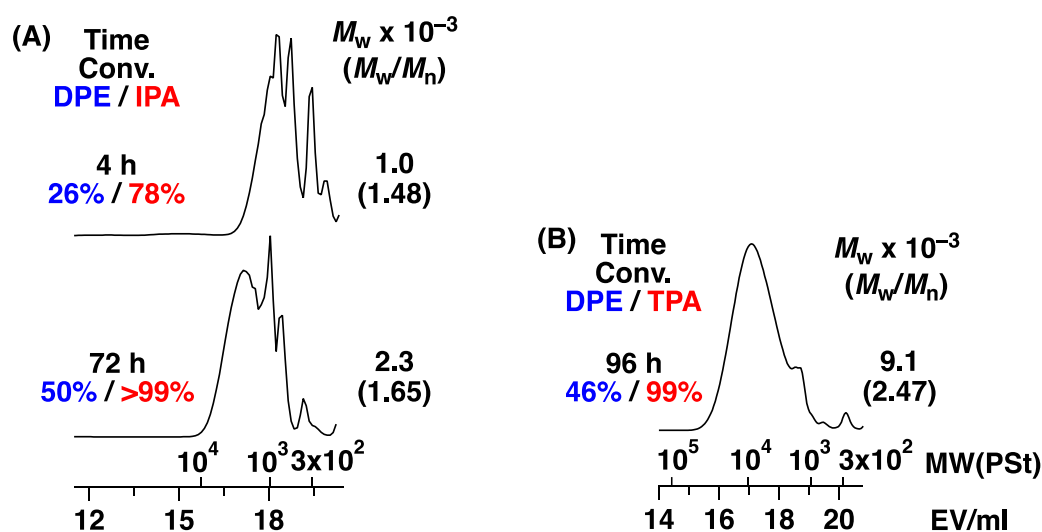


**Figure 7.** MWD curves of the products obtained by polyaddition via cyclotrimerization of DPE with (A) IPA or (B) TPA (entries 3 and 4 in Table 3).

### Thermal properties of the polymers

The poly(cyclic acetal)s obtained by the cyclotrimerization of vinyl monomers and dialdehydes exhibited superior thermal properties to the polyacetals produced by the alternating copolymerization of VEs and conjugated aldehydes (Table 4). DSC measurements revealed that  $T_g$  of poly(CEVE-*co*-IPA) was 56 °C (entry 1 in Table 4), which is higher than that of alternating poly(CEVE-*alt*-BzA)<sup>16</sup> (38 °C; entry 4). The higher  $T_g$  value was likely due to the cyclic acetal structures in the main chain. Furthermore, poly(DPE-*co*-IPA) had a very high  $T_g$  (193 °C; entry 2) likely because of the phenyl rings on the cyclic acetal structures. The 5% weight loss temperature ( $T_{5\%}$ ) value of poly(DPE-*co*-IPA) was also higher than those of poly(CEVE-*co*-IPA) and poly(CEVE-*alt*-BzA). Moreover, poly(DPE-*co*-TPA) had higher  $T_g$  value than poly(DPE-*co*-IPA), probably due to the symmetrical structures (entry 3).

**Table 4.**  $T_g$  and  $T_{5\%}$  values of polymers with cyclic or acyclic acetal in the main chain

entry	polymer	$M_w \times 10^{-3}$	$M_w/M_n$	$T_g$ (°C) <sup>a</sup>	$T_{5\%}$ (°C) <sup>b</sup>
1	poly(CEVE- <i>co</i> -IPA)	3.3	1.92	56	192
2	poly(DPE- <i>co</i> -IPA)	2.3	1.42	193	309
3	poly(DPE- <i>co</i> -TPA)	7.9	2.65	262	304
4 <sup>c</sup>	poly(CEVE- <i>alt</i> -BzA)	17.4	1.16	38	237

<sup>a</sup> The heating and cooling rates were 10 °C/min. The  $T_g$  values were determined by the second heating scan. <sup>b</sup> The 5% weight-loss temperature determined by TGA. <sup>c</sup> Reference 16.

### Conclusion

A polymer with cyclic acetal structures in the main chain was successfully produced via the successive cyclotrimerization of two conjugated dialdehydes and one vinyl monomer using a Lewis acid catalyst. The use of a suitable Lewis acid catalyst and vinyl monomers with appropriate reactivities was critical for the selective cyclotrimerization without homopolymerization reactions of vinyl monomers. The poly(cyclic acetal)s obtained via the cyclotrimerization reactions exhibited acid degradability and good thermal properties compared to alternating poly(CEVE-*alt*-BzA). Particularly, poly(DPE-*co*-IPA) and poly(DPE-*co*-TPA), which have three aromatic rings in each repeating unit, exhibited very high  $T_g$  values.

### References

1. Kolb, H. C.; Finn, M. G.; Sharpless, K. B. *Angew. Chem. Int. Ed.* **2001**, *40*, 2004–2021.
2. Espeel, P.; Du Prez, F. E. *Macromolecules* **2015**, *48*, 2–14.
3. Goodall, G. W.; Hayes, W. *Chem. Soc. Rev.* **2006**, *35*, 280–312.
4. Fournier, D.; Hoogenboom, R.; Schubert, U. S. *Chem. Soc. Rev.* **2007**, *36*, 1369–1380.
5. Binder, W. H.; Sachsenhofer, R. *Macromol. Rapid. Commun.* **2007**, *28*, 15–54.
6. Qin, A.; Lam, J. W. Y.; Tang, B. Z. *Chem. Soc. Rev.* **2010**, *39*, 2522–2544.
7. Qin, A.; Lam, J. W. Y.; Tang, B. Z. *Macromolecules* **2010**, *43*, 8693–8702.
8. Delaittre, G.; Guimard, N. K.; Barner-Kowollik, C. *Acc. Chem. Res.* **2015**, *48*, 1296–1307.
9. Moldenhauer, F.; Kakuchi, R.; Theato, P. *ACS Macro Lett.* **2016**, *5*, 10–13.



10. Yang, B.; Zhao, Y.; Wei, Y.; Fu, C.; Tao, L. *Polym. Chem.* **2015**, *6*, 8233–8239.
11. Solleder, S. C.; Meier, M. A. R. *Angew. Chem. Int. Ed.* **2014**, *53*, 711–714.
12. Oelmann, S.; Solleder, S. C.; Meier, M. A. R. *Polym. Chem.* **2016**, *7*, 1857–1860.
13. Deng, H.; Han, T.; Zhao, E.; Kwok, R. T. K.; Lam, J. W. Y.; Tang, B. Z. *Macromolecules* **2016**, *49*, 5475–5483.
14. Ishido, Y.; Aburaki, R.; Kanaoka, S.; Aoshima, S. *J. Polym. Sci., Part A: Polym. Chem.* **2010**, *48*, 1838–1843.
15. Ishido, Y.; Aburaki, R.; Kanaoka, S.; Aoshima, S. *Macromolecules* **2010**, *43*, 3141–3144.
16. Ishido, Y.; Kanazawa, A.; Kanaoka, S.; Aoshima, S. *J. Polym. Sci., Part A: Polym. Chem.* **2014**, *52*, 1334–1343.
17. Arundale, E.; Mikeska, L. A. *Chem. Rev.* **1952**, *51*, 505–555.
18. Hufendiek, A.; Lingier, S.; Du Prez, F. E. *Polym. Chem.* **2019**, *10*, 9–33.
19. Mizote, A.; Kusudo, S.; Higashimura, T.; Okamura, S. *J. Polym. Sci. Part A-1: Polym. Chem.* **1967**, *5*, 1727–1739.
20. Hoffmann, R.; Brückner, R. *Chem. Ber.* **1992**, *125*, 1471–1484.
21. Aoshima, S.; Kanaoka, S. *Chem. Rev.* **2009**, *109*, 5245–5287.
22. Battistuzzi, G.; Cacchi, S.; Fabrizi, G. *Org. Lett.* **2003**, *5*, 777–780.
23. Michels, H.-P.; Nieger, M.; Vögtle, F. *Chem. Ber.* **1994**, *127*, 1167–1170.
24. Okuyama, T.; Fueno, T.; Furukawa, J.; Uyeo, K. *J. Polym. Sci. Part A-1: Polym. Chem.* **1968**, *6*, 1001–1007.
25. Nuyken, O.; Raether, R. B.; Spindler, C. E. *Macromol. Chem. Phys.* **1998**, *199*, 191–196.
26. Jones, D. W. *J. Chem. Soc. C* **1966**, 1026–1028.
27. Qian, B.; Zhang, G.; Ding, Y.; Huang, H. *Chem. Commun.* **2013**, *49*, 9839–9841.

### Supporting Information

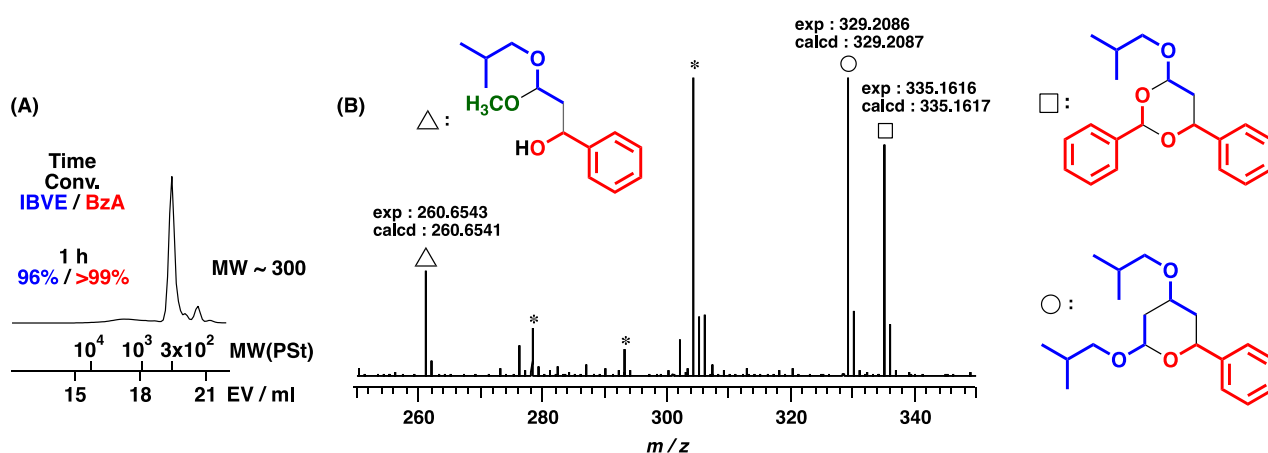
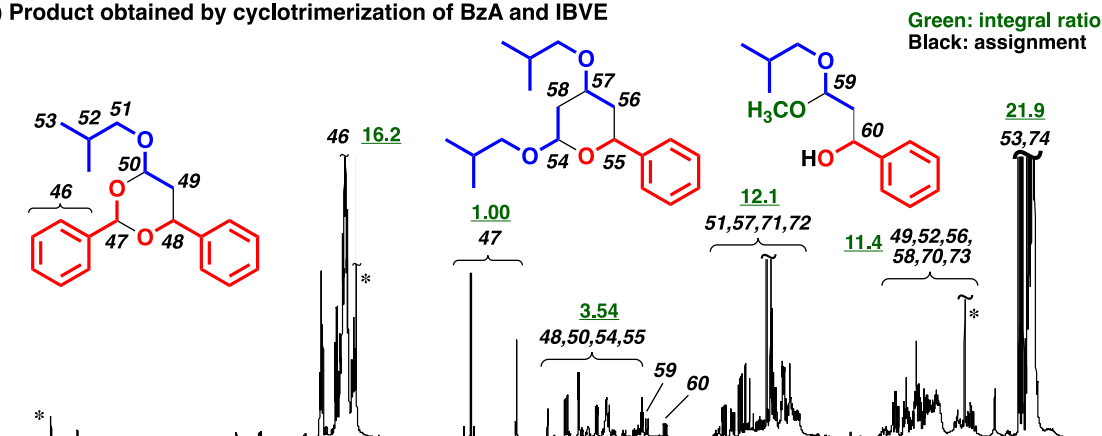
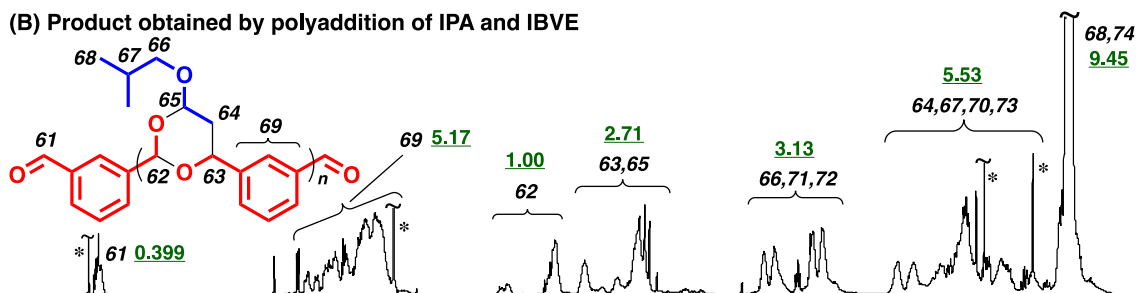


**Figure S1.** (A) MWD curve and (B) ESI-MS spectrum of the product obtained by the reaction of IBVE and BzA (entry 2 in Table 1).

(A) Product obtained by cyclotrimerization of BzA and IBVE



(B) Product obtained by polyaddition of IPA and IBVE



(C) IBVE homopolymer [for comparison]

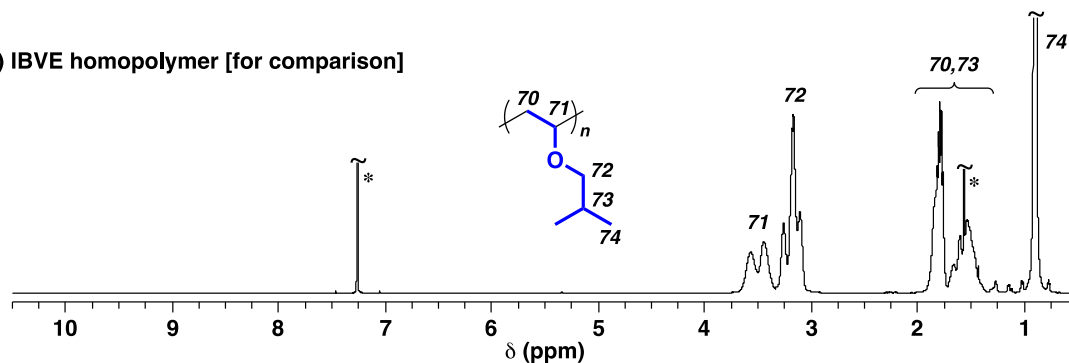


**Figure S2.**  $^1\text{H}$  NMR spectra of (A) the product obtained by the cyclotrimerization of BzA and IBVE (entry 2 in Table 1), (B) the product obtained by polymerization of IPA and IBVE (entry 3 in Table 2), and (C) IBVE homopolymer (\* solvent, residual monomer, water, etc.; number written in green: integral ratio).

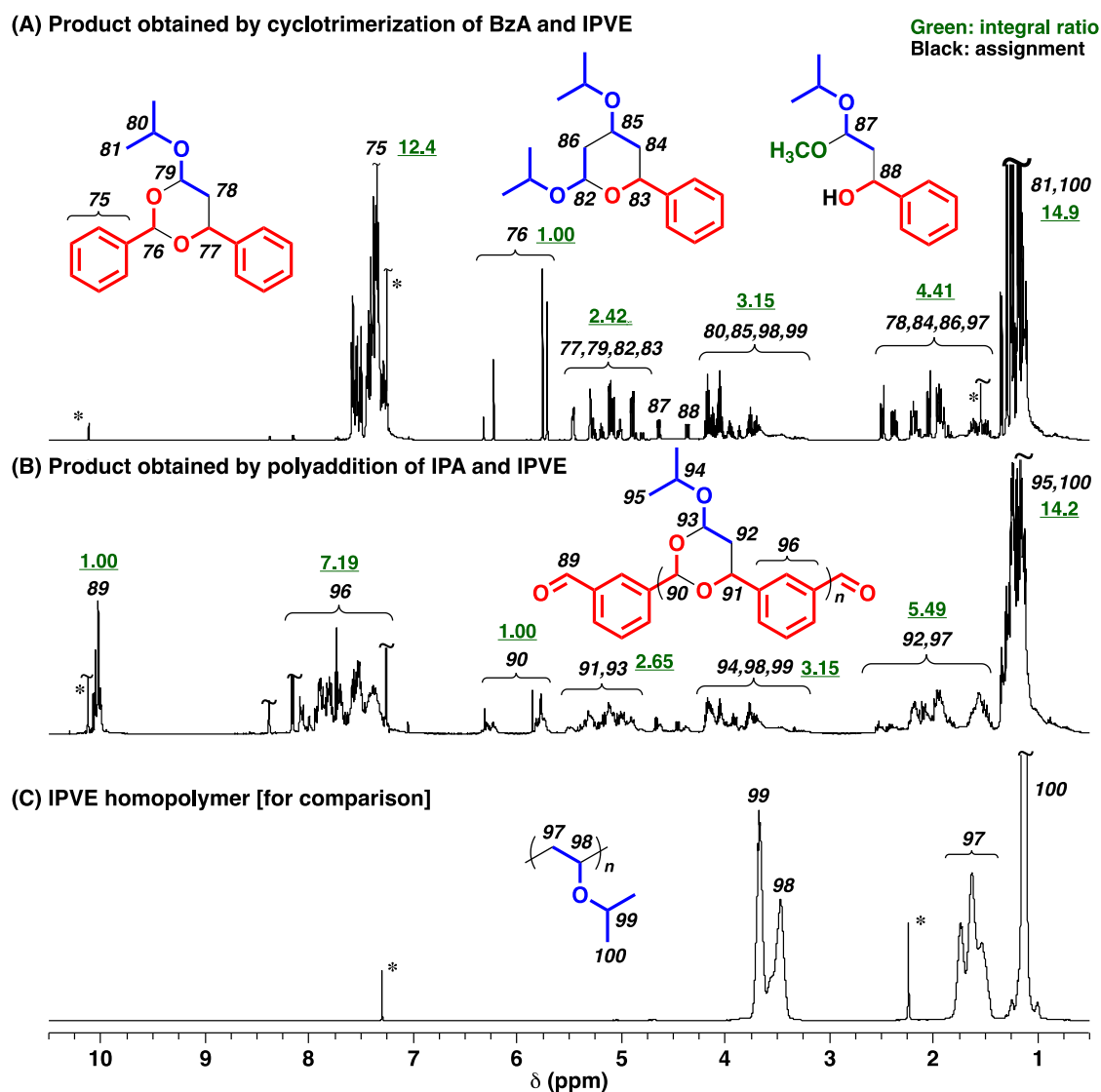


**Figure S3.**  $^1\text{H}$  NMR spectra of (A) the product obtained by the cyclotrimerization of BzA and IPVE (entry 3 in Table 1), (B) the product obtained by polymerization of IPA and IPVE (entry 4 in Table 2), and (C) IPVE homopolymer (\* solvent, residual monomer, or water; number written in green: integral ratio).

**Notes for Figures S2 and S3:**

The ratios of a cyclic trimer consisting of two BzA and one VE, a cyclic trimer consisting of one BzA and two VE, and other byproducts, which are listed in Table 1, were calculated from the integral ratios of peaks 47, 48, 50, 53, 54, 55, and 74 for IBVE (Figure S2) and peaks 76, 77, 79, 81, 82, 83 and 100 for IPVE (Figure S3). The ratio of products other than the cyclic trimers was standardized based on the number of IPVE units (e.g., the ratio is 1/1/8 when equal amounts of a cyclic trimer consisting of two BzA and one VE, a cyclic trimer consisting of one BzA and two VE, and a homopolymer composed of 8 units of IPVE are generated).

### *Chapter 3*

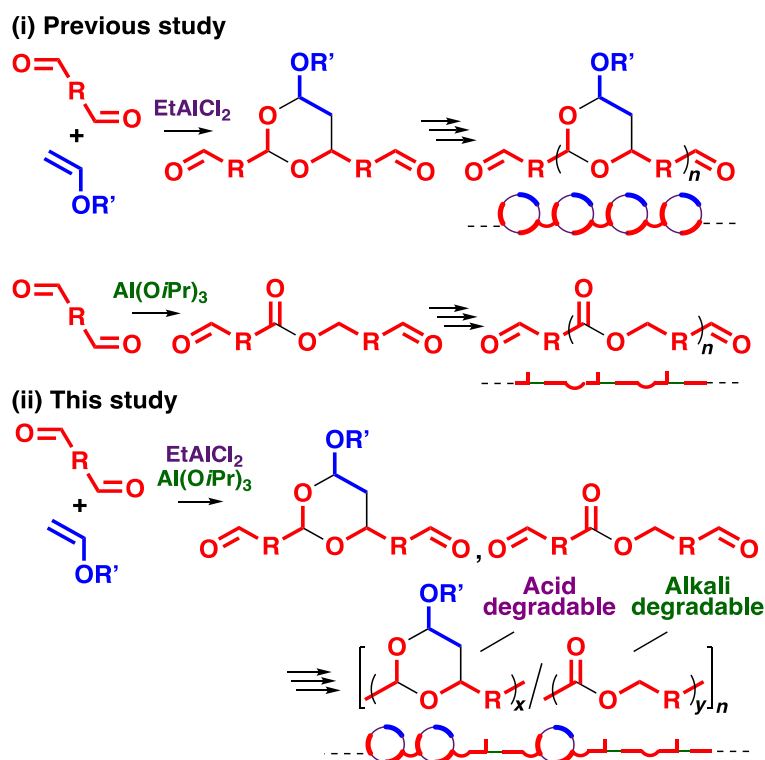
## **Tandem polymerization consisting of cyclotrimerization and the Tishchenko reaction: synthesis of acid- and alkali-degradable polymers with cyclic acetal and ester structures in the main chain**

### **Introduction**

A selective organic reaction is an indispensable tool for the synthesis of polymers with functional groups in the main chain via polyadditions and polycondensations. These polymers exert valuable functionalities that cannot be achieved by vinyl polymers with only carbon–carbon bonds in the main chain. For example, polyesters, polyamides, and polyurethanes, which play important roles in both dairy life and industries, are generally produced via step-growth polymerization reactions. Specifically, the utilization of novel organic reactions for a polymerization protocol enables the generation of a polymer inaccessible by conventional synthetic approaches. In fact, multicomponent reactions, such as the Ugi reaction and the Kabachnik–Fields reaction,<sup>1-5</sup> and tandem reactions have been recently applied in polymer chemistry as bond-forming reactions.<sup>6-11</sup> An important key to obtaining a high molecular weight (MW) polymer is the enhancement of the selectivity of the reactions.

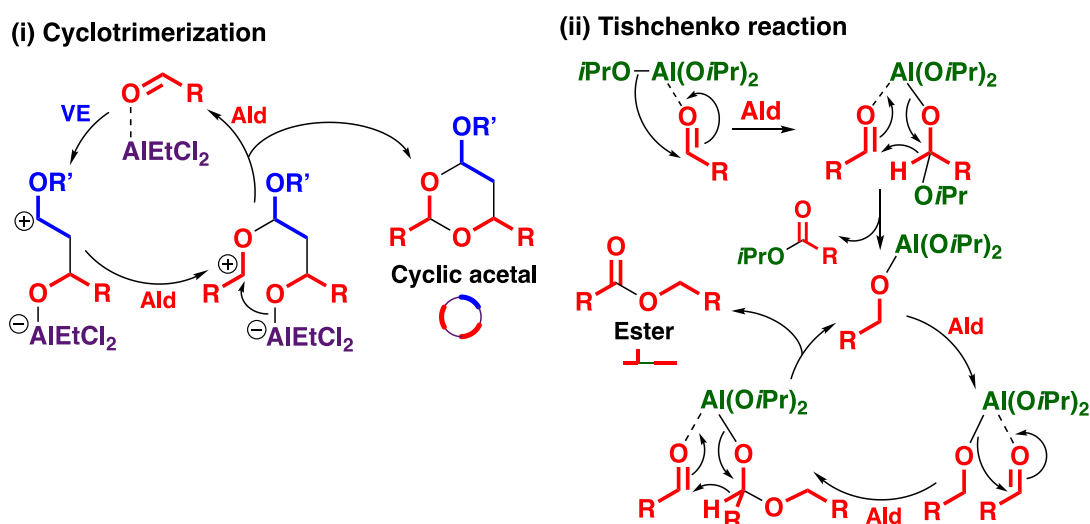
An advantage of tandem polymerization is that a complicated and well-defined polymer, which is difficult to obtain by other methods, is available via direct and simplified synthetic preparation without the additional time and yield losses associated with isolation and purification. A fundamental strategy for the construction of a tandem polymerization system is to design a catalyst that can simultaneously activate multiple reactions.<sup>12-14</sup> A synthetic approach using a tandem catalyst can combine polymerization reactions, such as insertion polymerization, radical polymerization, and cationic polymerization, and organic chemistry, such as Cu-catalyzed azide-alkyne cycloaddition and Diels-Alder reaction.<sup>15-18</sup> Specifically, when two different reactions occur through the same intermediate to form a polymer backbone, a polymer with different structures in the main chain is generated.<sup>8-10</sup>

For the construction of a novel tandem polymerization system,<sup>19-21</sup> the author has focused on Prins-type cycloaddition and the Tishchenko reaction, which are reactions involving aldehydes that yield a cyclic acetal and an ester, respectively.<sup>22-28</sup> These reactions have been individually employed as bond-forming reactions for polymer synthesis because these reactions proceed with high selectivity under appropriate conditions (Scheme 1 (i)).<sup>29-33</sup> Both reactions occur via the same intermediate that is generated by the coordination of a catalyst with an aldehyde. Therefore, the author anticipated that an appropriate catalyst system could permit the simultaneous occurrences of these two reactions and allow for the incorporation of both cyclic acetal and ester structures into one polymer chain (Scheme 1 (ii))



**Scheme 1.** Tandem polymerization consisting of cyclotrimerization and Tishchenko reaction using VEs and dialdehydes as monomers.

In Chapter 2 of this thesis, the author reported a novel polyaddition reaction of vinyl ethers (VEs) and bifunctional aldehydes via successive cyclotrimerization using  $\text{EtAlCl}_2$  as the catalyst (Scheme 2(i)). 1,1-diphenylethylene also underwent polyaddition with isophthalaldehyde (IPA), yielding a polymer with a high glass transition temperature (193 °C) and acid degradability.<sup>26</sup>



**Scheme 2.** Postulated mechanisms of cyclotrimerization and the Tishchenko reaction using  $\text{EtAlCl}_2$  and  $\text{Al}(\text{O}i\text{Pr})_3$ .

The Tishchenko reaction involves the dimerization reaction of two aldehydes to yield an ester through an atom economical route. A plausible mechanism of the Tishchenko reaction was suggested by Ogata and

Kawasaki.<sup>26</sup> In this model (Scheme 2(ii)), the initiation step involves the coordination of a catalyst with an aldehyde molecule and the subsequent generation of an aldehyde-derived alkoxide-bonded Al catalyst (Al–OCH<sub>2</sub>R) by transfer of the alkoxide ligand of the original catalyst along with the elimination of the corresponding ester. Subsequently, this catalyst coordinates with another aldehyde to transfer an alkoxide group on the Al catalyst to the carbonyl carbon of the aldehyde coordinated to the catalyst. Finally, a hydrogen atom on the carbon atom, which was originally the carbonyl carbon, transfers to a newly coordinated aldehyde, resulting in the generation of an ester and an aluminum alkoxide. Although the Tishchenko reaction has been employed in polymer chemistry as a bond-forming reaction,<sup>27–33</sup> a termination reaction,<sup>37</sup> and monomer synthesis,<sup>38</sup> there are no reports on the tandem polymerization consisting of the Tishchenko reaction and other organic reactions as far as the author knows.

In this study, the author aimed to develop a novel tandem polymerization system consisting of the two aforementioned reactions of aldehydes. Firstly, a model reaction was conducted with benzaldehyde (BzA) instead of bifunctional aldehydes to optimize reaction conditions. Based on the results of the model reaction, the tandem polymerization of bifunctional conjugated aldehydes and 2-chloroethyl VE (CEVE) was conducted, which resulted in polymers with cyclic acetal and ester structures in the main chain. Moreover, the author conducted three-component tandem polymerization by adding diethyl fumarate (DEF) as the third monomer that underwent transesterification reactions with Al-bonded alkoxy groups at polymer chain ends.<sup>39</sup> The thermal properties of the obtained polymers were tunable by the design of the backbone structures, such as the composition ratios of cyclic acetal to ester.

## **Experimental Section**

### **Materials**

DEF (TCI, >98.0%) and diisopropyl fumarate (DiPF; TCI, >98.0%) were distilled twice over calcium hydride under reduced pressure. IPA (TCI, >98.0%) and terephthalaldehyde (TPA; Nacalai Tesque, >98.0%) were recrystallized from *n*-hexane/toluene (1/1 v/v), vacuum dried for more than 3 h, and then dried by azeotropy with toluene. Commercially available Al(O*i*Pr)<sub>3</sub> (Nacalai Tesque, >98.0%), Al(OPh)<sub>3</sub> (Sigma–Aldrich, >99.9%), and Al(O*t*Bu)<sub>3</sub> (TCI, >98.0%) were used as received. DEF and DiPF were stored in brown ampules. Other materials were prepared and used as described in Chapter 2.

### **Polymerization procedure**

The following is a description of the typical polymerization procedure. A glass tube equipped with a three-way stopcock was dried using a heat gun (Ishizaki; PJ-206A; blow temperature of ~450 °C) under dry nitrogen. IPA was added into the tube in an N<sub>2</sub>-filled globe box (DBO-1B; MIWA MFG Co., Ltd.). Dichloromethane and CEVE were sequentially added to this tube using dry syringes. Al(O*i*Pr)<sub>3</sub> was added into another tube in the N<sub>2</sub>-filled globe box. To this tube, dichloromethane and an EtAlCl<sub>2</sub> solution were sequentially added by using dry syringes, and the mixture was kept at 0 °C for at least 10 min. The polymerization was initiated by adding the catalyst mixture solution to the monomer solution at 0 °C. After a predetermined time, the reaction was terminated by the addition of 1-propanol containing a small amount of aqueous ammonia. The quenched mixture was washed with water. Then, the volatiles were removed under reduced pressure at 50 °C to yield a polymer. The monomer and formyl group conversions were determined

by  $^1\text{H}$  NMR analysis of the quenched reaction mixture using *n*-hexane as an internal standard.

### Acid or alkali hydrolysis

Acid or alkali hydrolysis of the polymer was conducted with 1 M HCl (aq) or sodium hydroxide, respectively, in mixture of 1,2-dimethoxyethane/water at 60 °C for 4 or 8 h. The quenched mixture was diluted with dichloromethane and successively washed with an aqueous sodium hydroxide solution (only for acid hydrolysis) and water. The volatiles were removed under atmospheric pressure at room temperature.

### Characterization

The molecular weight distribution (MWD) of the polymers was measured by gel permeation chromatography (GPC) in chloroform at 40 °C with two polystyrene gel columns [TSKgel GMH<sub>HR</sub>-M  $\times$  2 (exclusive limit molecular weight =  $4 \times 10^6$ ; bead size = 5  $\mu\text{m}$ ; column size = 7.8 mm I.D.  $\times$  300 mm); flow rate = 1.0 mL min<sup>-1</sup>] connected to a JASCO PU-4580 pump, a Tosoh CO-8020 column oven, a UV-8020 ultraviolet detector, and an RI-8020 refractive index detector. Differential scanning calorimetry (DSC) was conducted with a Shimadzu DSC-60 Plus differential scanning calorimeter.  $M_w$ ,  $M_w/M_n$ ,  $^1\text{H}$  NMR spectra, and ESI-MS spectra were obtained in a manner similar to that described in Chapter 2.

## Results and Discussion

### *Tandem reaction of CEVE and BzA in dichloromethane using various Lewis acid catalysts*

First, appropriate conditions for tandem polymerization were investigated in a model reaction using BzA instead of a bifunctional aldehyde. The reaction of CEVE and BzA was conducted with EtAlCl<sub>2</sub> and/or Al(O*i*Pr)<sub>3</sub> as catalysts in dichloromethane at 0 °C. Only cyclotrimerization and CEVE homopolymerization (Scheme 2(i)) occurred when EtAlCl<sub>2</sub> was used (entry 1 in Table 1), yielding a cyclic trimer consisting of one CEVE and two BzA, which was supported by  $^1\text{H}$  NMR spectrum of the obtained product (Figure 1B; compound I obtained in the reaction under the different condition from entry 1 in Table 1; a mixture of diastereomers).<sup>40</sup> In contrast, only the Tishchenko reaction (Scheme 2(ii)) occurred with Al(O*i*Pr)<sub>3</sub> alone, even in the presence of both monomers (entry 2 in Table 1), which yielded benzyl benzoate (see Figure 1C for the  $^1\text{H}$  NMR spectrum of the obtained product; compound II).

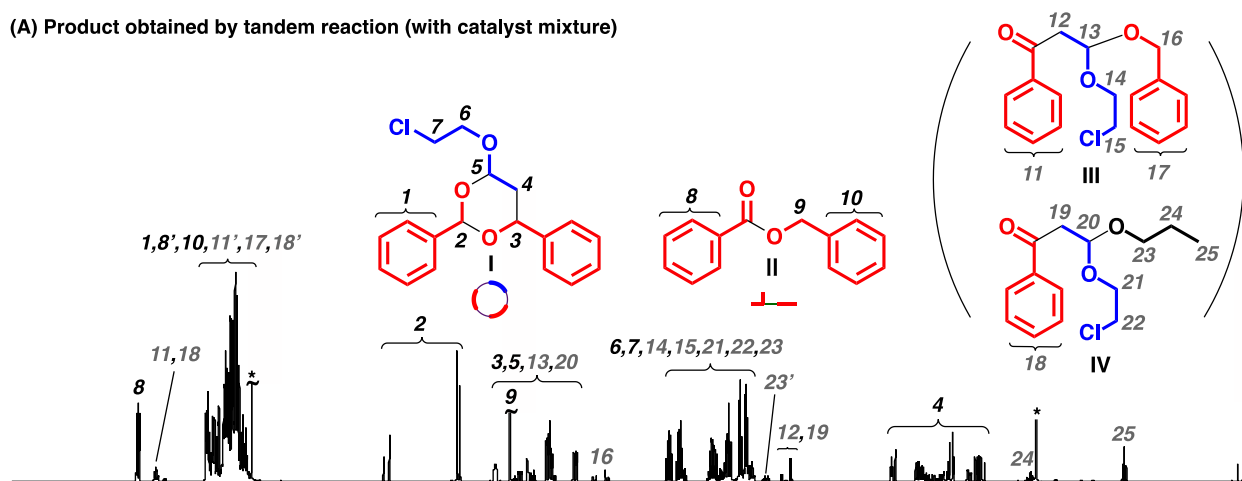
**Table 1.** Tandem reaction of CEVE and BzA<sup>a</sup>

entry	EtAlCl <sub>2</sub> (mM)	metal alkoxide	(mM)	time	conv. (%) <sup>b</sup>		ratio of products <sup>c</sup>			
					CEVE	BzA	cyclotrim- erization	Tishchenko reaction	VE homo- polymerization	linear acetal generation
1	50	Al(O <i>i</i> Pr) <sub>3</sub>	0	10 min	>99	95	88	–	12	–
2	0		100	72 h	0	22	–	>99	~0	–
3	30		10	168 h	88	96	74	18	2	6
4	30		20	144 h	3	73	–	91	–	9
5	30	Al(O <i>t</i> Bu) <sub>3</sub>	20	72 h	47	61	58	23	9	10
6	30	Al(OPh) <sub>3</sub>	20	4 h	40	60	30	13	14	43

<sup>a</sup> [CEVE]<sub>0</sub> = 0.50 M, [BzA]<sub>0</sub> = 1.0 M, in dichloromethane at 0 °C. <sup>b</sup> Determined by  $^1\text{H}$  NMR analysis of quenched reaction mixtures. <sup>c</sup> Estimated by  $^1\text{H}$  NMR analysis of the obtained products.

Both cyclotrimerization and the Tishchenko reaction simultaneously occurred when 30 mM EtAlCl<sub>2</sub> and 10 mM Al(OiPr)<sub>3</sub> were used as a catalyst mixture (entry 3 in Table 1). A GPC curve of the obtained product showed two sharp peaks in the low-MW region, which indicated that the polymerization of CEVE, a cationically homopolymerizable monomer, did not occur. In the <sup>1</sup>H NMR spectrum of the obtained product (Figure 1A), peaks for both the cyclic acetal and the ester were observed. The total proportion of the two desirable products was 92%, and small amounts (6%) of two linear acetals (compounds III and IV in Figure 1) were also produced via side reactions (*vide infra*).

(A) Product obtained by tandem reaction (with catalyst mixture)



(B) Product obtained by cyclotrimerization (with EtAlCl<sub>2</sub> alone)



(C) Product obtained by Tishchenko reaction (with Al(OiPr)<sub>3</sub> alone)

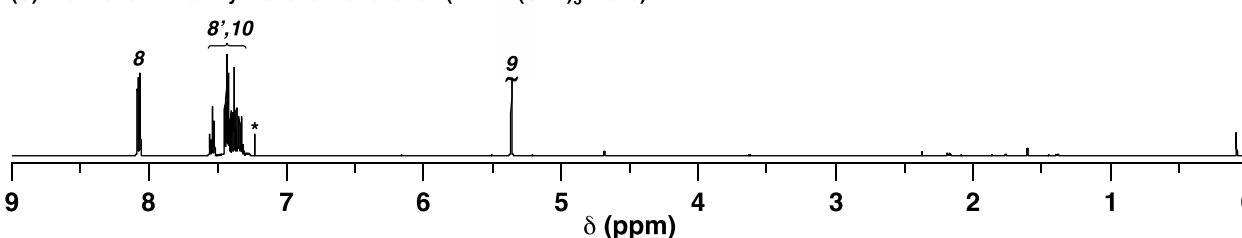


**Figure 1.** <sup>1</sup>H NMR spectra of the products obtained in the model reactions of CEVE and BzA with (A) both EtAlCl<sub>2</sub> and Al(OiPr)<sub>3</sub> (entry 3 in Table 1), (B) EtAlCl<sub>2</sub> alone ([CEVE]<sub>0</sub> = 0.50 M, [BzA]<sub>0</sub> = 1.0 M, [EtAlCl<sub>2</sub>]<sub>0</sub> = 50 mM, [THF] = 1.0 M, in dichloromethane at 0 °C), and (C) Al(OiPr)<sub>3</sub> alone (entry 2 in Table 1) (in CDCl<sub>3</sub> at 30 °C; \* CHCl<sub>3</sub>, water, or TMS).

The ratios and alkoxy ligand types of the catalysts combined with EtAlCl<sub>2</sub> are important for selective reactions. An increase in the concentration of Al(OiPr)<sub>3</sub> from 10 mM to 20 mM completely inhibited cyclotrimerization (entry 4 in Table 1). When different aluminum alkoxides were used (entries 5 and 6 in Table 1), the tandem reaction also proceeded. However, unlike the case with Al(OiPr)<sub>3</sub>, other linear acetals were partly formed as side products by transfers of the alkoxide ligands, which were confirmed by ESI-MS and <sup>1</sup>H NMR analyses of the obtained products.

The <sup>1</sup>H NMR spectrum of a catalyst mixture of EtAlCl<sub>2</sub> and Al(OiPr)<sub>3</sub> suggested that aluminum haloalkoxides were likely generated by ligand exchange reactions of chlorine atoms of EtAlCl<sub>2</sub> and isopropoxy



groups of  $\text{Al}(\text{O}i\text{Pr})_3$  (Figure 2). The aluminum haloalkoxides most likely exhibited appropriate catalytic activity for both cyclotrimerization and the Tishchenko reaction without interfering with each other due to their sufficient Lewis acidity for the generation of a carbocation and the ability to act as an alkoxide transfer agent.

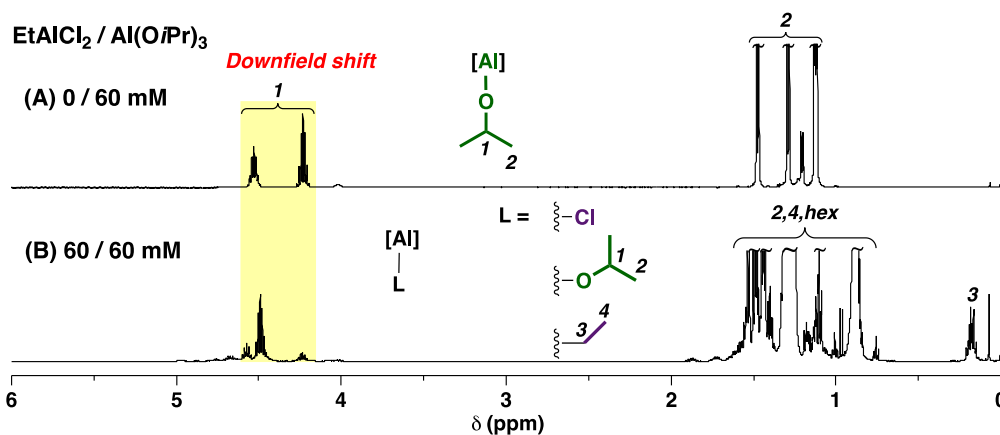
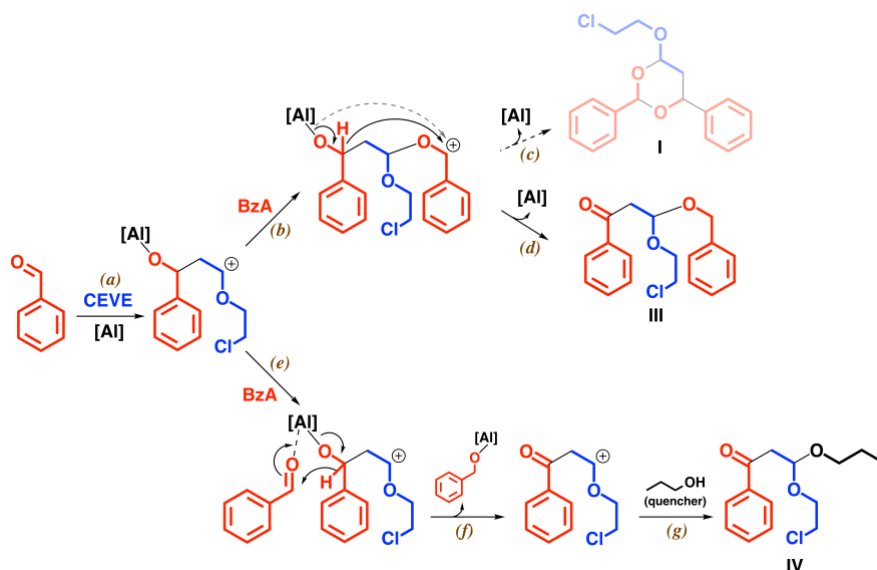


**Figure 2.**  $^1\text{H}$  NMR spectra of (A)  $\text{Al}(\text{O}i\text{Pr})_3$  and (B) the mixture of an equimolar amount of  $\text{EtAlCl}_2$  and  $\text{Al}(\text{O}i\text{Pr})_3$  (in  $\text{CDCl}_3$  at  $30\text{ }^\circ\text{C}$ ; L: other ligands; hex: *n*-hexane).

The two linear acetal side products (compounds III and IV in Figure 1A) were likely generated by the mechanisms shown in Scheme 3. A BzA molecule activated by the Al catalyst reacts with CEVE (path (a)) and another BzA (path (b)). The subsequent reaction of the Al-coordinated oxygen atom with the carbocation results in the cyclotrimerization (path (c); compound I), whereas the intramolecular hydride transfer results in a linear acetal consisting of one CEVE and two BzAs (path (d); compound III). The other linear acetal (path (g); compound IV) is produced by the reaction of 1-propanol, which was used as a quencher, with a carbocation derived from the undesired hydride transfer after the reaction of one BzA and one CEVE (paths (e) and (f)) (Scheme 3).



**Scheme 3.** Possible pathways of generation of two linear acetals ([Al]: aluminum haloalkoxide, such as  $\text{Al}(\text{OR})_n\text{Cl}_{2-n}$  and  $\text{Al}(\text{OR})_m\text{Cl}_{3-m}$ ; dormant species with a covalent bond, such as a carbon–chlorine bond, generated from carbocations are ignored)

### Tandem polymerization of CEVE or IBVE and IPA

Based on the results of the model reactions, the reaction of CEVE and IPA, which contains two aldehyde units at the *meta* positions, was examined using a catalyst mixture consisting of EtAlCl<sub>2</sub> and Al(OiPr)<sub>3</sub> in dichloromethane at 0 °C (entry 3 in Table 2). The appropriate catalyst mixture promoted both cyclotrimerization and Tishchenko reactions, resulting in a polymer of  $M_w = 3.5 \times 10^3$ . As shown in Figure 3A, IPA was almost completely consumed during the early stage of polymerization, whereas CEVE conversion plateaued at approximately 30% in 4 h. Even after both monomer consumptions plateaued via the reactions between monomers, the formyl groups, which exist at the oligomer and polymer chain ends, were gradually consumed (square symbols in Figure 3A) by the Tishchenko reactions between oligomers and polymers. The  $M_w$  values of the products exponentially increased along with the consumption of the formyl group for the tandem polymerization in the later stage (Figure 3B), which indicated that the polymerization proceeded in a step-growth manner. The MWD curves shifted to a higher-MW region even after the consumption of both monomers reached plateaus (Figure 3C), which also suggested that the Tishchenko reaction between the formyl groups of the polymer chains mainly occurred in the later stage.<sup>41</sup>

**Table 2.** Tandem polymerization of VEs and IPA<sup>a</sup>

entry	VE	Ald.	catalyst (mM)		conv. (%) <sup>b</sup>		$M_w \times 10^{-3}$ <sup>c</sup>	$M_w/M_n$ <sup>c</sup>	ratio of products <sup>d</sup>			
			EtAlCl <sub>2</sub> /Al(OiPr) <sub>3</sub>	time (h)	VE	Ald.			cyclotrim- erization	Tishchenko reaction	VE polym- erization	linear acetal generation
1	CEVE	IPA	30/0	4	>99	>99	1.2	1.87	96	–	4	–
2			0/100	144	~0	>99	0.7	2.90	–	>99	~0	~0
3			30/10	144	33	>99	3.5	4.11	21	69	5	5
4			40/10	144	88	>99	3.5	3.48	33	50	11	6
5			45/10	144	96	>99	3.5	3.74	49	38	6	7
6	IBVE	IPA	30/10	128	>99	>99	3.0	2.34	28	28	41	3

<sup>a</sup> [VE]<sub>0</sub> = 0.50 M, [IPA]<sub>0</sub> = 0.70 M, in dichloromethane at 0 °C. <sup>b</sup> Determined by <sup>1</sup>H NMR analysis of quenched reaction mixtures. <sup>c</sup> Determined by GPC (polystyrene standards). <sup>d</sup> Estimated by <sup>1</sup>H NMR analysis of the obtained polymers.

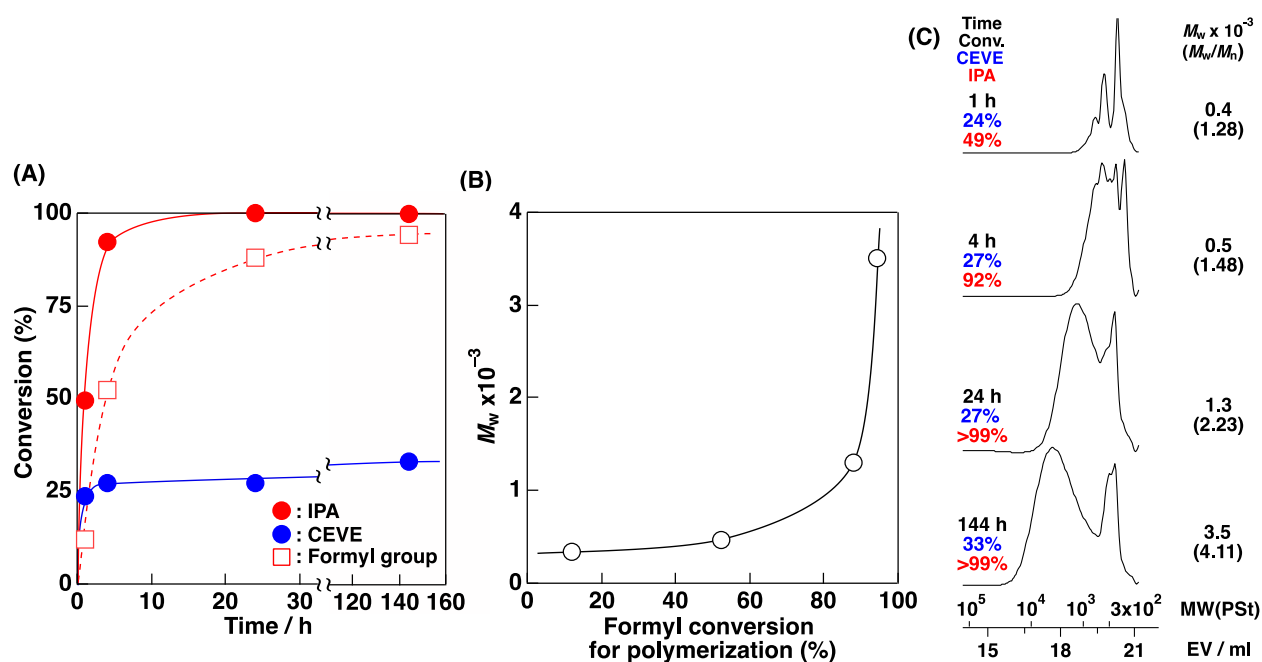


**Figure 3.** (A) Time–conversion curves of the tandem polymerization of CEVE and IPA, (B)  $M_w$  values [the formyl conversions for polymerization were calculated from the total amounts of remained formyl groups and the hydroxy groups converted from formyl groups (vide infra)], and (C) MWD curves of the obtained polymers (The data correspond to entry 3 in Table 2;  $[\text{CEVE}]_0 = 0.50$  M,  $[\text{IPA}]_0 = 0.70$  M,  $[\text{EtAlCl}_2]_0 = 30$  mM,  $[\text{Al}(\text{OiPr})_3]_0 = 10$  mM, in dichloromethane at 0 °C).

The  $^1\text{H}$  NMR spectrum of the obtained polymer (Figure 4A) indicated that the polymer was generated by both cyclotrimerization and the Tishchenko reaction. The spectrum had peaks with similar chemical shifts to those of the compounds obtained in the model reaction. For example, the peaks at 5.7–6.3 ppm (peak 2) were assigned to the methine proton adjacent to two oxygen atoms of cyclic acetal structures [see Figure 4B for  $^1\text{H}$  NMR spectrum of poly(cyclic acetal)]. In addition, ester peaks emerged at 5.4 ppm (peak 9), which was consistent with the poly(ester) produced by the successive Tishchenko reaction of IPA (Figure 4C). The remaining aldehyde ends were most likely converted into alcohol moieties, which could be generated by Meerwein-Ponndorf-Verley (MPV) reduction of the aldehyde ends after the addition of excess 1-propanol as the quencher (Scheme S1).<sup>42–44</sup> This reaction rarely operated during the polymerization because of the absence of a proton source except for adventitious water and impurity *i*PrOH. The amount of the converted hydroxy groups, which was used for the calculation of formyl conversion shown in Figure 3, was determined from the integral ratio of the methylene proton adjacent to a hydroxy group (peak 27) in the  $^1\text{H}$  NMR spectrum of the quenched reaction mixture.<sup>45</sup> Weak peaks of the methylene groups of the linear acetal side products were observed at 3.4 ppm (peaks 13 and 19).

(A) Polymer obtained by tandem polymerization (with catalyst mixture)

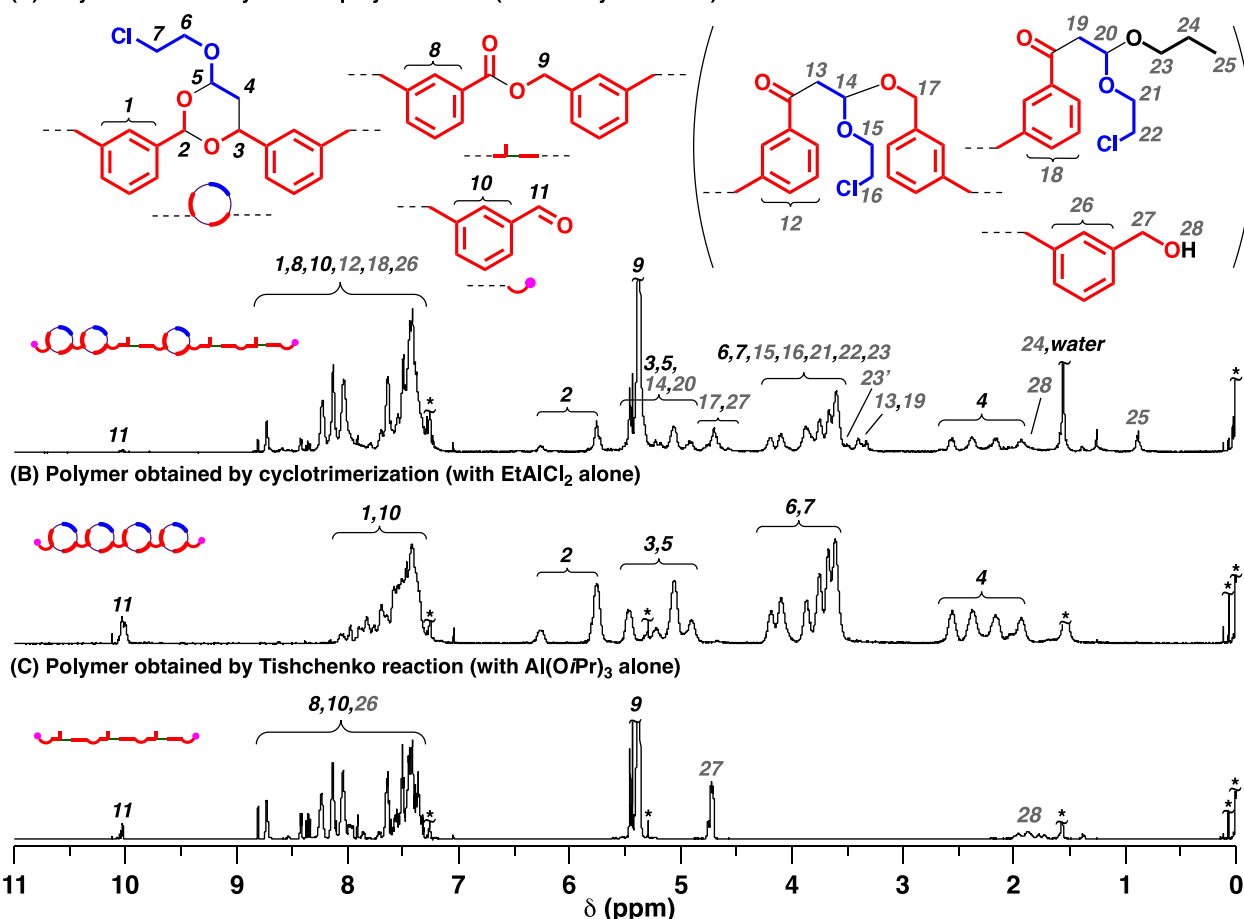


**Figure 4.**  $^1\text{H}$  NMR spectra of the products obtained by the tandem polymerization of CEVE and IPA with (A) both  $\text{EtAlCl}_2$  and  $\text{Al}(\text{O}i\text{Pr})_3$  (entry 3 in Table 2; after purification by reprecipitation in *n*-hexane), (B)  $\text{EtAlCl}_2$  alone [ $M_w(\text{GPC}) = 2.3 \times 10^3$ ,  $M_w/M_n(\text{GPC}) = 1.62$ ;  $[\text{CEVE}]_0 = 0.50$  M,  $[\text{IPA}]_0 = 0.50$  M,  $[\text{EtAlCl}_2]_0 = 50$  mM,  $[\text{THF}] = 1.0$  M, in dichloromethane at  $0^\circ\text{C}$ ; after purification by reprecipitation in methanol], and (C)  $\text{Al}(\text{O}i\text{Pr})_3$  alone [ $M_w(\text{GPC}) = 1.0 \times 10^3$ ,  $M_w/M_n(\text{GPC}) = 2.37$ ;  $[\text{IPA}]_0 = 0.50$  M,  $[\text{Al}(\text{O}i\text{Pr})_3]_0 = 100$  mM in dichloromethane at  $0^\circ\text{C}$ ] (in  $\text{CDCl}_3$  at  $30^\circ\text{C}$ ; \* solvents, residual monomer, water, grease, or TMS).

The ESI-MS spectrum also supported the generation of a polymer with both cyclic acetal and ester structures in the main chain (Figure 5). Peaks with  $m/z$  values consistent with the  $x$  units of CEVE and  $y$  units of IPA ( $y \geq x + 1$ ) were observed, which suggests that both cyclic acetal and ester structures were incorporated into one polymer chain. For example, a peak with an  $m/z$  value corresponding to a structure of one CEVE unit and three IPA units was observed, which indicates that an oligomer composed of one cyclic acetal and one ester structures was generated during the polymerization.

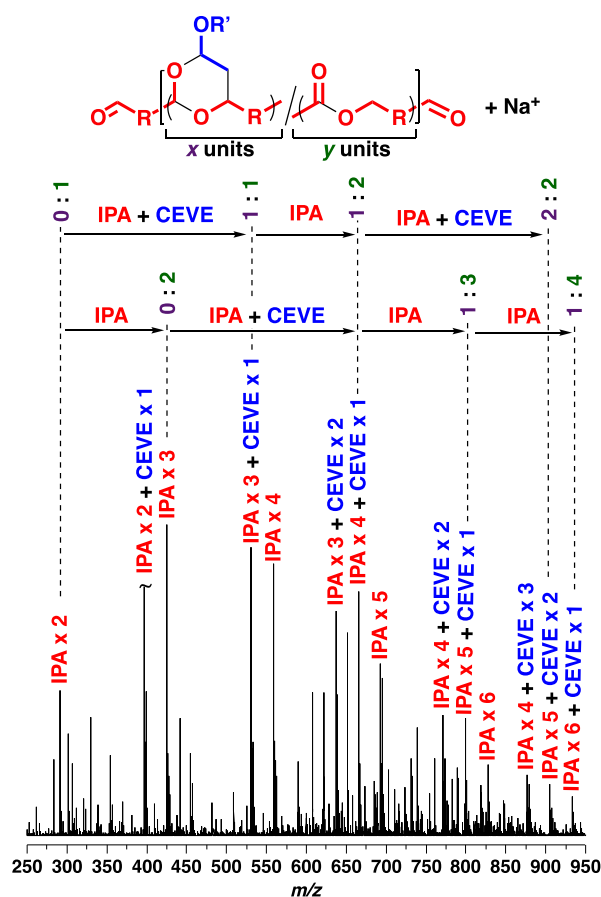
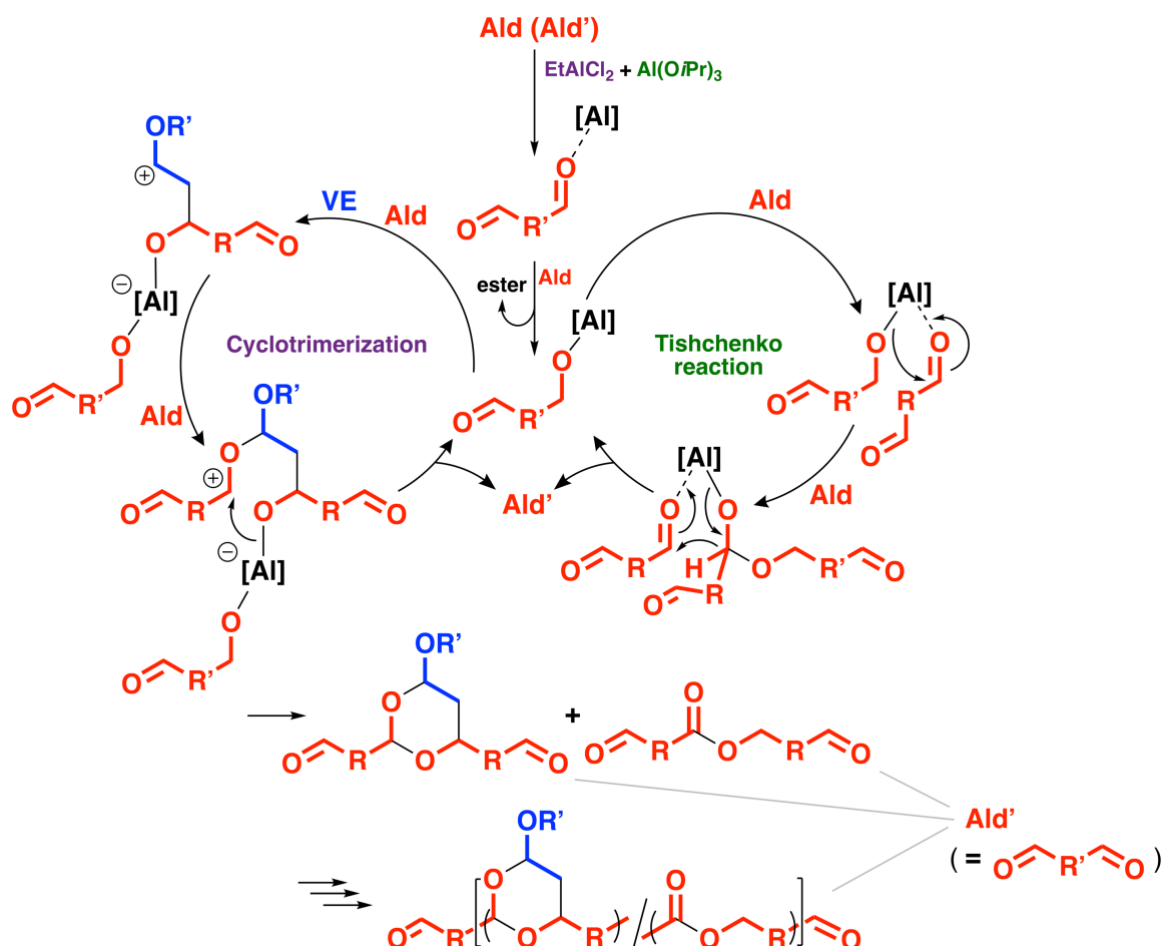


**Figure 5.** ESI-MS spectrum of the product obtained by the tandem polymerization of CEVE and IPA [ $M_w(\text{GPC}) = 0.5 \times 10^3$ ,  $M_w/M_n(\text{GPC}) = 1.66$ ;  $[\text{CEVE}]_0 = 0.50$  M,  $[\text{IPA}]_0 = 0.70$  M,  $[\text{EtAlCl}_2]_0 = 30$  mM,  $[\text{Al}(\text{OiPr})_3]_0 = 10$  mM, in dichloromethane at  $0^\circ\text{C}$  for 4 h].

A plausible mechanism of the tandem polymerization is shown in Scheme 4. The polymerization is initiated by the coordination of the catalyst with an aldehyde monomer. Subsequently, either cyclotrimerization or the Tishchenko reaction between monomers proceeds with the aluminum haloalkoxides. The obtained cyclic trimer and ester have two reactive aldehyde moieties (Ald' in Scheme 4). These products react with other aldehyde moieties of either an IPA monomer, a cyclic trimer, an ester, an oligomer, or a polymer via cyclotrimerization or via the Tishchenko reaction. For example, if an ester undergoes the cyclotrimerization with a VE and an aldehyde monomer, an oligomer consisting of one cyclic acetal and one ester structures is obtained. The successive reactions result in a polymer with cyclic acetal and ester structures in the main chain.



**Scheme 4.** Tandem polymerization consisting of cyclotrimerization and the Tishchenko reaction using VEs and dialdehydes as monomers ([Al]: aluminum haloalkoxide, such as Al(OR)<sub>n</sub>Cl<sub>2-n</sub> and Al(OR)<sub>m</sub>Cl<sub>3-m</sub>; Ald: dialdehyde (IPA or TPA); aldehydes coordinated with the aluminum catalyst could undergo cyclotrimerization).

The resulting polymer was hydrolyzed under acidic or alkaline conditions because of the degradation of the cyclic acetal and ester structures, respectively. Importantly, different products were obtained depending on the degradation conditions because ester and acetal moieties remained intact under acidic and alkaline conditions, respectively. After acid or alkali hydrolysis, the MWD curve shifted into the lower-MW region in relation to the original polymer (the purple and green curves in Figure 6A). Selective degradation was confirmed by <sup>1</sup>H NMR analysis of the hydrolysis products. After acid hydrolysis, the peaks assigned to the cyclic acetal structures completely disappeared and instead peaks assignable to a cinnamaldehyde moiety emerged at 6.8 and 9.7 ppm (Figure 6C).<sup>46,47</sup> On the other hand, the ester structures disappeared, and peaks for methylene protons (peak 27) adjacent to the alcohol moieties emerged after alkali hydrolysis (Figure 6D). These results indicated that the obtained polymer had both cyclic acetal and ester structures in one polymer chain.

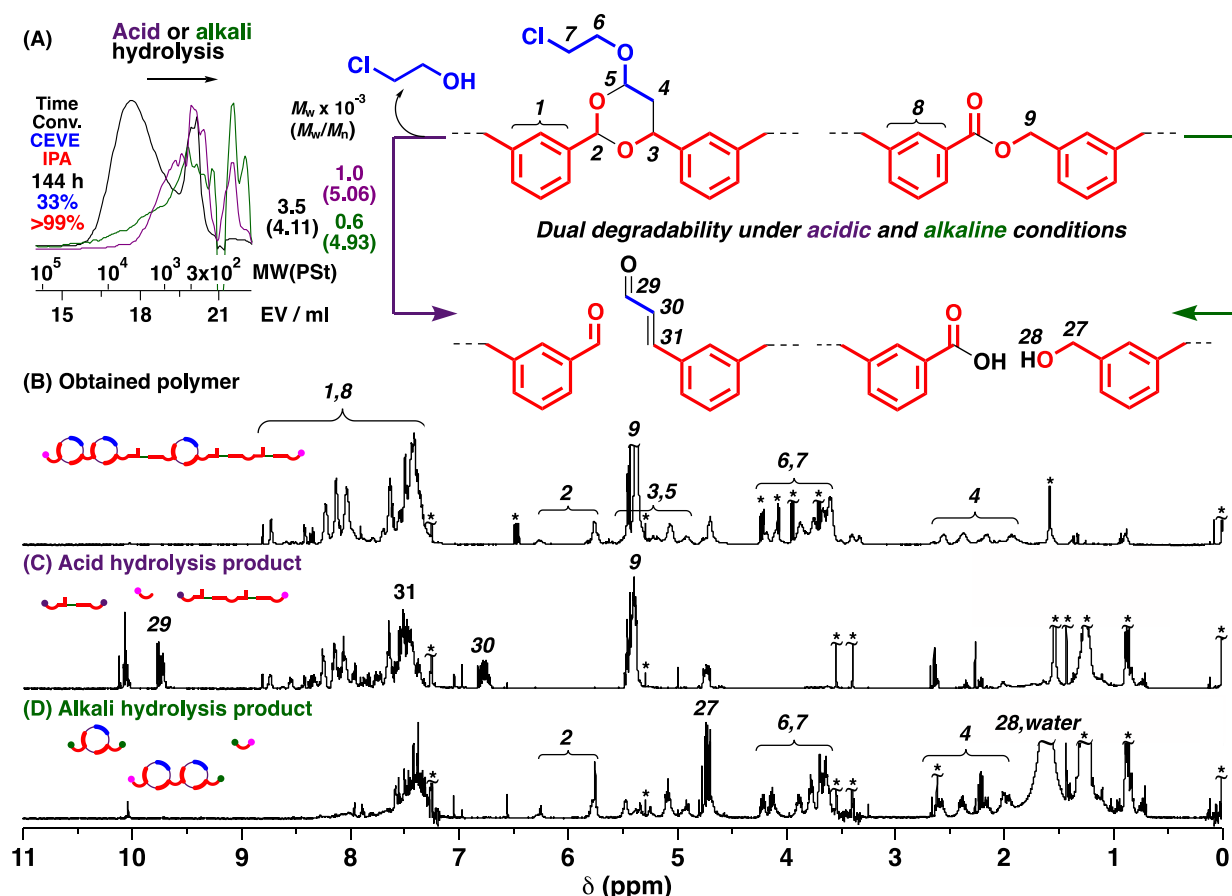


**Figure 6.** (A) MWD curves of the obtained polymer by the tandem polymerization (black) and its acid (purple) or alkali (green) hydrolysis products and  $^1\text{H}$  NMR spectra of (B) the obtained polymer (the same spectrum as that shown in Figure 4A) and its (C) acid or (D) alkali hydrolysis product (entry 3 in Table 2; in  $\text{CDCl}_3$  at  $30^\circ\text{C}$ ; \* solvents, residual monomer, water, or TMS).

The composition of the backbone constructed with the cyclic acetal and ester was controlled by adjusting the initial catalyst molar ratio because the kinetics of the cyclotrimerization and the Tishchenko reaction could be tunable (entries 3–5 in Table 2). For example, the Tishchenko reaction preferentially occurred with 30 mM  $\text{EtAlCl}_2$  and 10 mM  $\text{Al}(\text{OiPr})_3$ , yielding a polymer consisting of approximately 21% cyclic acetal and 69% ester structures (entry 3 in Table 2). In contrast, the polymer obtained with 40 mM  $\text{EtAlCl}_2$  and 10 mM  $\text{Al}(\text{OiPr})_3$  was composed of approximately 33% cyclic acetal and 50% ester structures (entry 4 in Table 2). Finally, the polymer with a larger amount of cyclic acetal than ester was obtained with 45 mM  $\text{EtAlCl}_2$  and 10 mM  $\text{Al}(\text{OiPr})_3$  (entry 5 in Table 2). The cyclic acetal structures became more frequently generated as the molar ratio of  $\text{EtAlCl}_2$  increased.

The reactivity of VE was important for selective tandem polymerization. Isobutyl VE (IBVE), which has a higher reactivity than that of CEVE, underwent the tandem polymerization with IPA (entry 6 in Table 2). Unlike CEVE, however, IBVE preferentially underwent side reactions, such as VE homopolymerization. Consequently, the low reactive vinyl monomer is favorable for tandem polymerization as in the case of the polyaddition by cyclotrimerization (Chapter 2).<sup>29</sup>

### Tandem polymerization of CEVE and TPA

To obtain higher-MW polymers, the effects of the initial molar concentrations of both monomers were investigated in the tandem polymerization of CEVE and IPA. However, the MWs of the polymers were comparable ( $M_w = 3\text{--}4 \times 10^3$ ) irrespective of the concentrations. The catalyst ratios were also ineffective for obtaining high-MW polymers as demonstrated above (entries 4 and 5 in Table 2). Notable amounts of low-MW oligomers, which are likely cyclic oligomers, were produced in any cases (see Figures S1 and S2 for the  $^1\text{H}$  NMR spectrum of the low-MW fraction separated by preparative GPC). The author anticipated that the suppression of the oligomer formation potentially led to higher-MW products.

**Table 3.** Tandem polymerization of CEVE and TPA<sup>a</sup>

entry	catalyst (mM)			conv. (%) <sup>b</sup>						side reaction <sup>d</sup>	
	TPA (M)	EtAlCl <sub>2</sub> / Al(O <sup><i>i</i></sup> Pr) <sub>3</sub>	time (h)	VE	TPA	$M_w \times 10^{-3}$ <sup>c</sup>	$M_w/M_n$ <sup>c</sup>	cyclotrim- erization <sup>d</sup>	Tishchenko reaction <sup>d</sup>	vinyl polymeri- zation	linear acetali- zation
1	0.20	30/10	360	50	>99	2.6	2.48	19	20	48	12
2	0.50	30/10	360	46	>99	5.1	3.20	12	67	13	8
3	0.70	30/10	168	47	>99	3.5	3.06	15	69	9	7
4	0.90	30/10	360	77	>99	6.7	4.13	19	65	10	6
5	0.90	40/10	360	88	>99	6.2	3.75	26	58	11	5

<sup>a</sup> [CEVE]<sub>0</sub> = 0.50 (entries 1–3), 0.49 (entry 4), or 0.52 (entry 5) M, in dichloromethane at 0 °C. <sup>b</sup> Determined by  $^1\text{H}$  NMR analysis of quenched reaction mixtures. <sup>c</sup> Determined by GPC (polystyrene standards). <sup>d</sup> Estimated by  $^1\text{H}$  NMR analysis of the obtained polymers.

The two formyl groups at the meta positions of IPA would be responsible for the cyclic oligomer generation; hence, the tandem polymerization was conducted with TPA, which contains two aldehyde units at the para positions, instead of IPA for the purpose of suppressing the intramolecular cyclization (Table 3). The polymerization proceeded well and yielded polymers with almost the same compositions of cyclic acetal and ester structures as those of the poly(CEVE-*co*-IPA)s obtained under the same conditions (entry 3 in Table 3). Interestingly, the obtained poly(CEVE-*co*-TPA)s had higher-MWs (entries 2–5 in Table 3) than those of poly(CEVE-*co*-IPA)s (entries 3–5 in Table 2), likely because of the decrease in cyclic oligomers (Figure 7A). Polymers with  $M_w$  values as high as  $6\text{--}7 \times 10^3$  were obtained with 0.90 M TPA at a long polymerization time (360 h; entries 4 and 5 in Table 3; black curve in Figure 7B). These polymers were hydrolyzed under acidic or alkaline conditions (purple and green curves in Figure 7B).



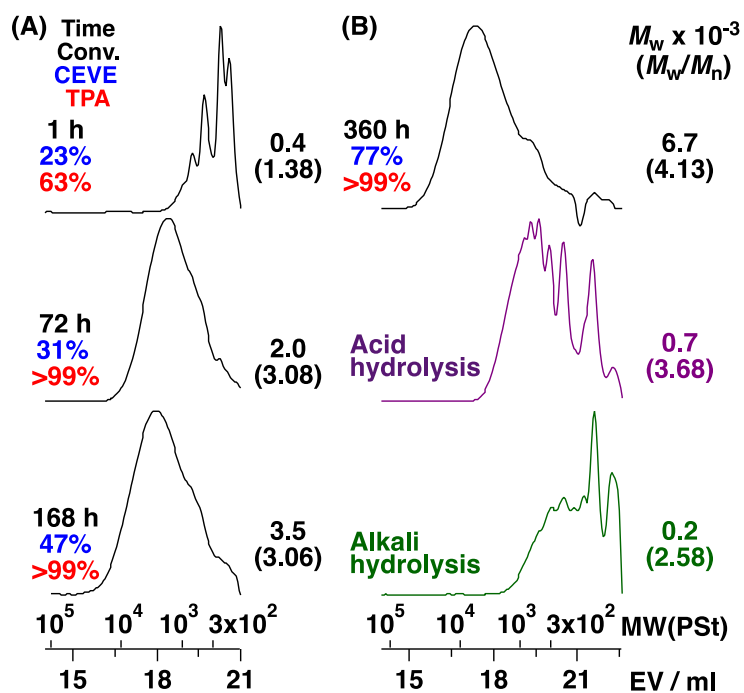
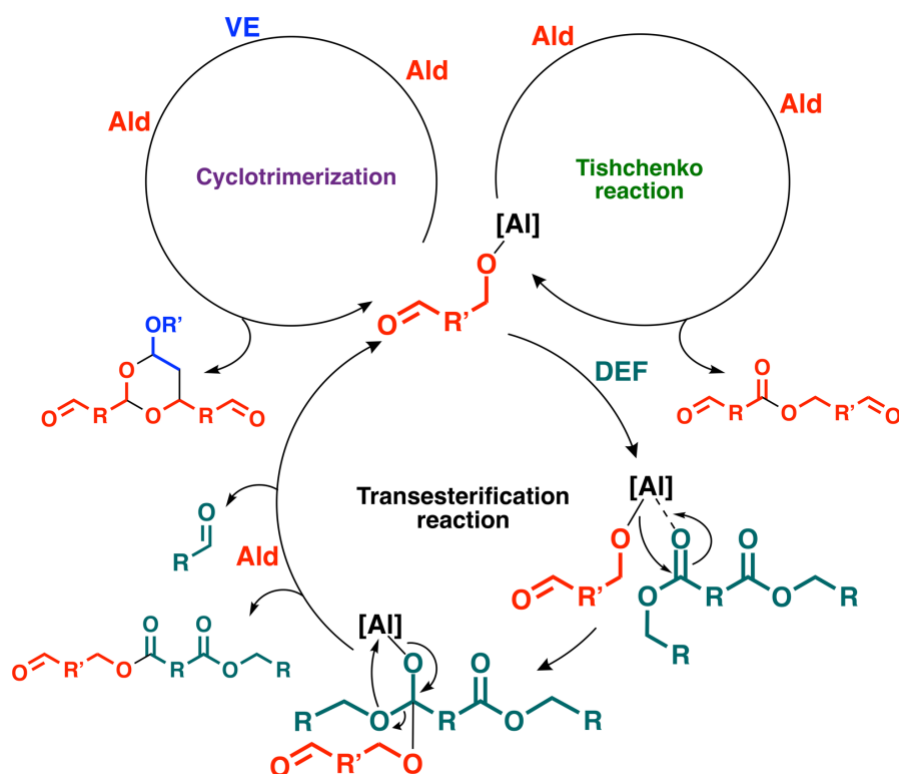


**Figure 7.** MWD curves of the polymers obtained by the tandem polymerization of CEVE and TPA (black) and its acid (purple) or alkali (green) hydrolysis product [entries (A) 3 and (B) 4 in Table 3].

#### Three-component tandem polymerization

To suppress VE homopolymerization during the tandem polymerization, ethyl acetate was used as a weak Lewis base;<sup>48,49</sup> however, the MW of the obtained polymer was lower than that obtained in the absence of ethyl acetate. The transesterification between ethyl acetate and the polymer chain ends, which was supported by the model reaction of CEVE and BzA in the presence of ethyl acetate (Figure S3), was likely responsible for the lower MW. An aldehyde-derived alkoxy group on the Al center reacted with an ethyl acetate molecule that was coordinated with the same Al center, resulting in an acetate ester and ethanol.<sup>50-53</sup>

From these results, the author devised a strategy to employ the transesterification for three-component tandem polymerization with DEF as the third component (Scheme 5). If the transesterification proceeds without interfering with both the cyclotrimerization and the Tishchenko reaction, the three-component tandem polymerization using CEVE, IPA, and DEF would be feasible to yield a polymer consisting of cyclic acetal and two different ester structures in the main chain.



**Scheme 5.** Three-component tandem polymerization of VEs, dialdehydes, and dicarboxylic acid esters [Al]:  $\text{Al}(\text{OR})_n\text{Cl}_{2-n}$ ; Ald: dialdehyde (IPA or TPA); see Scheme S1 for the liberation of a DEF-derived aldehyde and regeneration of a dialdehyde-derived Al alkoxide).

The three-component tandem polymerization of IPA, CEVE, and DEF was conducted under conditions similar to those used for the tandem polymerization by the cyclotrimerization and the Tishchenko reaction (entry 2 in Table 4). All three monomers were partly consumed in the polymerization (Figure 8A), which resulted in the generation of a polymer of  $M_w = 1.5 \times 10^3$  (Figure 8B). The  $^1\text{H}$  NMR spectrum of the product (Figure 9A) showed peaks assigned to the cyclic acetal and ester structures at the same chemical shifts as those of the polymer obtained by the tandem polymerization of CEVE and IPA (Figure 4A). In addition, the olefin structure derived from DEF was confirmed by the peak at 6.8 ppm (peaks 31 and 34 in Figure 9A). This chemical shift was consistent with that of the olefin proton of a DEF monomer (peak 45 in Figure 9B). From these results, the three-component tandem polymerization was demonstrated to occur successfully via cyclotrimerization, the Tishchenko reaction, and transesterification.<sup>54,55</sup> The initial concentrations of monomer and catalyst affected the frequency of each reaction. In addition, polymers obtained with TPA had higher MWs than those obtained with IPA (entries 5 and 6 in Table 4) as in the case of the polymerization in the absence of DEF. However, the MWs of the polymers obtained by the three-component tandem polymerization were relatively low because DEF was equivalent to a chain transfer agent. More specifically, the transesterification between a polymer chain end and a DEF molecule generated an ethoxy unit, which produced a new polymer chain. These results were consistent with those in the model reaction of BzA, CEVE, and DEF (Figure S4). When DiPF, which potentially releases *i*PrOH by transesterification, was used as the third component, transesterification did not occur at all.

**Table 4.** Three-component tandem polymerization of CEVE, dialdehydes, and DEF<sup>a</sup>

entry	dialdehyde	DEF (M)	DEF (M)	time (h)	conv. (%) <sup>b</sup>			ratio of products					
					CEVE	dialdehyde	DEF	$M_w$ x $10^{-3}$ <sup>c</sup>	$M_w$ / $M_n$ <sup>c</sup>	cyclotri- merization <sup>d</sup>	Tishchenko reaction <sup>d</sup>	transester- ification <sup>d</sup>	others <sup>d</sup>
1	IPA	0.70	0.20	96	32	>99	46	1.7	2.23	11	75	5	9
2		0.70	0.40	96	35	>99	38	1.5	1.99	9	74	8	9
3		0.70	0.60	96	25	>99	39	1.4	1.85	8	72	10	10
4		0.50	0.40	143	58	>99	52	1.2	1.81	17	60	14	9
5	TPA	0.70	0.40	144	25	>99	46	1.8	1.94	17	64	6	13
6		0.50	0.40	144	44	>99	47	1.5	1.79	9	66	11	14

<sup>a</sup> [CEVE]<sub>0</sub> = 0.50 (entries 1–3), 0.48 (entry 4), 0.51 (entry 5), or 0.49 (entry 6) M, [EtAlCl<sub>2</sub>]<sub>0</sub> = 30 mM, [Al(OiPr)<sub>3</sub>]<sub>0</sub> = 10 mM, in dichloromethane at 0 °C. <sup>b</sup> Determined by <sup>1</sup>H NMR analysis of quenched reaction mixtures. <sup>c</sup> Determined by GPC (polystyrene standards). <sup>d</sup> Estimated by <sup>1</sup>H NMR analysis of the obtained polymers.

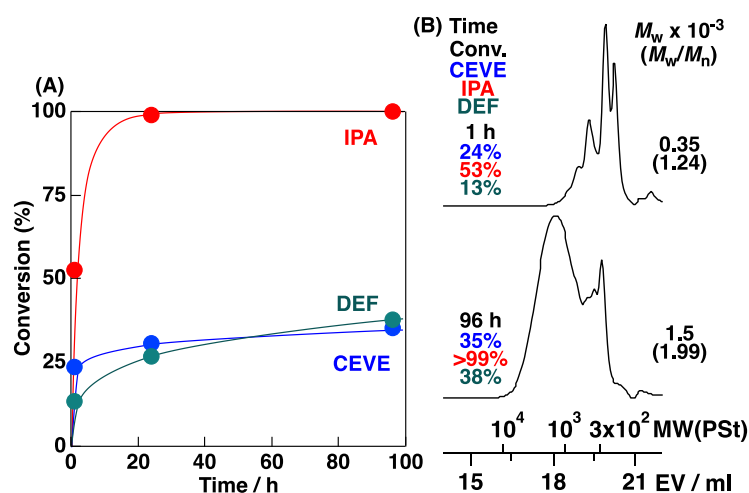


**Figure 8.** (A) Time–conversion curves of the three-component tandem polymerization and (B) MWD curves of the obtained products (entry 2 in Table 4; [CEVE]<sub>0</sub> = 0.50 M, [IPA]<sub>0</sub> = 0.70 M, [DEF]<sub>0</sub> = 0.40 M, [EtAlCl<sub>2</sub>]<sub>0</sub> = 30 mM, [Al(OiPr)<sub>3</sub>]<sub>0</sub> = 10 mM, in dichloromethane at 0 °C).

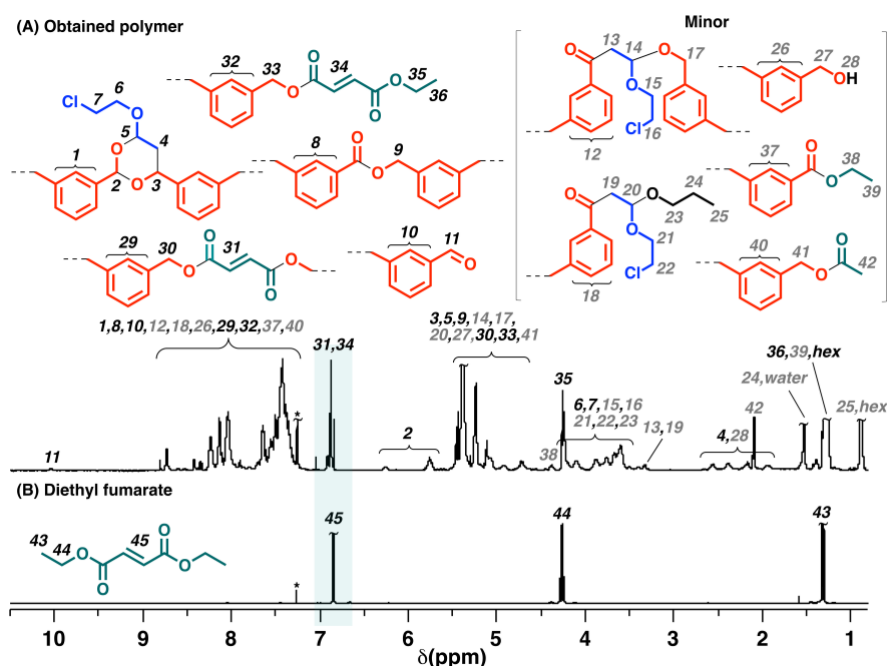


**Figure 9.**  $^1\text{H}$  NMR spectra of (A) the polymer obtained by the three-component tandem polymerization using CEVE, IPA, and DEF [entry 2 in Table 4;  $M_w(\text{GPC}) = 1.8 \times 10^3$ ,  $M_w/M_n(\text{GPC}) = 2.07$ ; after purification by reprecipitation in *n*-hexane] and (B) DEF monomer (in  $\text{CDCl}_3$  at  $30^\circ\text{C}$ ; \*  $\text{CHCl}_3$ ; hex: *n*-hexane).

#### Thermal properties of the polymers

DSC measurements were conducted to examine the thermal properties of the obtained polymers containing various structures in the main chain. The glass transition temperature ( $T_g$ ) of the obtained polymers was dependent on the backbone structures. Polymers consisting of higher ratios of the cyclic acetal structures exhibited higher  $T_g$  values, likely because of the rigidity of the structures (entries 2 and 3 in Table 5). Furthermore, the polymer obtained by the three-component tandem polymerization had a very low  $T_g$  ( $18^\circ\text{C}$ ; entry 5 in Table 5), likely because of the flexible fumarate structures. Moreover, poly(CEVE-*co*-TPA) (entry 4 in Table 5) had a higher  $T_g$  value than that of poly(CEVE-*co*-IPA) at comparable ratios of the cyclic acetal to ester moieties, probably due to the symmetrical nature of the structure, as in the case of the poly(imide)s with *meta* and *para* isomers.<sup>56</sup>

**Table 5.**  $T_g$  values of polymers with cyclic acetal and/or ester in the main chain<sup>a</sup>

entry	polymer <sup>b</sup>	composition		$M_w \times 10^{-3}$ <sup>d</sup>	$M_w/M_n$ <sup>d</sup>	$T_g$ ( $^\circ\text{C}$ )
		cyclic acetal <sup>c</sup>	ester <sup>c</sup>			
1	Poly(CEVE- <i>co</i> -IPA)	100	0	3.3	1.92	56
2		55	45	3.9	3.04	51
3		25	75	4.4	3.62	37
4	Poly(CEVE- <i>co</i> -TPA)	23	77	3.7	2.54	60
5	Poly(CEVE- <i>co</i> -IPA- <i>co</i> -DEF)	23	77	1.8	2.07	18

<sup>a</sup> The heating and cooling rates were  $10^\circ\text{C min}^{-1}$ . The  $T_g$  values were determined by the second heating scan.

<sup>b</sup> After purification by reprecipitation in methanol or *n*-hexane. <sup>c</sup> Estimated by  $^1\text{H}$  NMR analysis of the obtained polymers after purification by reprecipitation in methanol or *n*-hexane. <sup>d</sup> Determined by GPC (polystyrene standards).

## Conclusion

Tandem polymerization consisting of cyclotrimerization and the Tishchenko reaction successfully proceeded using the catalyst mixture of  $\text{EtAlCl}_2$  and  $\text{Al}(\text{OiPr})_3$ . The cyclotrimerization was a side reaction in the cationic polymerization of VEs and aldehydes, while the cyclotrimerization was effectively used as a bond-forming reaction for producing polymers with cyclic acetal structures in the main chain. The obtained polymers with cyclic acetal and ester structures in the main chain were hydrolyzed under acidic or alkaline conditions. The composition ratios of cyclic acetal to ester structures were tuned by an initial catalyst molar ratio of  $\text{EtAlCl}_2$  and  $\text{Al}(\text{OiPr})_3$ . Interestingly, higher-MW polymers were obtained when TPA was used instead of IPA probably due to the decrease in cyclic oligomerization. Moreover, the three-component tandem polymerization of CEVE, IPA, and DEF yielded a polymer with cyclic acetal and two different ester structures in the main chain by transesterification reaction with DEF in addition to cyclotrimerization and Tishchenko reaction. The results obtained in this study will contribute to both the development of novel orthogonal tandem polymerization reactions consisting of different organic reactions as bond-forming reactions and the production of degradable polymers by different stimuli.

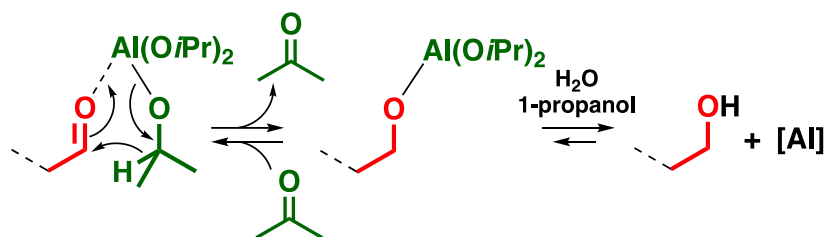
## Notes and References

1. Zhang, Y.; Zhao, Y.; Yang, B.; Zhu, C.; Wei, Y.; Tao, L. *Polym. Chem.* **2014**, *5*, 1857–1862.
2. Yang, B.; Zhao, Y.; Wei, Y.; Fu, C.; Tao, L. *Polym. Chem.* **2015**, *6*, 8233–8239.
3. von Czapiewski, M.; Gugau, K.; Todorovic, L.; Meier, M. A. R. *Eur. Polym. J.* **2016**, *83*, 359–366.
4. Xue, H.; Zhao, Y.; Wu, H.; Wang, Z.; Yang, B.; Wei, Y.; Wang, Z.; Tao, L. *J. Am. Chem. Soc.* **2016**, *138*, 8690–8693.
5. Kakuchi, R. *Polym. J.* **2019**, *51*, 945–953.
6. Lee, H.-K.; Bang, K.-T.; Hess, A.; Grubbs, R. H.; Choi, T.-L. *J. Am. Chem. Soc.* **2015**, *137*, 9262–9265.
7. Sample, C. S.; Kellstedt, E. A.; Hillmyer, M. A. *ACS Macro Lett.* **2022**, *11*, 608–614.
8. Xia, X.; Suzuki, R.; Gao, T.; Isono, T.; Satoh, T. *Nat. Commun.* **2022**, *13*, 163.
9. Aoshima, H.; Uchiyama, M.; Satoh, K.; Kamigaito, M. *Angew. Chem. Int. Ed.* **2014**, *53*, 10932–10936.
10. Kanazawa, A.; Kanaoka, S.; Aoshima, S. *J. Am. Chem. Soc.* **2013**, *135*, 9330–9333.
11. Higuchi, M.; Kanazawa, A.; Aoshima, S. *ACS Macro Lett.* **2020**, *9*, 77–83.
12. a) Mecerreyes, D.; Moineau, G.; Dubois, P.; Jérôme, R.; Hedrick, J. L.; Hawker, C. J.; Malmström, E. E.; Trollsas, M. *Angew. Chem. Int. Ed.* **1998**, *37*, 1274–1276. b) Mecerreyes, D.; Atthoff, B.; Boduch, K. A.; Trollsas, M.; Hedrick, J. L. *Macromolecules* **1999**, *32*, 5175–5182.
13. Nakatani, K.; Terashima, T.; Sawamoto, M. *J. Am. Chem. Soc.* **2009**, *131*, 13600–13601.
14. Higuchi, M.; Kanazawa, A.; Aoshima, S. *Macromolecules* **2020**, *53*, 3822–3831.
15. Johnson, J. A.; Finn, M. G.; Koberstein, J. T.; Turro, N. J. *Macromolecules* **2007**, *40*, 3589–3598.
16. Doran, S.; Yilmaz, G.; Yagci, Y. *Macromolecules* **2015**, *48*, 7446–7452.
17. Galbis, E.; de Paz, M. V.; McGuinness, K. L.; Angulo, M.; Valencia, C.; Galbis, J. A. *Polym. Chem.* **2014**, *5*, 5391–5402.
18. Matsumoto, S.; Kanazawa, A.; Kanaoka, S.; Aoshima, S. *J. Am. Chem. Soc.* **2017**, *139*, 7713–7716.
19. Lundberg, P.; Hawker, C. J.; Hult, A.; Malkoch, M. *Macromol. Rapid Commun.* **2008**, *29*, 998–1015.
20. Freudensprung, I.; Klapper, M.; Mullen, K. *Macromol. Rapid Commun.* **2016**, *37*, 209–214.

21. In references 19 and 20, the word "tandem polymerization" was explained to include polymerization systems consisting of two or more reactions proceeding simultaneously and/or orthogonally. The cyclotrimerization and the Tishchenko reaction are considered to proceed simultaneously and orthogonally in this study. Therefore, the polymerization demonstrated in this study can be regarded as tandem polymerization.
22. Arundale, E.; Mikeska, L. A. *Chem. Rev.* **1952**, *51*, 505–555.
23. Sabitha, G.; Reddy, K. B.; Bhikshapathi, M.; Yadav, J. S. *Tetrahedron Lett.* **2006**, *47*, 2807–2810.
24. Hirai, K.; Takeda, R.; Hutchison, J. A.; Uji-i, H. *Angew. Chem. Int. Ed.* **2020**, *59*, 5332–5335.
25. Luder, W. F.; Zuffanti, S. *Chem. Rev.* **1944**, *34*, 345–370.
26. Ogata, Y.; Kawasaki, A. *Tetrahedron* **1969**, *25*, 929–935.
27. Ooi, T.; Miura, T.; Takaya, K.; Muraoka, K. *Tetrahedron Lett.* **1999**, *40*, 7695–7698.
28. Matsuyama, T.; Yatabe, T.; Yabe, T.; Yamaguchi, K. *ACS Catal.* **2021**, *11*, 13745–13751.
29. Naito, T.; Kanazawa, A.; Aoshima, S. *Polym. Chem.* **2019**, *10*, 1377–1385.
30. Sweeny, W. J. *J. Appl. Polym. Sci.* **1963**, *7*, 1983–1989.
31. Yamaguchi, I.; Kimishima, T.; Osakada, K.; Yamamoto, T. *J. Polym. Sci., Part A: Polym. Chem.* **1997**, *35*, 1265–1273.
32. Onozawa, S.; Sakakura, T.; Tanaka, M.; Shiro, M. *Tetrahedron* **1996**, *52*, 4291–4302.
33. Karmel, I. S. R.; Fridman, N.; Tamm, M.; Eisen, M. S. *Organometallics* **2015**, *34*, 2933–2942.
34. Ishido, Y.; Aburaki, R.; Kanaoka, S.; Aoshima, S. *J. Polym. Sci., Part A: Polym. Chem.* **2010**, *48*, 1838–1843.
35. Ishido, Y.; Aburaki, R.; Kanaoka, S.; Aoshima, S. *Macromolecules* **2010**, *43*, 3141–3144.
36. Ishido, Y.; Kanazawa, A.; Kanaoka, S.; Aoshima, S. *J. Polym. Sci., Part A: Polym. Chem.* **2014**, *52*, 1334–1343.
37. Choi, S.-H.; Yashima, E.; Okamoto, Y. *Macromolecules* **1996**, *29*, 1880–1885.
38. Ren, T.; Chen, Q.; Zhao, C.; Zheng, Q.; Xie, H.; North, M. *Green Chem.* **2020**, *22*, 1542–1547.
39. Baker, R. H. *J. Am. Chem. Soc.* **1938**, *60*, 2673–2675.
40. Hoffmann R.; Brückner, R. *Chem. Ber.* **1992**, *125*, 1471–1484.
41. When 30 mM EtAlCl<sub>2</sub> and 10 mM Al(OiPr)<sub>3</sub> were used, the cyclotrimerization and Tishchenko reaction preferentially occurred at the early and later stage of polymerization, respectively. On the other hand, the difference in the reaction rates of both reactions was lowered when 40 mM EtAlCl<sub>2</sub> and 10 mM Al(OiPr)<sub>3</sub> were used, which resulted in the occurrence of the cyclotrimerization even at the later stage.
42. Meerwein, H.; Schmidt, R. *Justus Leibigs Ann. Chem.* **1925**, *444*, 221–238.
43. Ponndorf, W. *Angew. Chem.* **1926**, *39*, 138–143.
44. Flack, K.; Kitagawa, K.; Pollet, P.; Eckert, C. A.; Richman, K.; Stringer, J.; Dubay, W.; Liotta, C. L. *Org. Process Res. Dev.* **2012**, *16*, 1301–1306.
45. The integral ratio of peak 27 was determined by subtracting the integral ratio of the peak of a benzyl-type linear acetal (peak 17). The integral ratio of peak 17 was estimated from the integral ratios of peaks 13, 19, and 25.
46. Battistuzzi, G.; Cacchi, S.; Fabrizi, G. *Org. Lett.* **2003**, *5*, 777–780.
47. Michels, H.-P.; Nieger, M.; Vögtle, F. *Chem. Ber.* **1994**, *127*, 1167–1170.

48. Sawamoto, M. *Prog. Polym. Sci.* **1991**, *16*, 111–172.
49. Aoshima, S.; Kanaoka, S. *Chem. Rev.* **2009**, *109*, 5245–5287.
50. This mechanism is similar to the ring-opening polymerization of cyclic esters with  $\text{Al}(\text{OiPr})_3$  as the catalyst.<sup>51–53</sup> Another possible but minor pathway is the transesterification by a hydroxy group converted from the Al-bonded alkoxy group and protic impurities such as *i*PrOH and water.
51. Duda, A.; Penczek, S. *Macromolecules* **1995**, *28*, 5981–5992.
52. Mecerreyes, D.; Jérôme, R. *Macromol. Chem. Phys.* **1999**, *200*, 2581–2590.
53. Labet, M.; Thielemans, W. *Chem. Soc. Rev.* **2009**, *38*, 3484–3504.
54. A relatively large peak for an acetoxy group (peak 42 in Figure 9A) was observed in the  $^1\text{H}$  NMR spectrum of the polymer obtained by the three-component tandem polymerization. The acetoxy group was derived from the Tishchenko reaction between an aldehyde moiety and acetaldehyde, the latter of which was likely generated by the oxidation reaction [the reverse reaction of the MPV reduction (Scheme S1); Oppenauer oxidation] of ethanol eliminated from DEF.<sup>55</sup> The Tishchenko reaction of aliphatic aldehydes was reported to proceed faster than that of aromatic aldehydes.<sup>27</sup>
55. de Graauw, C. F.; Peters, J. A.; van Bekkum, H.; Huskens, J. *Synthesis* **1994**, 1007–1017.
56. Qu, W.; Ko, T. M.; Vora, R. H.; Chung, T. S. *Polymer* **2001**, *42*, 6393–6401.

### Supporting Information



**Scheme S1.** A postulated mechanism of the transformation of a formyl group into a hydroxy group after termination reaction (the MPV reduction).

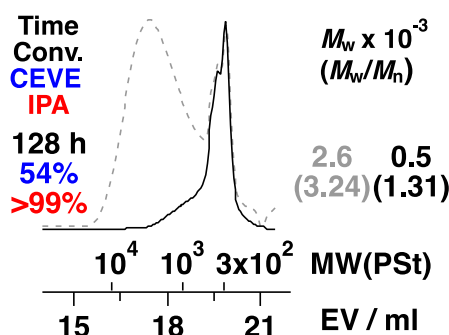


**Figure S1.** MWD curves of the obtained polymer (dashed line) by the tandem polymerization of CEVE and IPA and the low-MW fraction separated by preparative GPC (solid line) ( $[\text{CEVE}]_0 = 0.50$  M,  $[\text{IPA}]_0 = 0.70$  M,  $[\text{EtAlCl}_2]_0 = 30$  mM,  $[\text{Al}(\text{OiPr})_3]_0 = 10$  mM, in dichloromethane at  $0^\circ\text{C}$ ; a different sample from those shown in entry 3 in Table 2).

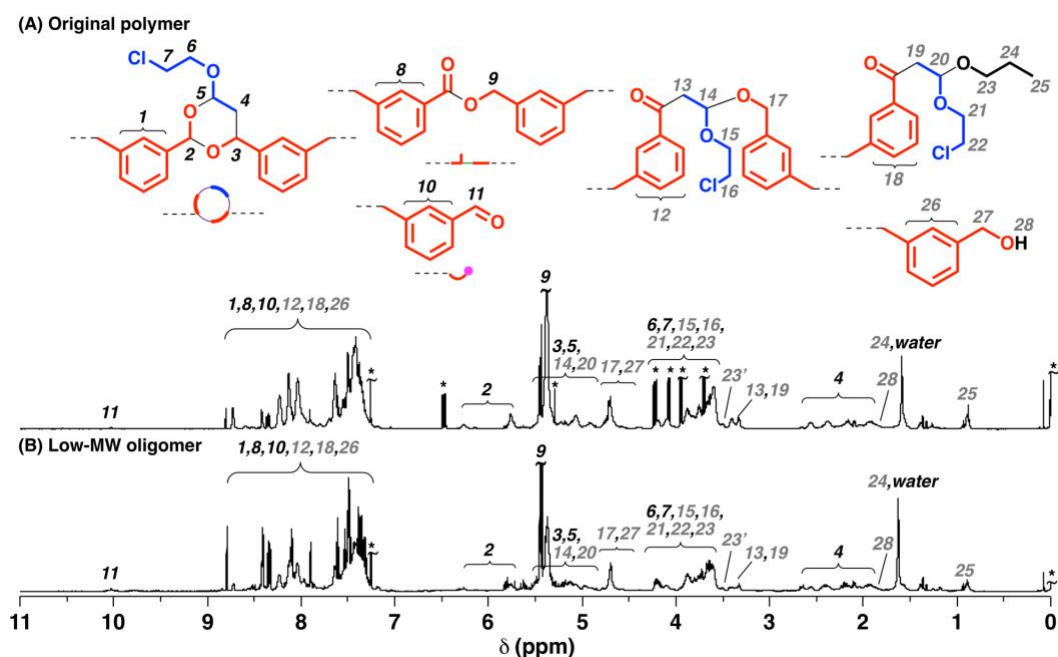


**Figure S2.**  $^1\text{H}$  NMR spectra of (A) the obtained polymer and (B) the low-MW fraction separated by preparative GPC (in  $\text{CDCl}_3$  at  $30^\circ\text{C}$ ;  $[\text{CEVE}]_0 = 0.50\text{ M}$ ,  $[\text{IPA}]_0 = 0.70\text{ M}$ ,  $[\text{EtAlCl}_2]_0 = 30\text{ mM}$ ,  $[\text{Al}(\text{OiPr})_3]_0 = 10\text{ mM}$ , in dichloromethane at  $0^\circ\text{C}$ ; a different sample from those shown in entry 3 in Table 2; \* solvents, residual monomer, water, grease, or TMS).

**Note for Figure S2.** In Figure S2B, the peaks of the remaining aldehyde and hydroxy moieties at polymer chain ends (peaks 11 and 27) are very small considering the MW determined by GPC. This result indicates that low molecular weight oligomers most likely had cyclic structures.

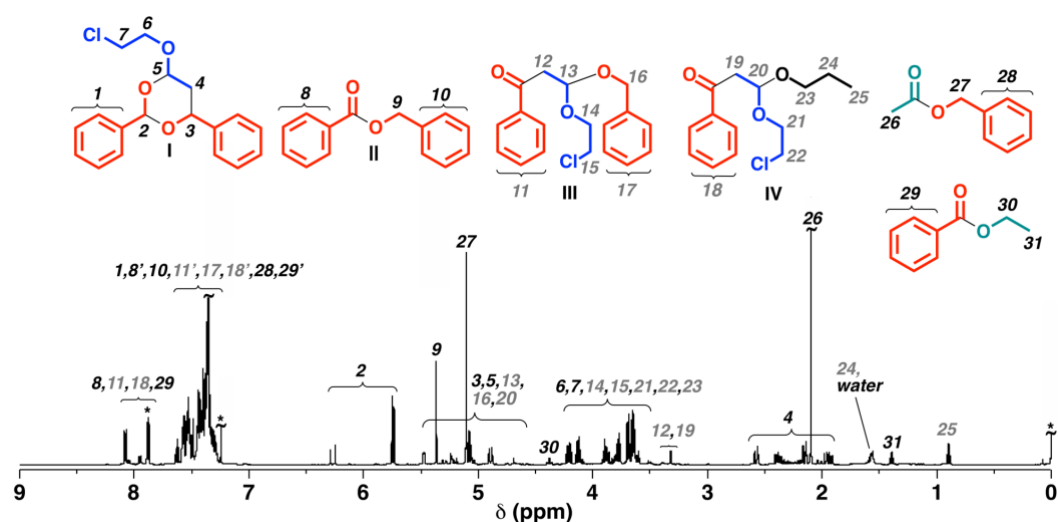


**Figure S3.**  $^1\text{H}$  NMR spectrum of the product obtained by the tandem reaction of CEVE and BzA in the presence of ethyl acetate (in  $\text{CDCl}_3$  at  $30^\circ\text{C}$ ;  $[\text{CEVE}]_0 = 0.50\text{ M}$ ,  $[\text{BzA}]_0 = 1.0\text{ M}$ ,  $[\text{ethyl acetate}]_0 = 1.0\text{ M}$ ,  $[\text{EtAlCl}_2]_0 = 30\text{ mM}$ ,  $[\text{Al}(\text{OiPr})_3]_0 = 10\text{ mM}$ , in dichloromethane at  $0^\circ\text{C}$ ; \* residual monomer,  $\text{CHCl}_3$ , or TMS).



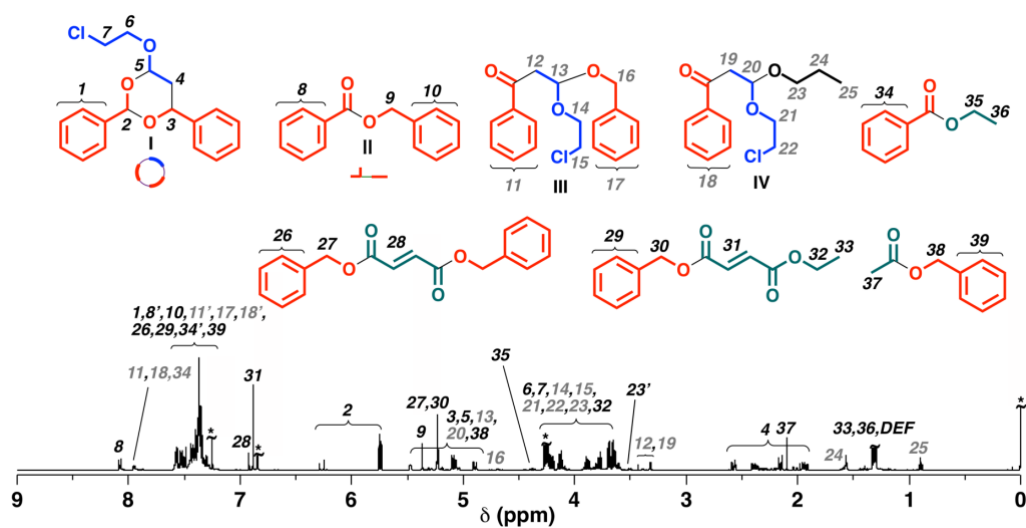


**Figure S4.**  $^1\text{H}$  NMR spectrum of the product obtained in the model reaction of CEVE, BzA, and DEF (in  $\text{CDCl}_3$  at  $30^\circ\text{C}$ ;  $[\text{CEVE}]_0 = 0.50\text{ M}$ ,  $[\text{BzA}]_0 = 1.0\text{ M}$ ,  $[\text{DEF}]_0 = 0.40\text{ M}$ ,  $[\text{EtAlCl}_2]_0 = 30\text{ mM}$ ,  $[\text{Al}(\text{O}i\text{Pr})_3]_0 = 10\text{ mM}$ , in dichloromethane at  $0^\circ\text{C}$  \*  $\text{CHCl}_3$ , residual monomer, or TMS; DEF: diethyl fumarate).

## **Part II**

### **Novel Sequence Periodic Polymer Synthesis Consisting of Cyclic Trimer Formation and Copolymerization with Vinyl Monomers**



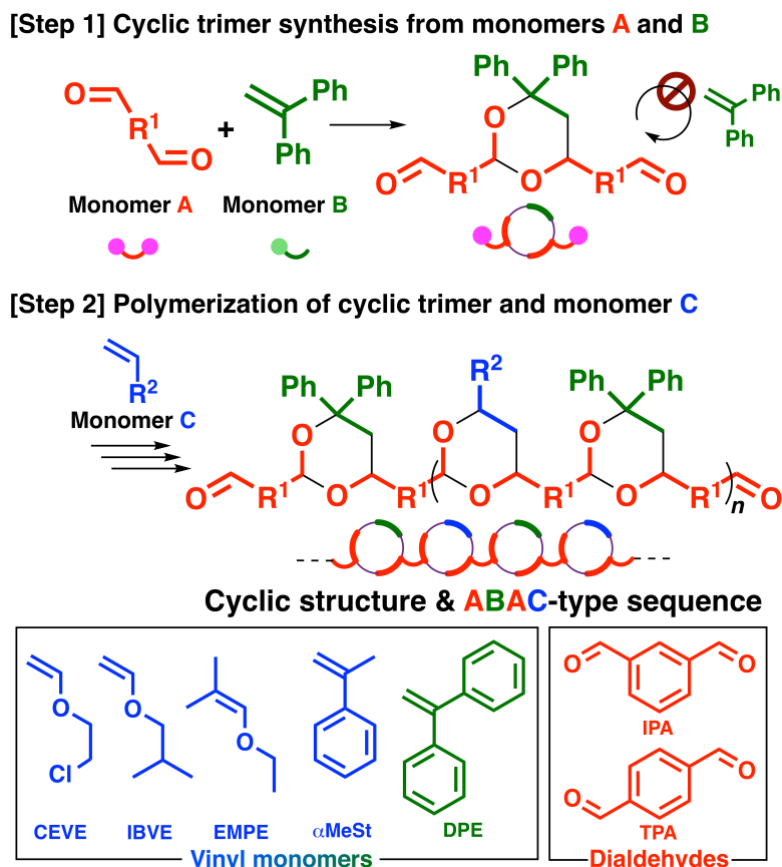
## *Chapter 4*

### **Two-step degradable ABAC-type periodic poly(cyclic acetal)s synthesized by sequence-programmed monomer formation and subsequent polyaddition based on cyclotrimerization of one vinyl monomer and two aldehydes**

#### **Introduction**

Monomer sequences greatly affect the functions and/or physical properties of polymers; for example, perfectly controlled monomer sequences in natural macromolecules, such as proteins and DNA, result in sophisticated functions.<sup>1–6</sup> Precisely controlling monomer sequences is a highly challenging goal in synthetic polymer chemistry, although a lower level of control, such as an alternating sequence, has been achieved by many studies.<sup>7–10</sup> In radical copolymerization, alternating copolymers are accessible by the copolymerizations of a pair of nonhomopolymerizable monomers, such as maleic anhydrides and  $\alpha$ -olefins.<sup>8–10</sup> The Aoshima's laboratory reported the alternating cationic copolymerization of vinyl ethers (VEs) and conjugated aldehydes,<sup>11–14</sup> the latter of which are nonhomopolymerizable due to the low ceiling temperature, such as benzaldehyde (BzA;  $-160\text{ }^{\circ}\text{C}$ ).<sup>15</sup> Alternating copolymers of VEs and conjugated aldehydes have acid-degradable acetal structures, which are derived from the crossover reaction from a VE to an aldehyde, in the main chain. As seen in the above examples, chain-growth polymerization is effective for alternating copolymer synthesis from two kinds of monomers. However, chain-growth polymerization is usually unsuitable for sequence regulation with more than two kinds of monomers (e.g., ABC- and ABAC-type periodic sequences) because a high selectivity is necessary for the addition reactions of each monomer with a specific propagating species.<sup>16–18</sup> Unlike chain-growth polymerization, step-growth polymerization based on selective multicomponent reactions is very suitable for synthesizing polymers with special monomer sequences.<sup>19–21</sup> For example, ABCB-type periodic terpolymers have been obtained by Passerini three-component polymerization.<sup>22,23</sup> In addition, ABAC-type periodic polymers have been synthesized by the chemoselective synthesis of polyurethanes using bis(six-membered cyclic carbonate) and two different diamines.<sup>24</sup> Successful reports on ABAC-type periodic polymerization are very limited.

The author has reported the synthesis of polymers with cyclic acetal structures in the main chain by the step-growth type, successive cyclotrimerization of VEs and dialdehydes in Chapter 2 of this thesis.<sup>25</sup> This polymerization starts via the generation of a cyclic trimer from a VE and two dialdehydes. The cyclic trimer contains two aldehyde moieties; hence, subsequent reactions proceed via cyclotrimerizations of a VE with dialdehydes as well as the cyclic trimers, oligo(cyclic trimer)s, and poly(cyclic trimer)s, resulting in an alternating copolymer of VE and dialdehyde.



**Scheme 1.** ABAC-type sequence-regulated poly(cyclic acetal)s using various vinyl monomers and dialdehydes.

In this study, the author devised a strategy to synthesize polymers with ABAC-type periodic sequences based on the cyclotrimerization of vinyl monomers and dialdehydes. If a cyclic trimer is selectively obtained without generating oligo(cyclic trimer)s (step 1 in Scheme 1), ABAC-type periodic polymers can be obtained by the subsequent cyclotrimerizations of the cyclic trimer with a different vinyl monomer from that used for the cyclic trimer synthesis (step 2 in Scheme 1). An essential requirement for efficient synthesizing a cyclic trimer is suppressing the successive cyclotrimerization and vinyl homopolymerization. Selecting an appropriate vinyl monomer, which effects the steric hindrance and electronic property of a resulting cyclic acetal structure, is probably essential for achieving single cyclotrimerization with high selectivity. Cyclotrimerization is initiated by the coordination of a catalyst with an aldehyde molecule, which provokes the reaction of the activated carbonyl carbon and a vinyl monomer.<sup>26–28</sup> The generated carbocation reacts with another aldehyde molecule, producing a carbocation. This carbocation subsequently reacts with the oxygen atom coordinated with the catalyst to yield a cyclic trimer. Considering this mechanism, styrene (St) derivatives with low reactivity and/or large steric hindrance may be promising as monomers for selective cyclotrimerization with dialdehydes.

The synthesis of ABAC-type periodic polymer was examined by performing a procedure that involved screening suitable monomers for selective cyclic trimer formation and subsequent polymerization of the cyclic trimer with a vinyl monomer. Various VEs and St derivatives were reacted, and 1,1-diphenylethylene (DPE) was found to be suitable for highly selective cyclotrimerization with isophthalaldehyde (IPA) as a result.

The obtained cyclic trimer consisting of DPE and IPA was subsequently copolymerized with VEs via cyclotrimerization, which resulted in polymers with ABAC-type periodic sequences. Interestingly, the copolymers exhibited two-step acid degradation behavior due to the difference in acid degradability between DPE- and VE-derived cyclic acetal structures. In addition, the copolymers exhibited high glass transition temperatures ( $T_g$ s) because of the rigidity of the cyclic acetal structures in the main chain.

## **Experimental Section**

### **Materials**

1,4-Dioxane (Nacalai Tesque; 99.5%) was distilled over calcium hydride and then lithium aluminum hydride.  $\alpha$ -Methylstyrene ( $\alpha$ MeSt; Nacalai Tesque, >98.0%) was distilled twice over calcium hydride under reduced pressure. Other materials were prepared and used as described in Chapter 2.

### **Synthesis of the sequenced-programmed cyclic trimer**

The following is a description of the typical reaction procedure. A glass tube equipped with a three-way stopcock was dried using a heat gun (Ishizaki; PJ-206A; blow temperature of  $\sim 450$  °C) under dry nitrogen. IPA was added to the tube in an  $N_2$ -filled glove box (DBO-1B; MIWA MFG Co., Ltd). Dichloromethane and DPE were sequentially added to this tube using dry syringes. The reaction was initiated by the addition of a prechilled  $GaCl_3$  solution ( $5.0 \times 10$  mM) in dichloromethane/*n*-hexane. After a predetermined time, the reaction was terminated by adding water that contained a small amount of ammonia. The quenched mixture was washed with water. Then, the volatile compounds were removed under reduced pressure at 50 °C. The crude product was purified by silica gel column chromatography (toluene/ethyl acetate (10/1 v/v)). When the obtained product contained significant fractions of impurities, it was recrystallized with *n*-hexane and toluene (white solid; melting point = 170–178 °C).

### **Polymerization procedure**

The following is a description of the typical polymerization procedure. A glass tube equipped with a three-way stopcock was dried using a heat gun under dry nitrogen. A solution of a cyclic trimer consisting of DPE and dialdehydes in dichloromethane was added to the tube using a dry syringe. This cyclic trimer was dried via azeotropic method using toluene for approximately 6 h. Dichloromethane, 1,4-dioxane, and 2-chloroethyl VE (CEVE) were sequentially added to this tube using dry syringes. The polymerization was initiated by adding a prechilled  $EtAlCl_2$  solution ( $5.0 \times 10^2$  mM) in dichloromethane/hexane. After a predetermined time, the reaction was terminated by adding a methanol solution that contained a small amount of aqueous ammonia. The quenched mixture was washed with water. Then, the volatile compounds were removed under reduced pressure at 50 °C to yield a polymer. The conversions of monomer and formyl group were determined by  $^1H$  NMR analysis of the quenched reaction mixture using *n*-hexane, pyridine, or THF as an internal standard.

### **Acid hydrolysis**

Acid hydrolysis of the polymer was conducted with 0.9 M HCl (aq) in 1,2-dimethoxyethane at 30 or 60 °C for a predetermined time. The quenched mixture was diluted with dichloromethane and successively

washed with an aqueous sodium hydroxide solution and water. The volatiles were removed under atmospheric pressure at room temperature.

## Characterization

Thermogravimetric analysis (TGA) was conducted with a HITACHI NEXTA STA300.  $M_w$ ,  $M_w/M_n$ ,  $^1\text{H}$  NMR spectra, ESI-MS spectra, and differential scanning calorimetry (DSC) data were obtained in a manner similar to that described in preceding chapters.

## Results and Discussion

### *Synthesis of sequence-programmed cyclic trimers with two unreacted aldehyde moieties*

Cyclotrimerization using various vinyl monomers and IPA (step 1 in Scheme 1) was conducted to obtain cyclic trimers with high selectivity. First, the cyclotrimerization of CEVE or isobutyl VE (IBVE) with IPA was conducted using  $\text{EtAlCl}_2$  as a Lewis acid catalyst at 0 °C (entries 1 and 2 in Table 1). Chapter 2 demonstrated that CEVE was effective for polymerization via successive cyclotrimerization when the concentrations of CEVE and IPA were equal.<sup>25</sup> In the present experiments, the concentration of IPA was twice that of CEVE to both promote the cyclotrimerization of one CEVE and two IPA molecules and suppress the successive trimerizations. However, the products contained both cyclic trimers and noticeable amounts of oligomers [the number-average degree of polymerization ( $\text{DP}_n$ ) = 1.5 (CEVE) or 1.9 (IBVE)] (see Figure S1 for the molecular weight distribution (MWD) curves of the obtained oligomers). The results indicate that the successive cyclotrimerization of the resulting cyclic trimers was suppressed, probably because the VE-derived cyclic trimer exhibited comparable reactivity to that of IPA.

**Table 1.** Synthesis of cyclic trimers using various vinyl monomers and dialdehydes <sup>a</sup>

entry	vinyl monomer	(M)	dialde- hyde	(M)	temp. (°C)	time (h)	conv. (%) <sup>b</sup>		$M_w \times 10^{-3}$ <sup>c</sup>	$M_w/M_n$ <sup>c</sup>	cyclic trimer formation/ polymerization/ others <sup>d</sup>	DP <sub>n</sub> <sup>d</sup>
							vinyl monomer	dialde- hyde				
1	CEVE	0.15	IPA	0.30	0	4	60	49	0.5	1.43	n.d. <sup>e</sup>	1.5
2	IBVE	0.15	IPA	0.30	0	1	>99	53	0.7	1.49	n.d. <sup>e</sup>	1.9
3	DPE	0.15	IPA	0.30	−78	72	>99	56	1.6	1.36	8/91/1	3.2
4		0.15		0.30	0	24	70	58	0.4	1.23	63/31/6	1.2
5		0.20		0.30	0	24	54	57	0.4	1.20	54/38/8	1.3
6	DPE	0.20	TPA	0.30	0	24	51	54	0.5	1.27	40/55/5	1.3

<sup>a</sup>  $[\text{EtAlCl}_2]_0 = 50$  (entries 1 and 2) or 0 (entries 3–6) M,  $[\text{GaCl}_3]_0 = 0$  (entries 1 and 2), 10 (entry 3), or 5.0 (entries 4–6) M,  $[\text{THF}] = 1.0$  (entries 1 and 2) or 0 (entries 3–6) M, in dichloromethane. <sup>b</sup> Determined by  $^1\text{H}$  NMR analysis of the quenched reaction mixtures (entries 1–3) or obtained products (entries 4–6). <sup>c</sup> Determined by gel permeation chromatography (GPC) (polystyrene standards). <sup>d</sup> Estimated by  $^1\text{H}$  NMR analysis of the obtained products. The ratio of products other than the cyclic trimers was standardized based on the number of DPE units. <sup>e</sup> Not determined because the peaks of the cyclic trimer overlapped with those of other products derived from successive cyclotrimerization.

The author next focused on St derivatives instead of VEs. To optimize the reaction conditions, model reactions were conducted using *p*-methylstyrene (pMeSt),  $\alpha$ MeSt, and DPE as St derivatives in conjunction with BzA as a conjugated monoaldehyde in the presence of various Lewis acid catalysts, such as EtAlCl<sub>2</sub>, Bi(OTf)<sub>3</sub>, and GaCl<sub>3</sub>. As a result, DPE underwent selective cyclotrimerization with BzA when GaCl<sub>3</sub>, which exhibited strong acidity compared to that of EtAlCl<sub>2</sub>, was used as a Lewis acid catalyst at –78 °C.

Based on the model reactions, the synthesis of cyclic trimers was conducted using DPE and IPA under the optimized conditions. However, the reaction of DPE and IPA with GaCl<sub>3</sub> at –78 °C resulted in polymer (oligomer) formation ( $M_w = 1.6 \times 10^3$ ; entry 3 in Table 1 and Figure 1A) rather than a selective generation of cyclic trimer. In contrast, the cyclic trimer was selectively generated at 0 °C because of the large steric hindrance of the two phenyl rings, resulting in cyclic trimer formation/polymerization by successive trimerization/other reactions ratios of 63/31/6 (entry 4 in Table 1). When terephthalaldehyde (TPA), a *para*-disubstituted dialdehyde, was used instead of IPA, the cyclic trimer was also produced, but the yield of the cyclic trimer decreased, likely because successive cyclotrimerization frequently occurred (entry 6 in Table 1).

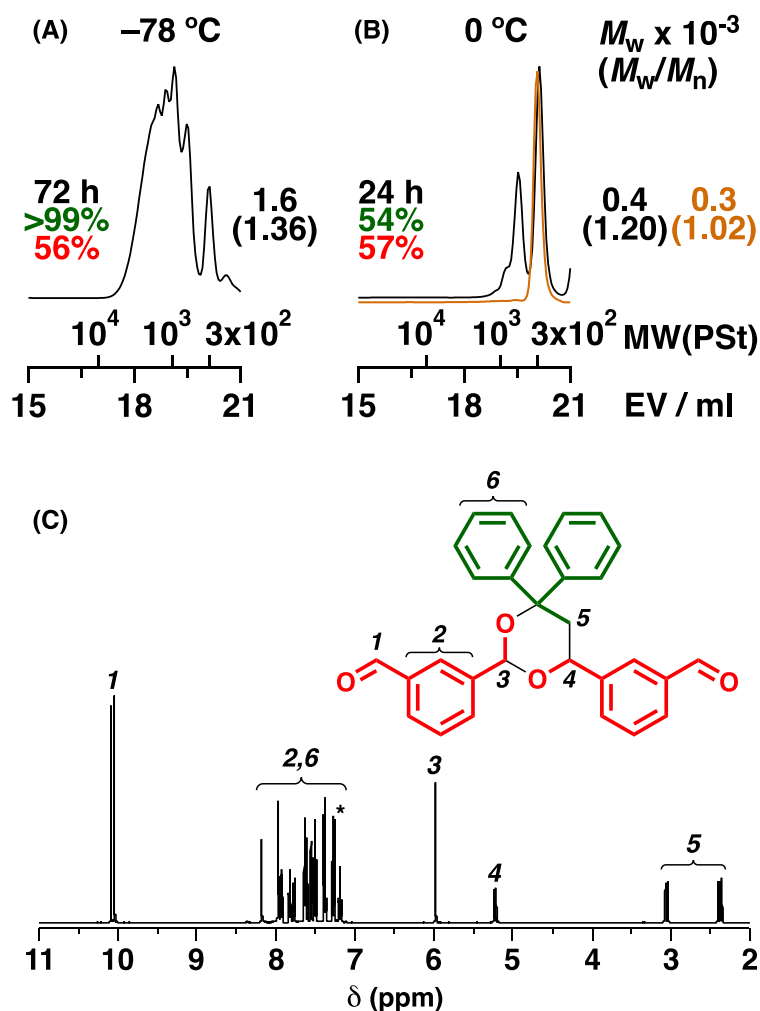


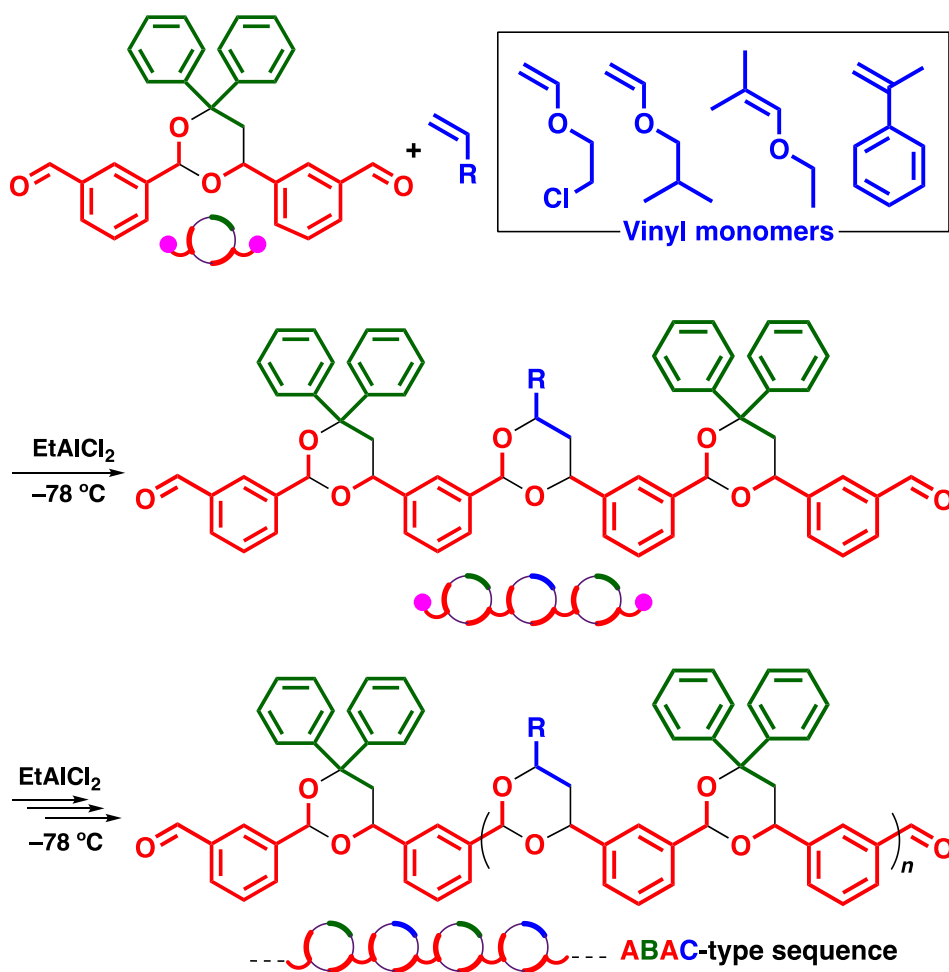
**Figure 1.** MWD curves of the obtained products after cyclotrimerization of DPE and IPA (black) at (A) –78 (entry 3 in Table 1) or (B) 0 (entry 5 in Table 1) °C and the cyclic trimer separated by silica gel column chromatography and recrystallization (orange). (C) <sup>1</sup>H NMR spectrum of the separated cyclic trimer (in CDCl<sub>3</sub> at 30 °C; \* CHCl<sub>3</sub>).



The MWD curves of the obtained products using DPE and IPA at 0 °C showed multimodal peaks in the low-MW region (black curve in Figure 1B; entry 5 in Table 1 as an example). The largest peak was assigned to the cyclic trimer, while the higher-MW peaks were due to oligomers resulting from successive cyclotrimerizations. The cyclic trimer was successfully separated by silica gel column chromatography (orange curve in Figure 1B). The isolation of the pure cyclic trimer was confirmed by  $^1\text{H}$  NMR analysis (Figure 1C). The integral ratios of the aldehyde peak (peak 1) and the peak of the acetal methine proton (peak 3) were accurately 2.0, which indicated that an oligomer and other side products were completely removed.

ABAC-type periodic polymerization of CEVE and a cyclic trimer consisting of DPE–IPA or DPE–TPA

The above-obtained cyclic trimers are regarded as ABA-type sequence-programmed cyclic acetal monomers consisting of two dialdehydes (unit A) and one DPE (unit B). This cyclic trimer possesses two unreacted aldehyde moieties. The remaining reactive sites potentially undergo successive cyclotrimerization with VEs or St derivatives (unit C) and thus result in ABAC-type periodic poly(cyclic acetal)s (Scheme 2). ABAC-type polymers have two different kinds of cyclic acetal structures as well as two phenyl rings and vinyl monomer-derived side chains that are alternately arranged. Such polymers show the potential to exhibit characteristic degradability and good thermal properties because of the acid degradability and rigidity of cyclic acetal structures.



**Scheme 2.** Successive cyclotrimerization of the sequence programmed cyclic trimer and vinyl monomers.

**Table 2.** ABAC-type sequence-regulated polymerization of VEs and the cyclic trimers <sup>a</sup>

entry	vinyl monomer	(M)	cyclic trimer	cyclic trimer (M)	temp. (°C)	time	conv. (%) <sup>b</sup>		$M_w \times 10^{-3}^c$	$M_w/M_n^c$	cyclotrimerization/others <sup>d</sup>
							vinyl monomer	cyclic trimer			
1	CEVE	0.50	DPE-IPA	0.50	0	24 h	26	71	0.9	1.28	64/36
2		0.20	DPE-IPA	0.20	-78	24 h	94	>99	7.5	2.84	97/3
3	IBVE	0.20	DPE-IPA	0.20	-78	15 min	>99	>99	5.7	2.50	93/7
4	$\alpha$ MeSt	0.30	DPE-IPA	0.30	-40	196 h	56	98	1.2	1.16	80/20
5	CEVE	0.20	DPE-TPA	0.20	-78	24 h	88	>99	7.5	2.19	94/6

<sup>a</sup> [EtAlCl<sub>2</sub>]<sub>0</sub> = 50 (entries 1–3 and 5) or 0 (entry 4) mM, [Bi(OTf)<sub>3</sub>]<sub>0</sub> = 0 (entries 1–3 and 5) or 10 (entry 4) mM, [THF] = 1.0 (entry 1), 0 (entries 2, 3, and 5), or 0.54 (entry 4) M, [1,4-dioxane] = 0 (entries 1 and 4) or 1.0 (entries 2, 3, and 5) M, in dichloromethane. <sup>b</sup> Determined by <sup>1</sup>H NMR analysis of the quenched reaction mixtures. <sup>c</sup> Determined by GPC (polystyrene standards). <sup>d</sup> Estimated by <sup>1</sup>H NMR analysis of the obtained products after purification by reprecipitation in methanol.

First, the cyclotrimerization of CEVE and the cyclic trimer consisting of DPE and IPA was conducted with EtAlCl<sub>2</sub> in the presence of THF in dichloromethane at 0 °C (entry 1 in Table 2). These conditions were the most suitable for the polyaddition of CEVE and IPA in Chapter 2.<sup>25</sup> The cyclotrimerization somehow selectively proceeded; however, VE homopolymerization also occurred as a side reaction (selectivity of cyclotrimerization: 64%), and the conversion was low, resulting in oligomers of  $M_w = 0.9 \times 10^3$ . To promote cyclotrimerization, the polymerization temperature was lowered to -78 °C (entry 2 in Table 2), which was inspired by the unsuppressed cyclotrimerization of DPE and IPA at low temperatures (vide supra, entry 3 in Table 1). Compared to THF, 1,4-dioxane is a weaker Lewis base;<sup>29,30</sup> thus, 1,4-dioxane was used instead of THF. Under these conditions, cyclotrimerization was obviously promoted, resulting in a polymer with an  $M_w$  of  $7.5 \times 10^3$ . Moreover, the selectivity of the cyclotrimerization was improved to 97%.<sup>31</sup>

The time course of the polymerization was investigated, as shown in Figure 2. Both monomers were smoothly consumed to reach near quantitative conversion in 24 h (Figure 2A). The remaining aldehyde moieties (square symbols in Figure 2A), which were present in the monomer, oligomer, and polymer, were gradually consumed even after the cyclic trimer was completely consumed, which indicated that reactions between oligomers (polymers) and oligomers (polymers) mainly occurred at the later stage of polymerization. Importantly, the polymerization proceeded in a step-growth manner, which was supported by an exponential increase in the  $M_w$  values in the later stage of polymerization (Figure 2B). Furthermore, the MWD curves shifted to the higher-MW region as the monomer conversion increased (Figure 2C).

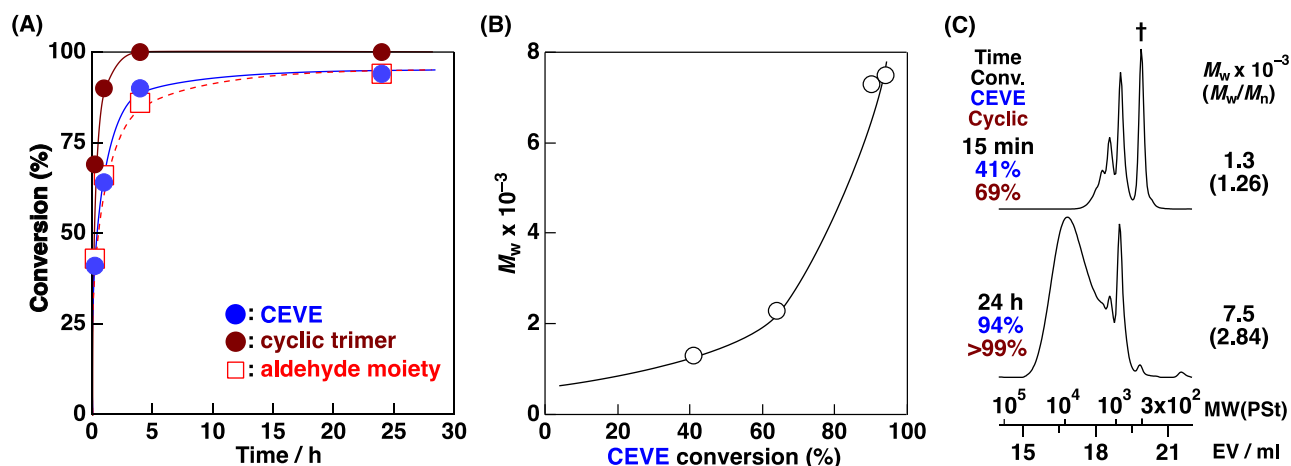


**Figure 2.** (A) Time–conversion curves of the polymerization of CEVE and the cyclic trimer consisting of DPE and IPA, (B)  $M_w$  values, and (C) MWD curves of the obtained polymers (entry 2 in Table 2;  $[\text{CEVE}]_0 = 0.20$  M,  $[\text{cyclic trimer (DPE-IPA)}]_0 = 0.20$  M,  $[\text{EtAlCl}_2]_0 = 50$  mM,  $[\text{1,4-dioxane}] = 1.0$  M, in dichloromethane at  $-78$  °C; † unreacted cyclic trimer).

The  $^1\text{H}$  NMR spectrum of the obtained polymer (Figure 3A) indicated that the obtained polymer was generated by successive cyclotrimerization. The spectrum contained peaks with similar chemical shifts to those of both poly(DPE-*co*-IPA) (Figure 3B) and poly(CEVE-*co*-IPA) (Figure 3C). For example, the peaks at 5.9 ppm (peak 2) were assigned to the methine proton adjacent to two oxygen atoms of the cyclic acetal structures consisting of DPE. The diastereotopic methylene protons (peak 4) of the cyclic acetal structures exhibited peaks at 2.4 and 3.0 ppm. The acetal methine and diastereotopic methylene protons of the CEVE-derived cyclic acetal structures exhibited peaks at 5.7–6.3 ppm (peak 7) and 1.8–2.6 ppm (peak 9), respectively. Additionally, the peaks of the CEVE side chains (peaks 11 and 12) emerged at 3.5–4.3 ppm. These results were also confirmed by the  $^{13}\text{C}$  NMR spectra of the three polymers. Furthermore, the number average degree of polymerization ( $\text{DP}_n$ ) was determined to be 17 from the peak integral ratio of the methine protons of cyclic acetal structures (peaks 2 and 7) and the chain end protons of the aldehyde moieties [peak 14; the methoxy peak (peak 17) converted from aldehyde moieties by the reaction with methanol quencher was also used]. The experimental integral ratios of all the peaks were relatively consistent with the theoretical values calculated from the estimated  $\text{DP}_n$  value (17), which supported that the ABAC-type periodic poly(cyclic acetal) was successfully obtained. In addition, the ESI-MS spectrum (Figure S2) contained a series of peaks with constant intervals of  $m/z = 554$ , which agrees with the total molar mass of one CEVE and one cyclic trimer.

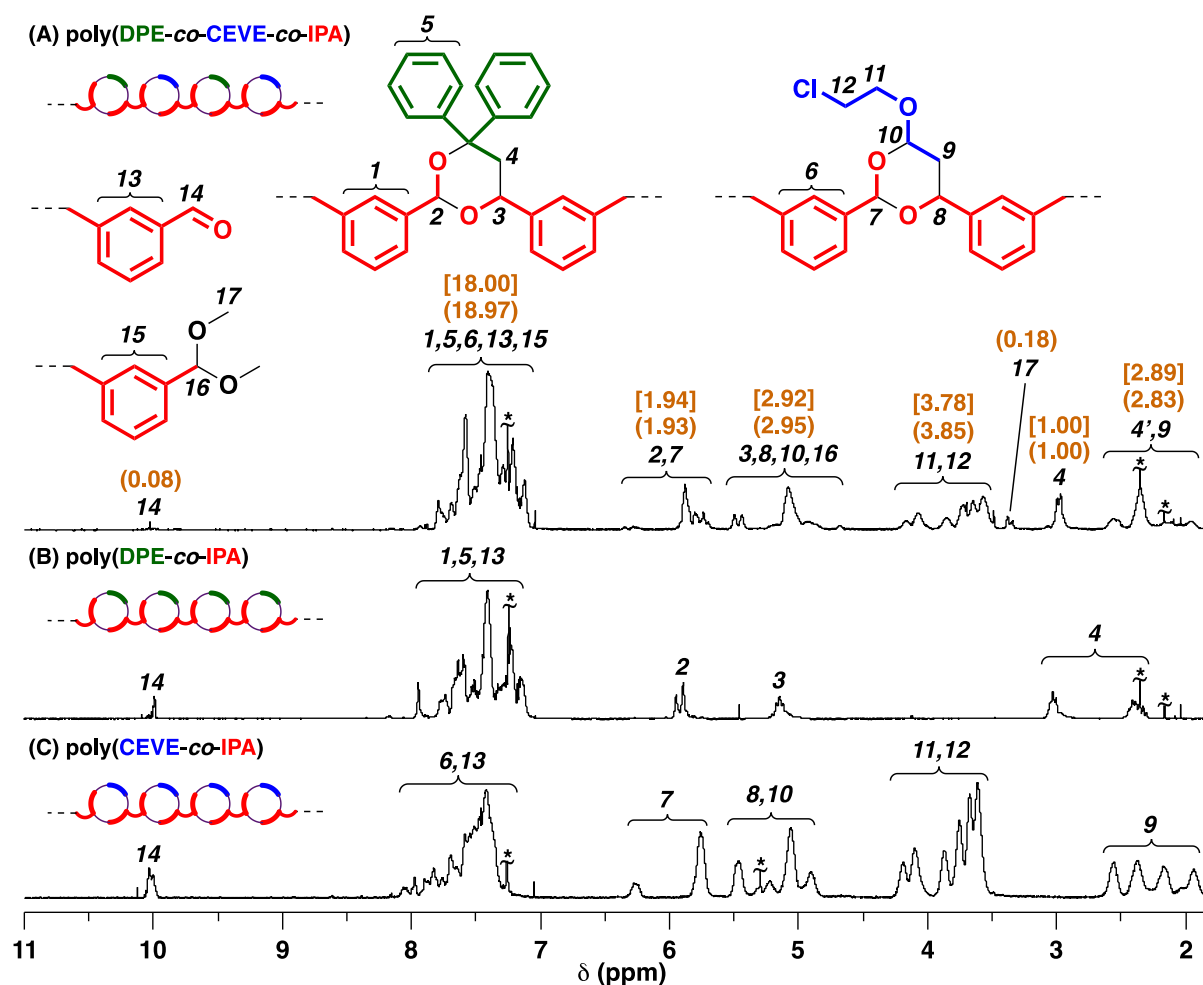


**Figure 3.** <sup>1</sup>H NMR spectra of (A) the polymer obtained by the copolymerization of CEVE and the cyclic trimer consisting of DPE and IPA (entry 2 in Table 2), (B) poly(DPE-co-IPA) [ $M_w(\text{GPC}) = 2.2 \times 10^3$ ,  $M_w/M_n(\text{GPC}) = 1.51$ ;  $[\text{DPE}]_0 = 0.40$  M,  $[\text{IPA}]_0 = 0.20$  M,  $[\text{GaCl}_3]_0 = 10$  mM, in dichloromethane at  $-78$  °C; after purification by reprecipitation in methanol], and (C) poly(CEVE-co-IPA) [ $M_w(\text{GPC}) = 2.3 \times 10^3$ ,  $M_w/M_n(\text{GPC}) = 1.62$ ;  $[\text{CEVE}]_0 = 0.50$  M,  $[\text{IPA}]_0 = 0.50$  M,  $[\text{EtAlCl}_2]_0 = 50$  mM,  $[\text{THF}] = 1.0$  M, in dichloromethane at  $0$  °C; after purification by reprecipitation in methanol] (in  $\text{CDCl}_3$  at  $30$  °C; \*  $\text{CHCl}_3$ , dichloromethane, or others; numbers written in orange parentheses: the observed integral ratio; numbers written in orange square brackets: the theoretical integral ratios of the ABAC-type sequence-regulated polymer with a  $\text{DP}_n$  value of 17).

When IBVE, a more reactive VE than CEVE, was used for copolymerization, the MW of the obtained polymer decreased due to the decreased selectivity of cyclotrimerization (entry 3 in Table 2). In contrast to CEVE, the highly reactive VE preferentially underwent homopolymerization.  $\alpha\text{MeSt}$  underwent copolymerization with the cyclic trimer; however, a low-MW oligomer ( $M_w = 1.2 \times 10^3$ ) was obtained rather than a polymer, likely because of the steric hindrance of the methyl substituent on the  $\alpha$ -carbon (entry 4 in Table 2). Furthermore, the cyclic trimer consisting of DPE and TPA was found to undergo successive cyclotrimerization with CEVE under the same conditions as those for the cyclic trimer that contained DPE and IPA (entry 5 in Table 2). The MWD curve and <sup>1</sup>H and <sup>13</sup>C NMR spectra indicated that the obtained polymer exhibited an MW and structure similar to those obtained from its IPA counterpart.

ABAC-type periodic polymer synthesis from EMPE and cyclic trimers

The above result suggested that a low reactive VE was important for suppressing side reactions, such as VE homopolymerization. The author anticipated that ethyl 2-methyl-1-propenyl ether (EMPE), which is a  $\beta,\beta$ -dimethyl VE that does not homopolymerize or copolymerize with aromatic aldehydes,<sup>14,32,33</sup> may undergo more selective cyclotrimerization with cyclic trimers than that of CEVE. Therefore, copolymerization of EMPE and the cyclic trimer consisting of DPE and IPA was conducted under the same conditions as those for copolymerization with CEVE (entry 1 in Table 3). The copolymerization successfully proceeded (Figure 4A), which resulted in a polymer with a higher MW than that obtained with the CEVE counterpart (Figure 4B). <sup>1</sup>H NMR analysis (Figure 4C) indicated that the polymer contained ABAC-type periodic sequences consisting of EMPE, DPE, and IPA, which was also supported by the <sup>1</sup>H NMR spectra of poly(DPE-*co*-IPA) and poly(EMPE-*co*-IPA) (Figure 4D and E). The selective reaction with EMPE is consistent with a previous study on the successive cyclotrimerization of EMPE and bifunctional conjugated aldehydes (Chapter 2).<sup>25</sup> A polymer of  $M_w = 14.3 \times 10^3$  was obtained at the EMPE concentration = 0.30 M (entry 3 in Table 3). In addition, the copolymerization of EMPE and a cyclic trimer consisting of DPE and TPA was conducted under the same conditions as those for the synthesis of poly(EMPE-*co*-DPE-*co*-IPA) (entry 4 in Table 3), which resulted in a polymer of  $M_w = 17.1 \times 10^3$  [see Figure 5 for the MWD curve and <sup>1</sup>H NMR spectrum of poly(EMPE-*co*-DPE-*co*-TPA)]. The generation of the higher-MW polymer is likely attributed to the suppression of intramolecular cyclization as in the case of on the tandem polymerization consisting of cyclotrimerization and the Tishchenko reaction (Chapter 3).<sup>34</sup>

**Table 3.** ABAC-type sequence regulated polymerization of EMPE and the cyclic trimers <sup>a</sup>

entry	EMPE (M)	cyclic trimer	cyclic trimer (M)	temp. (°C)	time (h)	conv. (%) <sup>b</sup>		$M_w$ $\times 10^{-3}$ <sup>c</sup>	$M_w/M_n$ <sup>c</sup>	cyclotrimerization/ others <sup>d</sup>
						EMPE	cyclic trimer			
1	0.20	DPE-IPA	0.20	-78	24	>99	>99	9.3	2.78	>99/~0
2	0.20	DPE-IPA	0.20	-100	24	98	97	8.3	2.52	>99/~0
3	0.30	DPE-IPA	0.20	-78	24	77	>99	14.3	2.86	90/10
4	0.20	DPE-TPA	0.20	-78	24	98	>99	17.1	2.88	>99/~0

<sup>a</sup> [EtAlCl<sub>2</sub>]<sub>0</sub> = 50 (entries 1, 2, and 4) or 54 (entry 3) mM, [1,4-dioxane] = 1.0 (entries 1, 2, and 4) or 0.98 (entry 3) M, in dichloromethane. <sup>b</sup> Determined by <sup>1</sup>H NMR analysis of the quenched reaction mixtures. <sup>c</sup> Determined by GPC (polystyrene standards). <sup>d</sup> Estimated by <sup>1</sup>H NMR analysis of the obtained products after purification by reprecipitation in methanol.

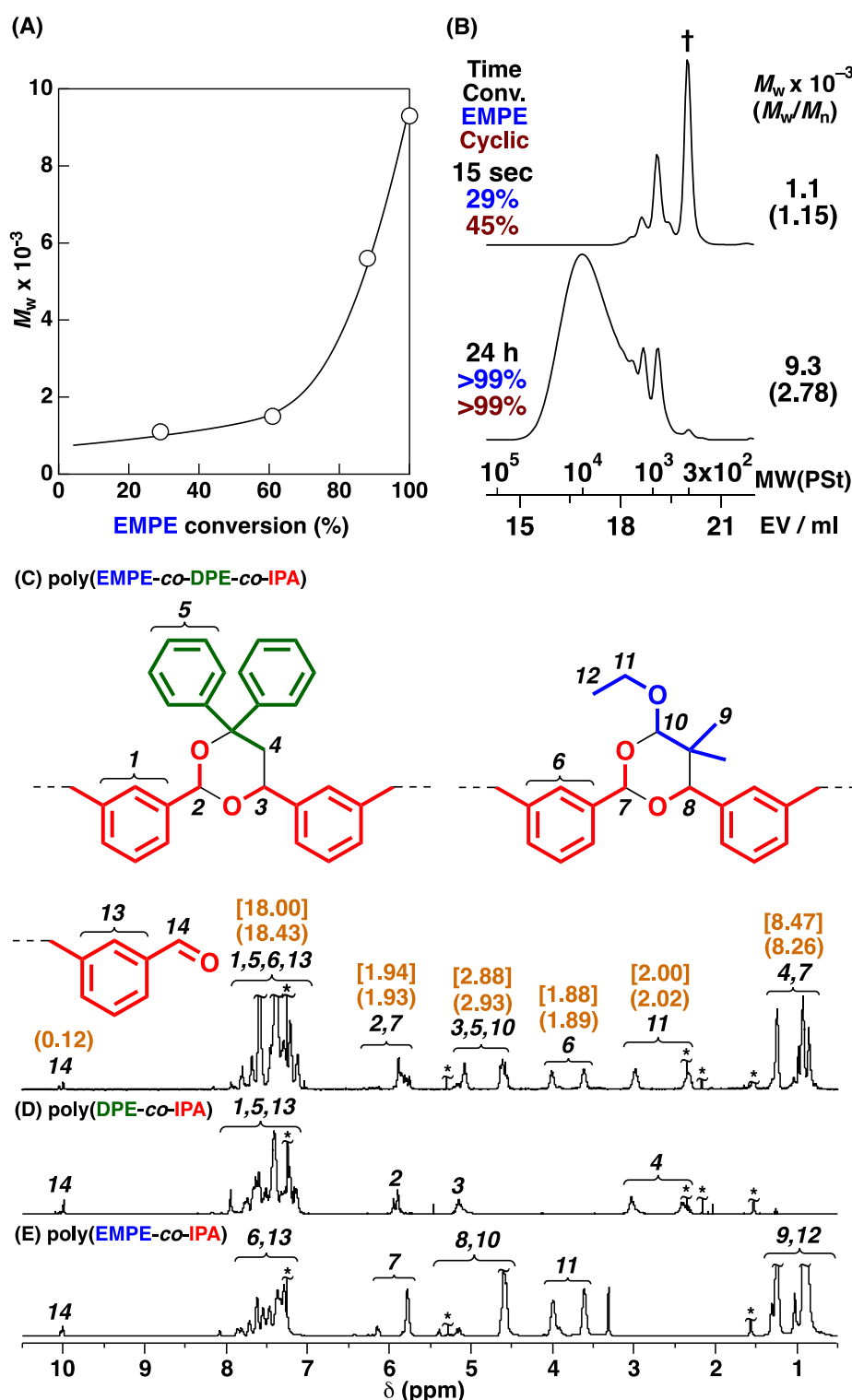


**Figure 4.** (A)  $M_w$  values, (B) MWD curves, and  $^1H$  NMR spectra (after purification by reprecipitation in methanol) of the polymers obtained by the successive cyclotrimerization of (C) EMPE and the cyclic trimer (entry 1 in Table 3; after purification by reprecipitation in methanol), (D) DPE and IPA (the same  $^1H$  NMR spectrum as that shown in Figure 3B), and (E) EMPE and IPA [ $M_w(GPC) = 3.7 \times 10^3$ ,  $M_w/M_n(GPC) = 1.37$ ;  $[EMPE]_0 = 0.50$  M,  $[IPA]_0 = 0.50$  M,  $[EtAlCl_2]_0 = 50$  mM,  $[THF] = 1.0$  M, in dichloromethane at 0 °C; after purification by reprecipitation in methanol] (in  $CDCl_3$  at 30 °C; \*  $CHCl_3$ , dichloromethane, water, or others; numbers written in orange parentheses: the observed integral ratio; numbers written in orange square brackets: the theoretical integral ratio of the ABAC-type periodic polymer; † unreacted cyclic trimer).

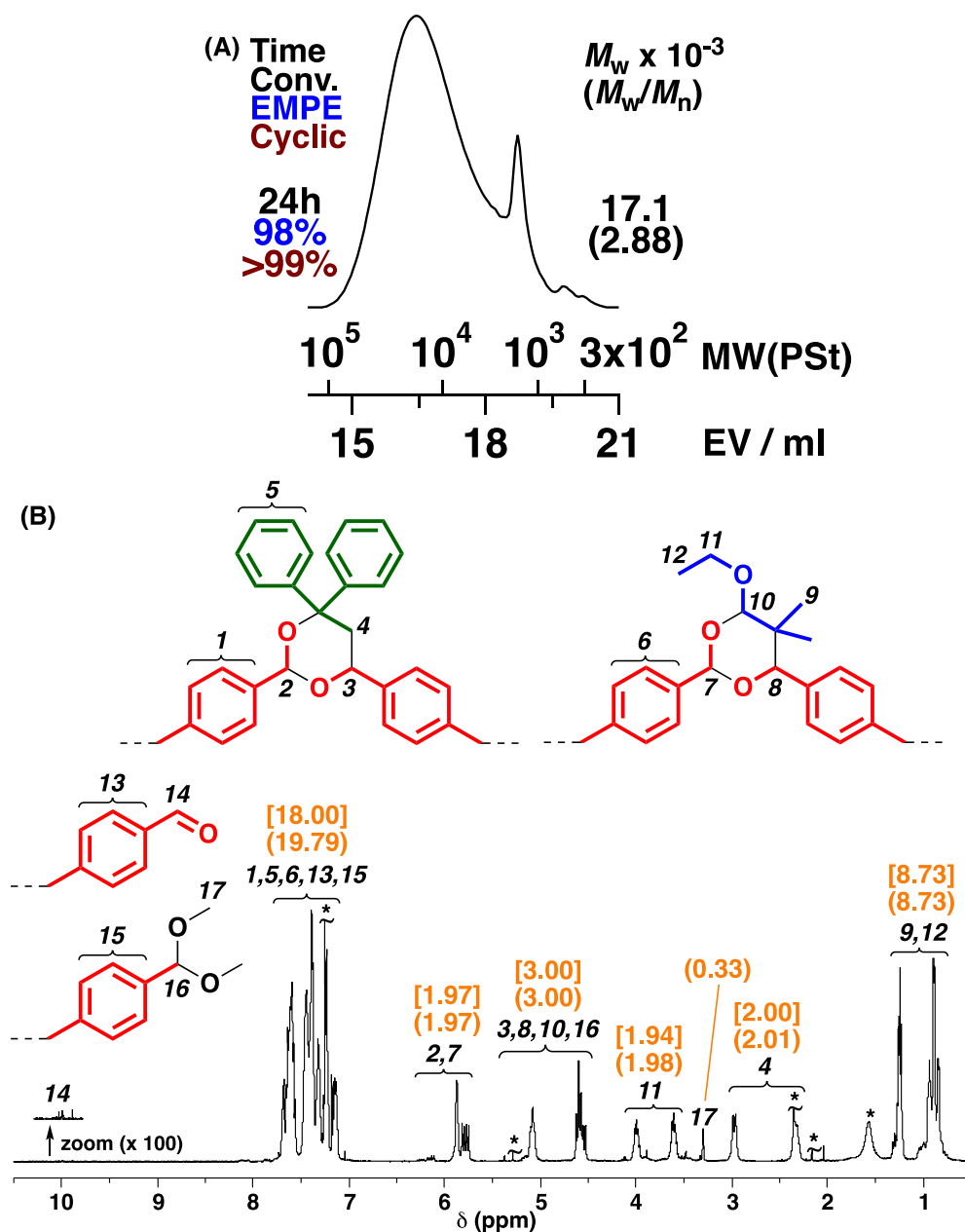


**Figure 5.** (A) MWD curve and (B)  $^1\text{H}$  NMR spectrum (after purification by reprecipitation in methanol) of the polymer obtained by the copolymerization of EMPE and the cyclic trimer consisting of DPE and TPA (entry 4 in Table 3; in  $\text{CDCl}_3$  at 30 °C; \*  $\text{CHCl}_3$ , dichloromethane, water, or others; numbers written in orange parentheses: the observed integral ratio; numbers written in orange square brackets: the theoretical integral ratio of the ABAC-type periodic polymer).

#### Degradation behavior of the obtained polymers

The ABAC-type periodic terpolymers obtained above contain cyclic acetal structures that are degraded under acidic conditions. An acid hydrolysis experiment of the polymer obtained from CEVE, DPE, and IPA (Figure 6A; compound I) was conducted with 0.9 M HCl in 1,2-dimethoxyethane at 60 °C. After 15 min, the polymer peak disappeared, and instead, a sharp peak emerged in the low-MW region in the MWD curve (B in Figure 6(i)).  $^1\text{H}$  NMR analysis revealed that the cyclic acetal structures derived from CEVE were selectively degraded, while the cyclic trimer structures derived from DPE remained intact, which was also

supported by the ESI-MS spectrum (Figure S3). This selective degradation was confirmed by the disappearance of some key peaks, such as the peaks assignable to the CEVE-derived side chain methylenes (peaks 11 and 12), and the emergence of peaks assignable to a cyclic acetal compound consisting of a DPE unit and a cinnamaldehyde-type moiety.<sup>35,36</sup> For example, the sharp peaks assigned to the methine protons (peaks 17 and 18) and the methylene proton (peak 19) on a cyclic acetal ring, a formyl group (peak 13), and two extra carbon atoms on the extended conjugation system (peaks 14 and 15) were observed (B in Figure 6(ii); compound II).

More interestingly, the above product, which was obtained by acid hydrolysis for 15 min, was further degraded after a prolonged reaction time (24 h). The two peaks observed in GPC analysis (C in Figure 6(i)) were assignable to compounds III and IV, which were suggested by the <sup>1</sup>H NMR spectrum (C in Figure 6(ii)). Compound III is an allyl alcohol-type compound derived from an acid-mediated cleavage of compound II. Compound IV contains DPE and conjugated dialdehydes. DPE was derived from the depolymerization of compound III. Conjugated dialdehydes were derived from the degradation of compounds II and III. This degradation behavior was characteristic of the ABAC-type periodic polymer that contained two kinds of cyclic acetal structures in the main chain. Indeed, a polymer synthesized by the copolymerization of CEVE and oligo(DPE-co-IPA), which had average DPE-IPA/CEVE-IPA units of 4.4/1.0, was hydrolyzed into oligomers, which corresponded to the oligo(DPE-co-IPA) used as the monomer, in a short time.

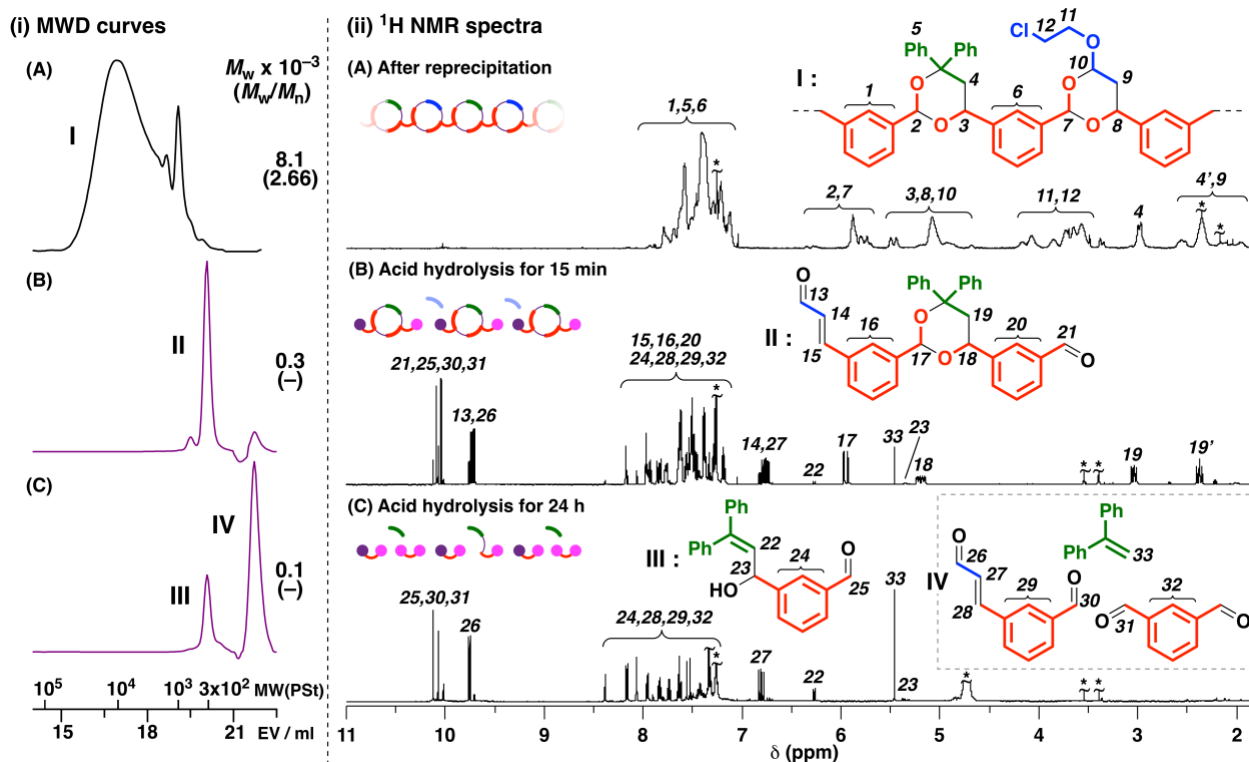


**Figure 6.** (i) MWD curves and (ii) <sup>1</sup>H NMR spectra of (A) poly(CEVE-co-DPE-co-IPA) after purification by reprecipitation in methanol (the same <sup>1</sup>H NMR spectrum as that shown in Figure 3A) and its acid hydrolysis products for (B) 15 min or (C) 24 h [in CDCl<sub>3</sub> at 30 °C; \* CHCl<sub>3</sub>, 1,2-dimethoxyethane, or others; entry 2 in Table 2; acid hydrolysis conditions: 0.9 M HCl in 1,2-dimethoxyethane, approximately 0.9 wt% polymer; examples of the structures (compound I–IV) were drawn (the other products were illustrated in Scheme S1)].



The solid and dashed lines in Figure 7 show the ratios of residual cyclic acetal structures at different hydrolysis times at 60 and 30 °C, respectively. In acid hydrolysis at 60 °C, the CEVE-derived cyclic acetal structures were quantitatively degraded in 15 min (blue circles and solid line), whereas the DPE-derived structures were very slowly degraded and were almost completely degraded in 24 h (green circles and solid line). These results were consistent with the significant difference in the degradation rates of poly(CEVE-*co*-IPA) and poly(DPE-*co*-IPA) (green and blue triangles, respectively, in Figure S4). Interestingly, the difference in degradability was greatly magnified at 30 °C (dashed line in Figure 7). The CEVE-derived cyclic acetal structures were completely degraded in 9 h (blue circles), while 96% of the DPE-derived cyclic acetal structures remained undegraded (green circles).

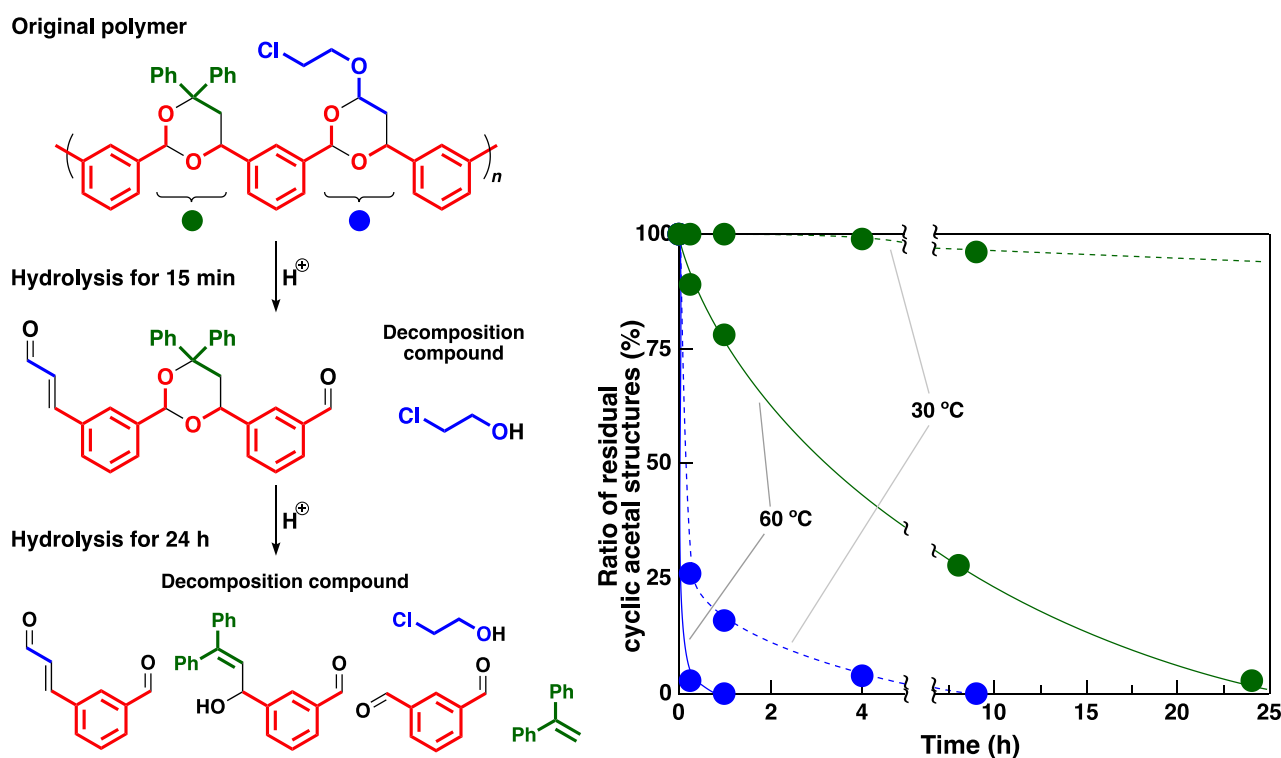


**Figure 7.** The ratios of residual cyclic acetal structures in acid hydrolysis of the ABAC-type periodic polymer (entry 2 in Table 2; green circle: DPE-derived unit; blue circle: CEVE-derived unit) at 60 (solid line) and 30 (dashed line) °C (conditions: 0.9 M HCl in 1,2-dimethoxyethane, approximately 0.9 wt% polymer). The values were estimated by <sup>1</sup>H NMR spectra. The polymers were used after purification by reprecipitation in methanol.

The substituents on the cyclic acetal structures were responsible for the difference in the degradation rates. Specifically, the CEVE-derived cyclic acetal structures show an exocyclic acetal structure, which is probably responsible for the enhanced acid lability. In contrast, the two bulky phenyl rings retarded the degradation of the DPE-derived cyclic acetal structures. In addition, poly(EMPE-*co*-DPE-*co*-IPA) also exhibited two-step degradation behavior under conditions similar to those for the acid hydrolysis of poly(CEVE-*co*-DPE-*co*-IPA) at 60 °C (see Figure S5 for the ratio of residual cyclic acetal structures in acid hydrolysis of poly(EMPE-*co*-DPE-*co*-IPA)).<sup>37,38</sup>

### Thermal properties of the ABAC-type periodic polymers

DSC analysis of the obtained ABAC-type periodic polymers detected single  $T_g$  values, which is consistent with the sequences being periodic rather than blocky (Table 4 and Figure 8A). The  $T_g$  values were related to the ratio of DPE units, likely due to the rigidity of the two phenyl rings (entries 1–3 in Table 4 and Figure 8A). For example, poly(DPE-*co*-IPA), poly(CEVE-*co*-DPE-*co*-IPA), and poly(CEVE-*co*-IPA) exhibited  $T_g$  values of 218, 164, and 66 °C, respectively (entries 2, 1, and 3 in Table 4). Additionally, the obtained ABAC-type periodic polymer containing EMPE as unit C exhibited a much higher  $T_g$  (210 °C; entry 4 in Table 4) than that of the CEVE counterpart (164 °C) due to the  $\beta,\beta$ -dimethyl moieties of EMPE. Utilizing TPA instead of IPA also resulted in higher  $T_g$  values (entries 6 and 7 in Table 4). The  $T_g$  value (264 °C; entry 7 in Table 4) of poly(EMPE-*co*-DPE-*co*-TPA) was comparable to poly(DPE-*co*-TPA). Furthermore, poly(EMPE-*co*-DPE-*co*-TPA) of  $M_w = 17.2 \times 10^3$  had the highest  $T_g$  value (above 300 °C;  $T_g$  cannot be observed below this temperature; entry 8 in Table 4).

The 5% weight loss temperature ( $T_{5\%}$ ) exhibited trends similar to those of  $T_g$  (Figure 8B). For example, the  $T_{5\%}$ s of poly(DPE-*co*-IPA) (288 °C, entry 2 in Table 4), poly(CEVE-*co*-DPE-*co*-IPA) (237 °C, entry 1 in Table 4), and poly(CEVE-*co*-IPA) (211 °C, entry 3 in Table 4) decreased in this order. Poly(EMPE-*co*-DPE-*co*-IPA) exhibited a higher  $T_{5\%}$  (280 °C, entry 4 in Table 4) than that of its CEVE counterpart, although poly(EMPE-*co*-IPA) was superior (307 °C, entry 5 in Table 4) to the corresponding ABAC-type periodic terpolymer. Polymers with TPA units exhibited higher  $T_{5\%}$  values (entries 6–9 in Table 4) than that of their IPA counterparts. In particular, poly(EMPE-*co*-DPE-*co*-TPA) exhibited the highest  $T_{5\%}$  value (345 °C) (entry 7 in Table 4) among the polymer examined.

**Table 4.**  $T_g$  and  $T_{5\%}$  values of polymers with cyclic acetal structures in the main chain

entry	polymer <sup>a</sup>	$M_w \times 10^{-3}$	$M_w/M_n$	$T_g$ (°C) <sup>b</sup>	$T_{5\%}$ (°C) <sup>c</sup>
1	poly(CEVE- <i>co</i> -DPE- <i>co</i> -IPA)	8.1	2.66	164	237
2	poly(DPE- <i>co</i> -IPA)	3.0	1.65	218	288
3	poly(CEVE- <i>co</i> -IPA)	3.9	2.60	66	211
4	poly(EMPE- <i>co</i> -DPE- <i>co</i> -IPA)	10.0	2.44	210	280
5	poly(EMPE- <i>co</i> -IPA)	3.7	1.37	154	307
6	poly(CEVE- <i>co</i> -DPE- <i>co</i> -TPA)	8.0	2.01	170	263
7	poly(EMPE- <i>co</i> -DPE- <i>co</i> -TPA)	8.9	1.73	264	345
8		17.2	3.03	– <sup>d</sup>	339
9	poly(DPE- <i>co</i> -TPA)	7.7	2.21	262	304

<sup>a</sup> After purification by reprecipitation in methanol. <sup>b</sup> The heating and cooling rates were 10 (entries 1–7 and 9) or 20 (entry 8) °C min<sup>−1</sup>. The  $T_g$  values were determined by the second heating scan. <sup>c</sup> The 5% weight-loss temperature determined by thermogravimetric analysis (TGA). <sup>d</sup> The  $T_g$  was not observed below 300 °C, which suggests that the polymer has a  $T_g$  value above 300 °C.

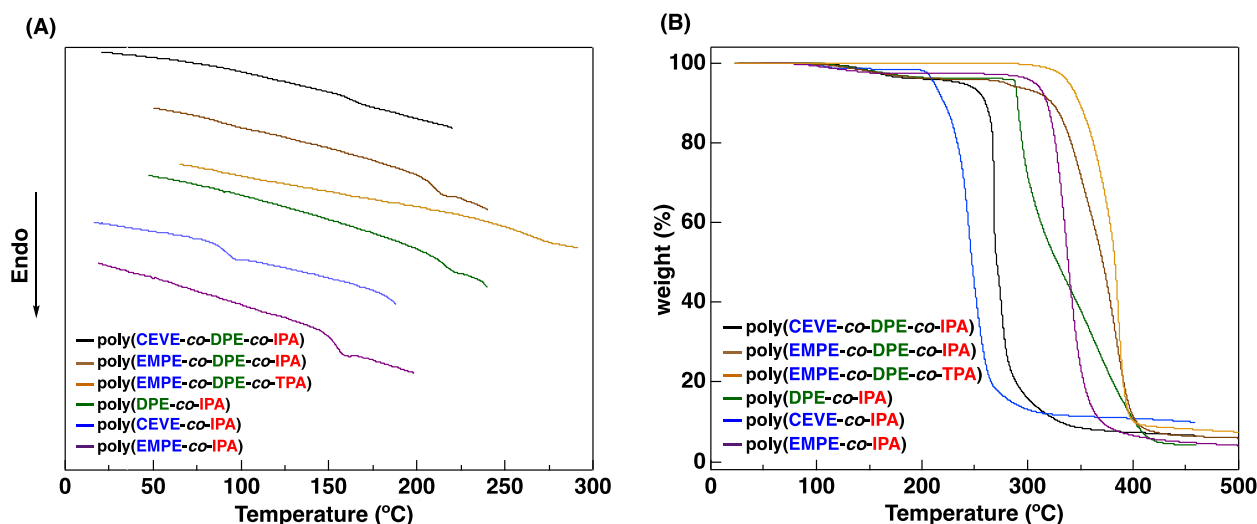


**Figure 8.** (A) DSC thermograms and (B) TGA analysis of poly(CEVE-co-DPE-co-IPA), poly(EMPE-co-DPE-co-IPA), poly(EMPE-co-DPE-co-TPA), poly(DPE-co-IPA), poly(CEVE-co-IPA), and poly(EMPE-co-IPA) (the samples listed in Table 4).

## Conclusion

Cyclotrimerization of vinyl monomers and sequence-programmed cyclic trimers bearing two unreacted aldehyde moieties was successfully performed with ABAC-type periodic polymerizations. This cyclic trimer was generated by the selective cyclic trimer formation of DPE and dialdehydes. DPE was effective in suppressing the successive cyclotrimerization and vinyl homopolymerization reactions due to steric hindrance. The obtained cyclic trimer underwent successive cyclotrimerization with various vinyl monomers. In particular, copolymerization with EMPE proceeded quantitatively. The obtained ABAC-type periodic polymers exhibited two-step degradation behavior under acidic conditions. In the first step, VE-derived cyclic acetal structures were selectively hydrolyzed into cyclic trimers consisting of DPE and dialdehydes. These products were further degraded for prolonged reaction time as the second-step. DSC and TGA measurements supported that the obtained polymer possessed good thermal properties, which were derived from the cyclic acetal structures.

## References and Notes

1. Badi, N.; Lutz, J.-F. *Chem. Soc. Rev.* **2009**, *38*, 3383–3390.
2. Lutz, J.-F.; Ouchi, M.; Liu, D. R.; Sawamoto, M. *Science* **2013**, *341*, 1238149.
3. Lutz, J.-F. *Macromol. Rapid Commun.* **2017**, *38*, 1700582.
4. Szymański, J. K.; Abul-Haija, Y. M.; Cronin, L. *Acc. Chem. Res.* **2018**, *51*, 649–658.
5. Meier, M. A. R.; Barner-Kowollik, C. *Adv. Mater.* **2019**, *31*, 1806027.
6. Dolui, S.; Kumar, D.; Banerjee, S.; Ameduri, B. *Acc. Mater. Res.* **2021**, *2*, 242–251.
7. Rzaev, Z. M. O. *Prog. Polym. Sci.* **2000**, *25*, 163–217.
8. Braun, D.; Hu, F. *Prog. Polym. Sci.* **2006**, *31*, 239–276.
9. Shahab, Y.; Mohamed, A.; Khettab, A.; Siddiq, A. *Eur. Polym. J.* **1991**, *27*, 227–229.
10. Yang, J.-Z.; Otsu, T. *Macromolecules* **1992**, *25*, 102–107.

11. Ishido, Y.; Aburaki, R.; Kanaoka, S.; Aoshima, S. *J. Polym. Sci., Part A: Polym. Chem.* **2010**, *48*, 1838–1843.
12. Ishido, Y.; Aburaki, R.; Kanaoka, S.; Aoshima, S. *Macromolecules* **2010**, *43*, 3141–3144.
13. Ishido, Y.; Kanazawa, A.; Kanaoka, S.; Aoshima, S. *Macromolecules* **2012**, *45*, 4060–4068.
14. Ishido, Y.; Kanazawa, A.; Kanaoka, S.; Aoshima, S. *J. Polym. Sci., Part A: Polym. Chem.* **2014**, *52*, 1334–1343.
15. Aso, C.; Tagami, S.; Kunitake, T. *Kobunshi Kagaku* **1996**, *23*, 63–68.
16. Hsieh, H. L. *J. Macromol. Sci., Part A: Chem.* **1973**, *7*, 1525–1535.
17. Saegusa, T.; Kobayashi, S.; Kimura, Y. *Macromolecules* **1977**, *10*, 68–72.
18. Mimura, M.; Kanazawa, A.; Aoshima, S. *Macromolecules* **2019**, *52*, 7572–7583.
19. Rudick, J. G. *J. Polym. Sci., Part A: Polym. Chem.* **2013**, *51*, 3985–3991.
20. Hu, R.; Li, W.; Tang, B. Z. *Macromol. Chem. Phys.* **2016**, *217*, 213–224.
21. Kakuchi, R. *Angew. Chem. Int. Ed.* **2014**, *53*, 46–48.
22. Kreye, O.; Tóth, T.; Meier, M. A. R. *J. Am. Chem. Soc.* **2011**, *133*, 1790–1792.
23. Deng, X.-X.; Li, L.; Li, Z.-L.; Lv, A.; Du, F.-S.; Li, Z.-C. *ACS Macro Lett.* **2012**, *1*, 1300–1303.
24. Ousaka, N.; Endo, T. *Macromolecules* **2021**, *54*, 2059–2067.
25. Naito, T.; Kanazawa, A.; Aoshima, S. *Polym. Chem.* **2019**, *10*, 1377–1385.
26. Arundale, E.; Mikeska, L. A. *Chem. Rev.* **1952**, *51*, 505–555.
27. Sabitha, G.; Reddy, K. B.; Bhikshapathi, M.; Yadav, J. S. *Tetrahedron Lett.* **2006**, *47*, 2807–2810.
28. Hirai, K.; Takeda, R.; Hutchison, J. A.; Uji-I, H. *Angew. Chem. Int. Ed.* **2020**, *59*, 5332–5335.
29. Aoshima, S.; Fujisawa, T.; Kobayashi, E. *J. Polym. Sci., Part A: Polym. Chem.* **1994**, *32*, 1719–1728.
30. Arnett, E. M.; Wu, C. Y. *J. Am. Chem. Soc.* **1962**, *84*, 1684–1688.
31. The author conducted the cyclotrimerization of CEVE and BzA as the model reaction under the same conditions as those of the successive cyclotrimerization of CEVE and the cyclic trimer consisting of DPE and IPA because the alternating cationic copolymerization of VEs and conjugated aldehydes proceed at –78 °C as reported in the previous studies in the Aoshima’s laboratory.<sup>11–14</sup> The results of the model reaction indicated that EtAlCl<sub>2</sub> promoted selective cyclotrimerization even at –78 °C.
32. Okuyama, T.; Fueno, T.; Furukawa, J.; Uyeo, K. *J. Polym. Sci., Part A-1: Polym. Chem.* **1968**, *6*, 1001–1007.
33. Nuyken, O.; Raether, R. B.; Spindler, C. E. *Macromol. Chem. Phys.* **1998**, *199*, 191–196.
34. Naito, T.; Kanazawa, A.; Aoshima, S. *Polym. Chem.* **2022**, *13*, 5757–5768.
35. Battistuzzi, G.; Cacchi, S.; Fabrizi, G. *Org. Lett.* **2003**, *5*, 777–780.
36. Michels, H.-P.; Nieger, M.; Vögtle, F. *Chem. Ber.* **1994**, *127*, 1167–1170.
37. The acid hydrolysis product obtained in 15 min was consistent with the cyclic trimer used as the monomer, whose aldehyde moieties were not converted into cinnamaldehyde structures unlike the case of the CEVE counterpart. The plausible hydrolysis mechanism of the EMPE-derived cyclic acetal structures is shown in Scheme S2.<sup>38</sup>
38. Späth, E.; Lorenz, R.; Altmann, E. *Ber. Dtsch. Chem. Ges.* **1943**, *76*, 513–517.

## Supporting Information

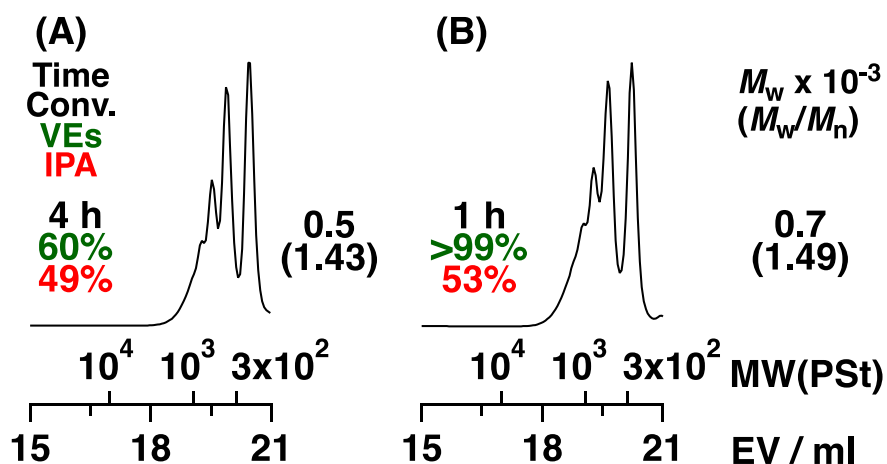


**Figure S1.** MWD curves of the products obtained by the cyclotrimerization of (A) CEVE or (B) IBVE with IPA (entries 1 and 2 in Table 1).

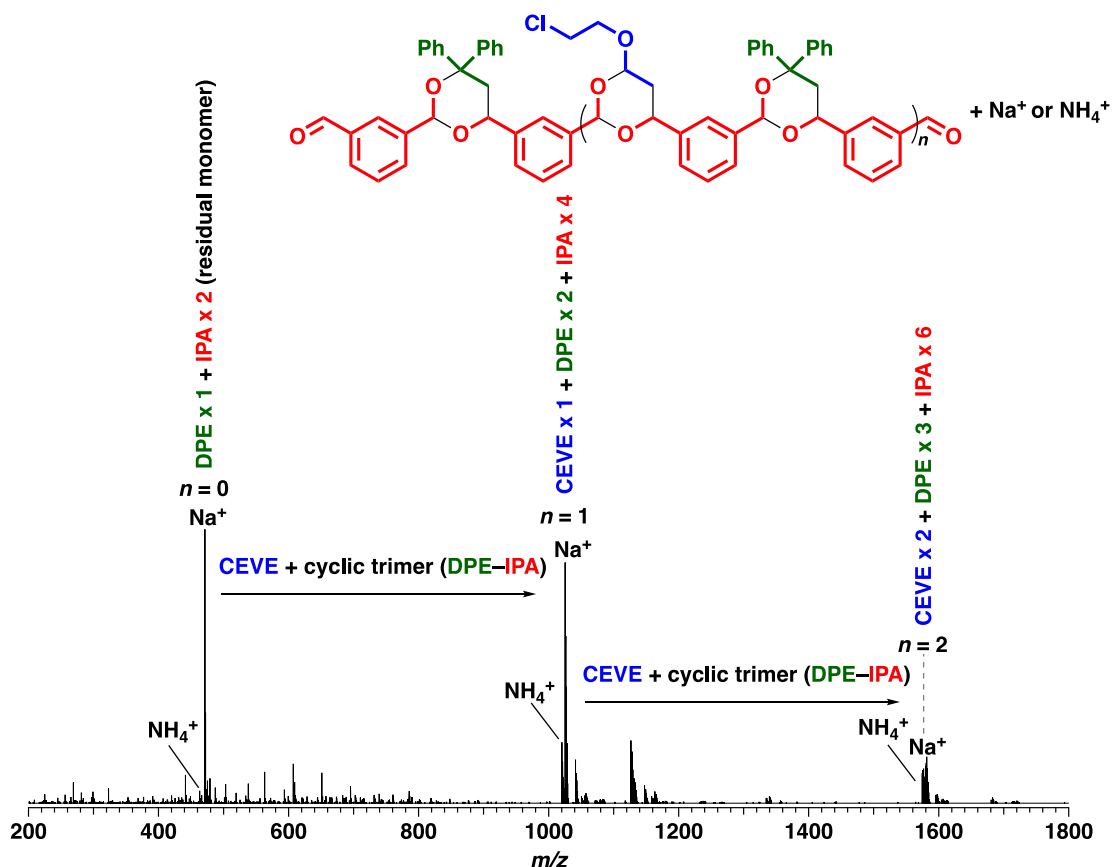


**Figure S2.** ESI-MS spectrum of the polymer obtained by the copolymerization of CEVE and the cyclic trimer consisting of DPE and IPA (entry 2 in Table 2; after reprecipitation in methanol;  $M_w(\text{GPC}) = 2.3 \times 10^3$ ,  $M_w/M_n(\text{GPC}) = 1.59$ ;  $[\text{CEVE}]_0 = 0.20 \text{ M}$ ,  $[\text{cyclic trimer (DPE-IPA)}]_0 = 0.20 \text{ M}$ ,  $[\text{EtAlCl}_2]_0 = 50 \text{ mM}$ ,  $[\text{1,4-dioxane}]_0 = 1.0 \text{ M}$ , in dichloromethane at  $-78^\circ\text{C}$  for 1 h).

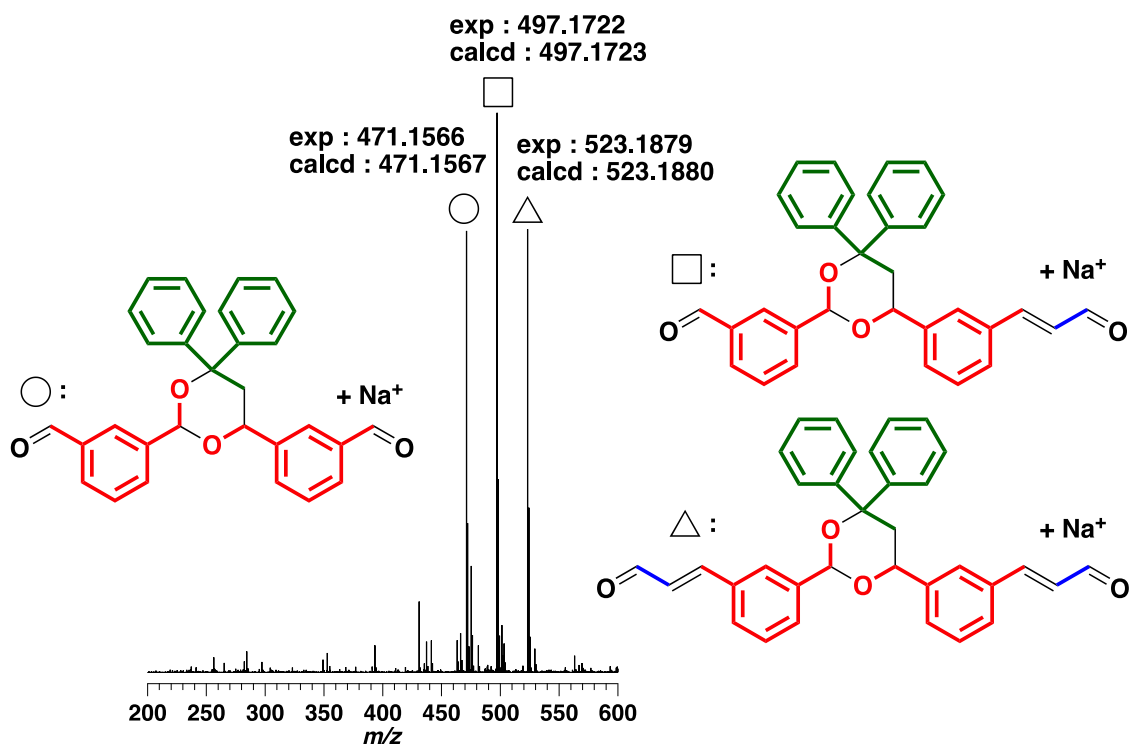
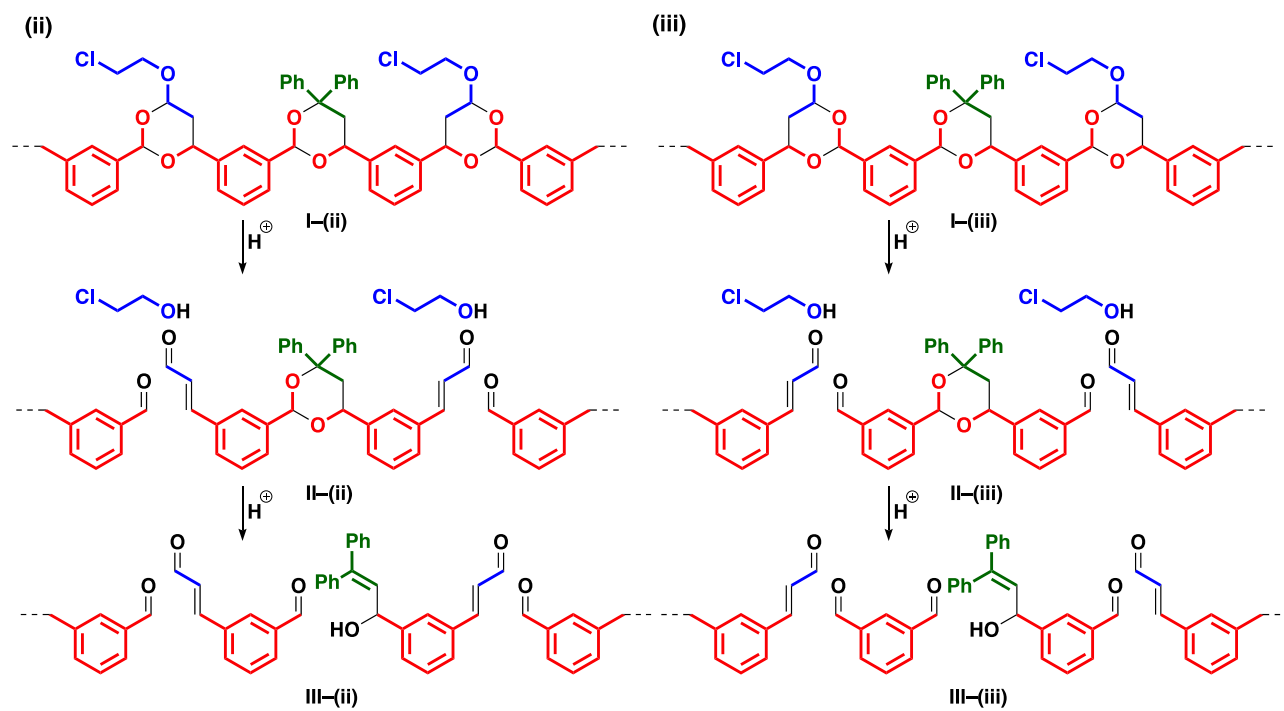
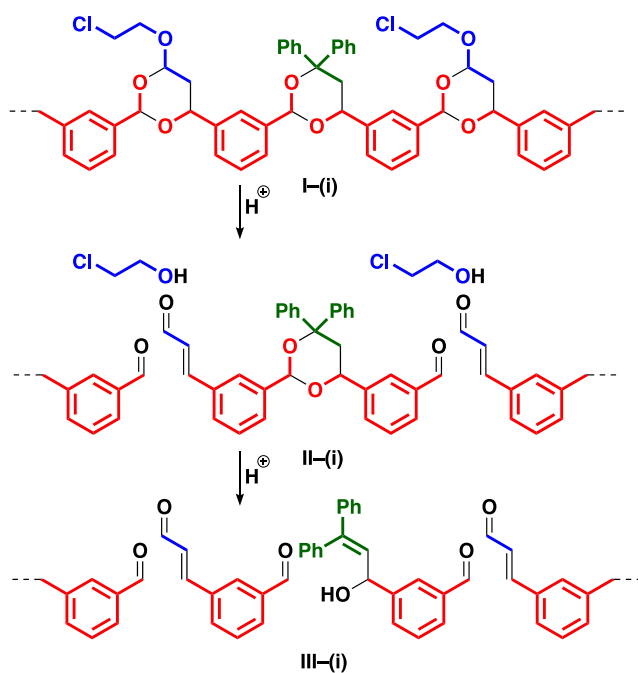


**Figure S3.** ESI-MS spectrum of the product obtained by the acid hydrolysis of poly(CEVE-*co*-DPE-*co*-IPA) (acid hydrolysis for 15 min).

(i) The same with Figure 6 and 7



**Scheme S1.** The possible structures of poly(CEVE-*co*-DPE-*co*-IPA) and its hydrolysis products.

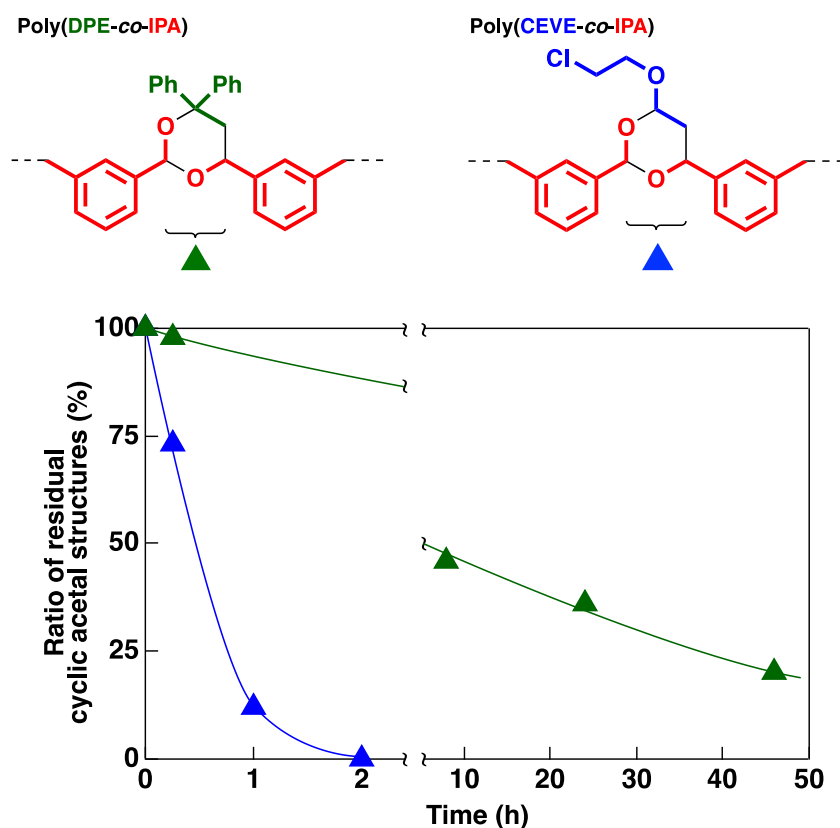


**Figure S4.** The ratio of residual cyclic acetal structures in acid hydrolysis of poly(DPE-co-IPA) (green triangle;  $M_w(\text{GPC}) = 3.6 \times 10^3$ ,  $M_w/M_n(\text{GPC}) = 2.01$ ;  $[\text{DPE}]_0 = 0.40$  M,  $[\text{IPA}]_0 = 0.20$  M,  $[\text{GaCl}_3]_0 = 10$  mM, in dichloromethane at  $-78$  °C; conditions: 0.9 M HCl in 1,2-dimethoxyethane, approximately 0.8 wt% polymer at 60 °C) and poly(CEVE-co-IPA) (blue triangle;  $M_w(\text{GPC}) = 3.9 \times 10^3$ ,  $M_w/M_n(\text{GPC}) = 2.60$ ;  $[\text{CEVE}]_0 = 0.50$  M,  $[\text{IPA}]_0 = 0.50$  M,  $[\text{EtAlCl}_2]_0 = 50$  mM,  $[\text{THF}] = 1.0$  M, in dichloromethane at 0 °C; conditions: 0.9 M HCl in 1,2-dimethoxyethane, approximately 1 wt% polymer at 60 °C). The values were estimated from the  $^1\text{H}$  NMR spectra. The polymers were used after purification by reprecipitation in methanol.



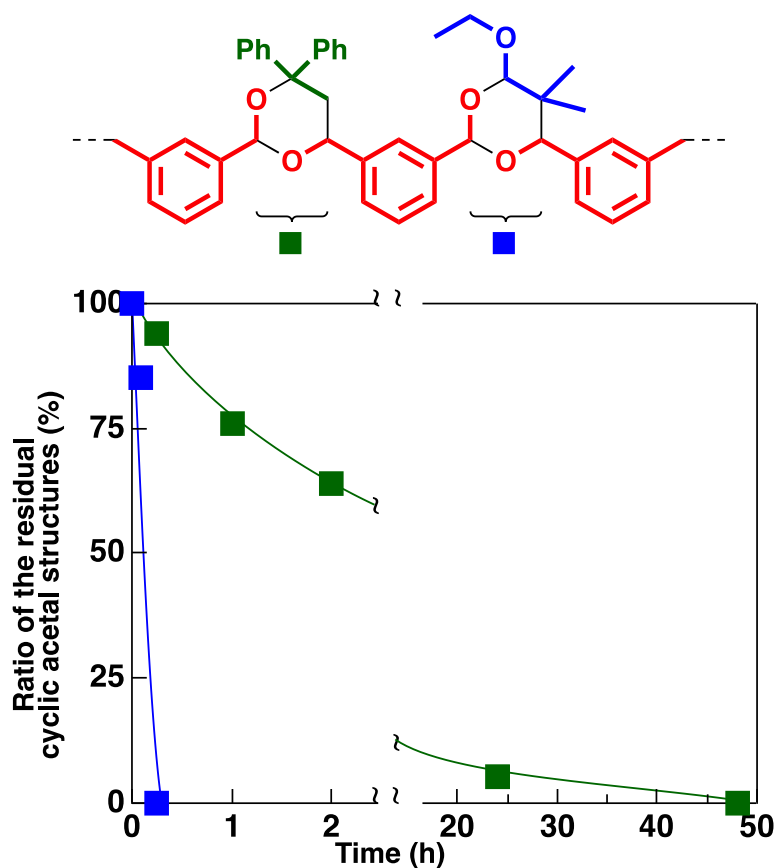
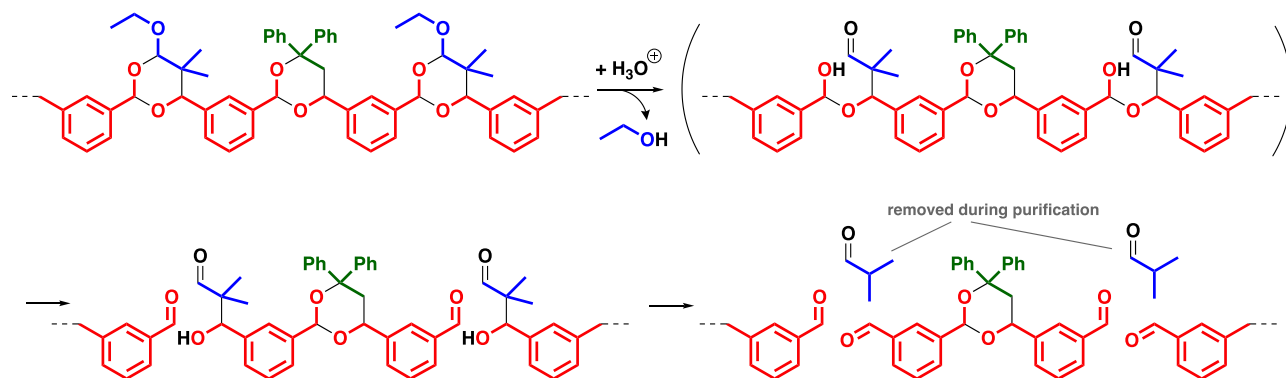


**Figure S5.** The ratio of residual cyclic acetal structures in acid hydrolysis of poly(EMPE-*co*-DPE-*co*-IPA) (entry 1 in Table 3; green square: DPE-derived unit; blue square: EMPE-derived unit; conditions: 0.9 M HCl in 1,2-dimethoxyethane, approximately 0.9 wt% polymer at 60 °C). The values were estimated from the  $^1\text{H}$  NMR spectra. The polymer was used after purification by reprecipitation in methanol.



**Scheme S2.** The plausible mechanism of the acid hydrolysis of poly(EMPE-*co*-DPE-*co*-IPA).

## Chapter 5

### **Alternating cationic copolymerization of vinyl ethers and sequence-programmed cyclic trimer consisting of one vinyl ether and two aldehydes for ABCC-type periodic terpolymer**

#### **Introduction**

Ring-opening polymerization is a powerful tool for introducing heteroatoms into the main chain.<sup>1-3</sup> Various functional polymers, such as polyesters, polyamides, polyurethanes, and polycarbonates, are available through the ring-opening polymerizations of corresponding cyclic monomers under mild conditions.<sup>4-10</sup> In addition, the copolymerizations of cyclic and other types of monomers,<sup>11-28</sup> which polymerize by different mechanisms through generating different types of propagating species, have great potential for yielding polymers with unprecedented structures inaccessible by traditional copolymerization. These polymerization systems permit the incorporation of two or more kinds of functional groups into the polymer main chain, resulting in polymers with characteristic properties, such as degradability and crystallinity. The persistence and structural integrity characteristics of vinyl polymers cause the accumulation of plastic waste in the environment; hence, vinyl-addition and ring-opening polymerization, which can introduce the labile bonds into the main chains of vinyl polymers, is of great interest. Examples of copolymerization reactions consisting of vinyl-addition and ring-opening polymerization include radical copolymerizations of methyl methacrylates and cyclic ketene acetals<sup>11-17</sup> and anionic copolymerizations of methyl methacrylates and  $\epsilon$ -caprolactone.<sup>20</sup> However, very few studies have achieved these copolymerizations due to the difficulty in realizing crossover reactions between different types of monomers, which produce different types of propagating species.

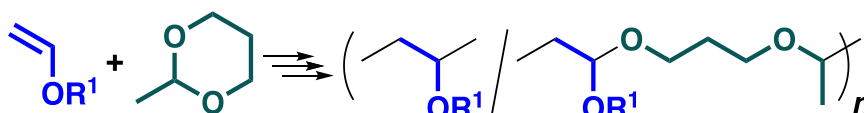
The structures of active chain ends derived from vinyl monomers and cyclic monomers are highly important for successful copolymerization by frequent crossover reactions. During cationic copolymerization, oxonium ions, which are active species of oxygen-containing cyclic monomers, do not react with vinyl monomers. Therefore, carbocation generation by ring-opening reactions of oxonium ions is indispensable for copolymerizing vinyl monomers and oxygen-containing cyclic monomers by crossover reactions.<sup>21-23</sup> For example, ring-opening reactions of cyclic acetals generate alkoxy-adjacent carbocations that are structurally similar to vinyl ether (VE)-derived carbocations. The cationic copolymerization processes of vinyl monomers and cyclic acetals were reported several decades ago.<sup>24,25</sup> The Aoshima's group has conducted systematic studies of the effects of the ring members and substituents of cyclic acetals on copolymerization behaviors.<sup>26-28</sup> Additionally, a one-pot synthesis of ABC-type periodic terpolymers has been achieved by AB-type sequence-programmed cyclic acetal synthesis and subsequent alternating cationic copolymerization with VEs (unit C).<sup>29</sup>

In this chapter, a novel system for sequence-regulated polymer synthesis was developed based on sequence-incorporated monomer synthesis and alternating cationic copolymerization (Scheme 1). The author focused on cyclic trimers consisting of one vinyl monomer and two aldehydes, which were generated by side reactions during the cationic alternating copolymerizations of vinyl monomers and conjugated aldehydes.<sup>30-33</sup> These cyclic trimers are regarded as cyclic acetal monomers with structures that are similar to 2-methyl-1,3-dioxane (MDOX). Thus, cyclic trimers potentially undergo cationic copolymerization with vinyl monomers. According to a systematic investigation of monomer structures, alternating cationic copolymerization were shown to proceed when 2-nonenal (NNE)-containing cyclic trimers were used under optimized conditions.

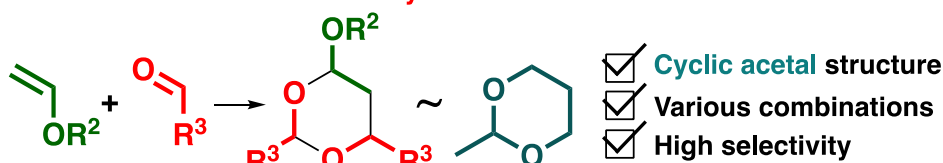
The alternating copolymer potentially has three different monomer sequence types—ABCC,<sup>34,35</sup> ACCB, and ACBC—due to three possible ring-opening modes. The monomer sequences of the obtained polymers could be determined by structurally analyzing acid methanolysis products. The results indicated that ABCC- and ACBC-type periodic sequences were obtained via ring-opening reactions of cyclic trimers. The ratios of the two types of sequences were affected by polymerization conditions. Specifically, ABCC-type periodic sequences were mainly generated by copolymerizing 2-chloroethyl VE (CEVE) and a cyclic trimer consisting of isobutyl VE (IBVE) and NNE without added bases (ABCC-type ratio = 83 %).

## Previous studies

### Cationic copolymerization of VEs and MDOX

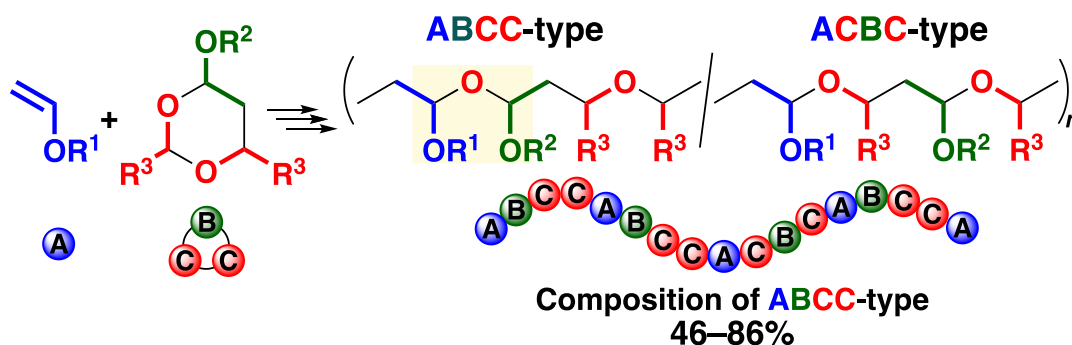


### Cyclotrimerization of VEs and aldehydes



## This study

### Cationic copolymerization of VEs and cyclic trimers



**Scheme 1.** Synthesis of ABCC-type periodic terpolymer via cationic copolymerization of VEs and cyclic trimers.

## Experiment

### Materials

NNE (TCI, > 95.0%) was distilled over calcium hydride twice under reduced pressure before use. Other materials were prepared and used as described in Chapter 2.

### Sequenced programmed cyclic trimer synthesis

Cyclic trimers other than those of VEs and NNEs were synthesized in a manner similar to that described in Chapter 2. When the obtained product contained a significant amount of impurities, the crude product was purified by silica gel column chromatography [*n*-hexane/ethyl acetate (EA)]. During the cyclotrimerizations of VEs and NNE, the second portion of VEs was added to the reaction mixture at a predetermined time to increase NNE conversion. For example, the cyclotrimerizations of NNE and isopropyl

VE (IPVE) were conducted by the following steps. Toluene (17.4 mL), tetrahydrofuran (THF; 2.4 mL) as an added base, IPVE (1.7 mL), and NNE (4.1 mL) were charged successively into a glass tube by using dry syringes. The reaction was initiated by adding a prechilled EtAlCl<sub>2</sub> solution in *n*-hexane/toluene (500 mM; 3.0 mL) at 0 °C. Then, 1.7 mL of IPVE was added at a predetermined interval (10 min). The reaction was terminated by adding water with a small amount of aqueous ammonia (approximately 10 mL; 0.3wt%). The quenched reaction mixture was diluted with dichloromethane and washed with water. The organic layer was evaporated under reduced pressure to remove the remaining volatiles. The crude product was purified by silica gel column chromatography (*n*-hexane/EA = 22/1 v/v; final yield = 32%).

### **Polymerization procedure**

The following is a description of the typical polymerization procedure. A glass tube equipped with a three-way stopcock was dried using a heat gun under dry nitrogen. A cyclic trimer solution consisting of VEs and aldehydes in toluene was added to the tube using a dry syringe. This cyclic trimer was dried via an azeotropic method using toluene for approximately 6 h. Toluene, *n*-hexane, 1,4-dioxane (1,4-DO), and CEVE were sequentially added to this tube using dry syringes. This solution was cooled at 0 °C in advance; a prechilled 40 mM EtSO<sub>3</sub>H solution in toluene was added to this solution using a dry syringe. The tube was then placed in a cooling bath set at –78 °C, 10 min after adding EtSO<sub>3</sub>H. The reaction was initiated by adding a prechilled Lewis acid solution. The reaction mixture was terminated with methanol containing a small amount of aqueous ammonia. The quenched mixture was washed with water. Then, volatile compounds were removed under reduced pressure at 50 °C to yield a polymer. The monomer conversions were determined by <sup>1</sup>H NMR analyses of the quenched reaction mixtures using pyridine as an internal standard.

### **Acid methanolysis of product copolymers**

The acid methanolysis of the polymers was conducted with 0.5 M aq. HCl in methanol at room temperature for 2 h. Other procedures were conducted in a manner similar to that in hydrolysis.

### **Characterization**

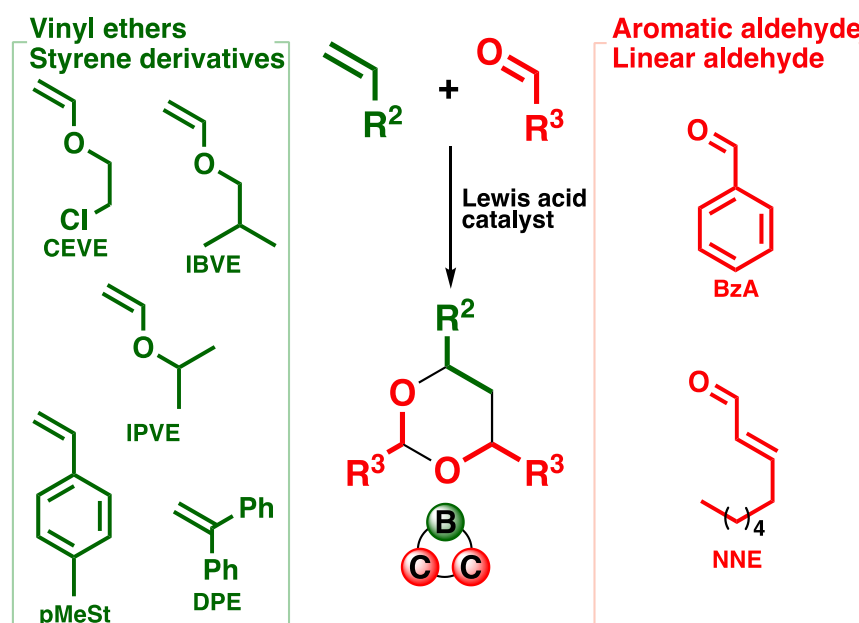
The molecular weight distributions (MWDs), <sup>1</sup>H and <sup>13</sup>C NMR spectra, and ESI–MS spectra were obtained in manners similar to those described in the preceding chapters.

## **Results and Discussion**

### **Selective cyclotrimerizations of various vinyl monomers and aldehydes**

Cyclotrimerizations of various vinyl monomers and aldehydes were conducted to obtain cyclic trimers bearing various structures (Scheme 2). The electronic and steric environments around the carbocations generated via ring-opening reactions of cyclic trimers were tunable by the types of vinyl monomers and aldehydes incorporated into cyclic trimers (Table 1). First, a cyclic trimer consisting of IBVE and benzaldehyde (BzA) was produced using EtAlCl<sub>2</sub> as a Lewis acid catalyst with 1,4-DO at –78 °C (entry 1 in Table 1). A cyclic trimer was generated quantitatively, as in the case of the previous study on the cationic alternating copolymerizations of IBVE and BzA.<sup>30,31</sup> NNE, which is a linear conjugated aldehyde, underwent relatively selective cyclotrimerizations with VEs (yields of cyclic trimers = 33–53%; entries 2–4 in Table 1)

to yield a cyclic trimer; a 3,4-dihydro-2*H*-pyran derivative and a VE homopolymer were obtained as side products (Figure S1). The cyclic trimer was isolated by silica gel column chromatography (Figure S2). The reactions of styrene (St) derivatives, such as *p*-methylstyrene (pMeSt) and 1,1-diphenylethylene (DPE) (entries 5 and 6 in Table 1), were examined. The cyclotrimerizations of St derivatives and BzA were promoted by GaCl<sub>3</sub>, unlike the highly selective cyclotrimerizations of VEs and BzA by EtAlCl<sub>2</sub>. For pMeSt, the concentration of BzA was set approximately a fifth of that of pMeSt to promote cyclotrimerization and suppress pMeSt homopolymerization. However, the yield of the cyclic trimer was lower than in the cases with VEs (entry 5 in Table 1). In contrast, DPE was demonstrated to be efficient for selective cyclotrimerization (cyclotrimerization/side reaction = >99/~0) (entry 6 in Table 1). The cyclotrimerization reactions of various vinyl monomers, including St derivatives, and BzA were described in Chapter 2.



**Scheme 2.** Cyclotrimerization of various vinyl monomers and conjugated aldehydes.

**Table 1.** Cyclotrimerization of various vinyl monomers and aldehydes <sup>a</sup>

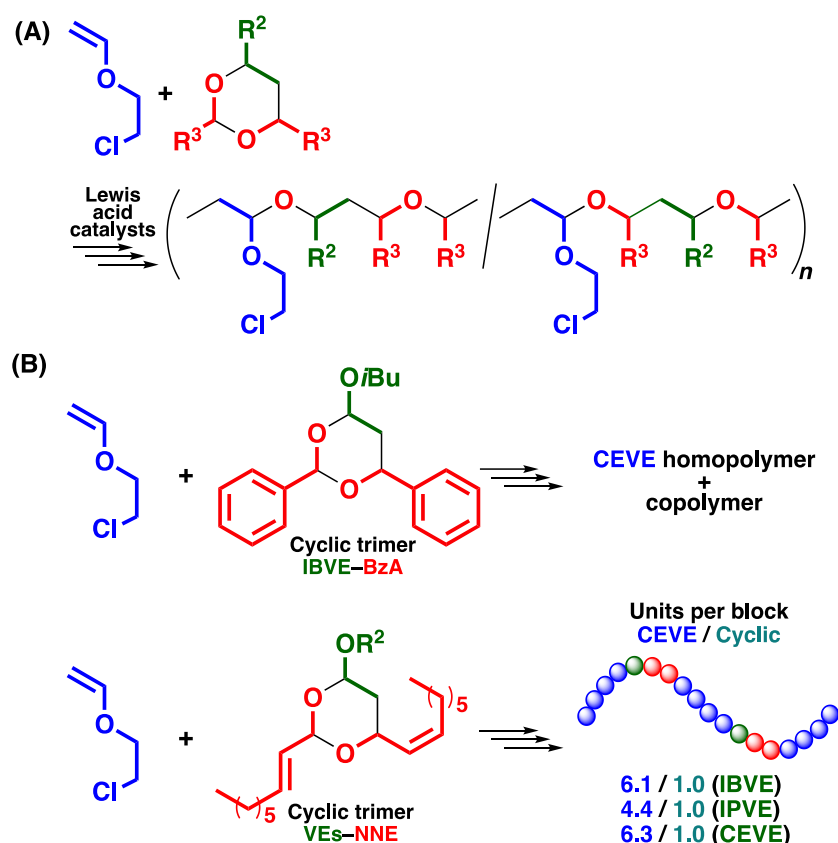
entry	vinyl monomer	(M)	Ald	(M)	catalyst	(mM)	time	conv.(%) <sup>b</sup>		conv. for cyclic trimer <sup>c</sup>
								vinyl monomer	Ald	
1	IBVE	0.50	BzA	1.0	EtAlCl <sub>2</sub>	20	24 h	95	>99	92
2	IBVE	0.50	NNE	1.0	EtAlCl <sub>2</sub>	50	4 h	>99	76	53
3	CEVE	0.50	NNE	1.0	EtAlCl <sub>2</sub>	50	24 h	>99	73	42
4	IPVE	0.50	NNE	1.0	EtAlCl <sub>2</sub>	50	10 min	>99	62	33
5	pMeSt	0.19	BzA	1.0	Bi(OTf) <sub>3</sub>	5.0	48 h	>99	15	21
6	DPE	0.50	BzA	1.0	GaCl <sub>3</sub>	5.0	168 h	92	92	>99

<sup>a</sup> [THF] = 0 (entries 1 and 6), 1.0 (entries 2–4), or 0.58 (entry 5) M, [1,4-DO] = 1.0 (entry 1) or 0 (entries 2–6) M, in toluene (entry 1) or dichloromethane (entries 2–6), at –78 (entries 1 and 6) or 0 (entries 2–5) °C.

<sup>b,c</sup> Determined by <sup>1</sup>H NMR analysis of quenched reaction mixtures.

*Cationic copolymerization of CEVE and various cyclic trimers*

The cyclic trimer consisting of IBVE and BzA was employed in a cationic copolymerization with CEVE using an initiating system suited for controlled alternating copolymerizations of various VEs and conjugated aldehydes (Scheme 3A).<sup>30–33</sup> Both CEVE and the cyclic trimer were consumed in a reaction using GaCl<sub>3</sub> as a Lewis acid catalyst in conjunction with EtSO<sub>3</sub>H with 1,4-DO in toluene at –78 °C. A product of  $M_n = 1.1 \times 10^3$  was obtained under these conditions (entry 1 in Table 2). <sup>1</sup>H NMR analysis of the polymer revealed that the cyclic trimer was introduced into the main chain by crossover reactions. However, the average numbers of CEVE/cyclic trimer units per block were about 25/1.0 (these values are based on the assumption that CEVE homopolymer chains are not generated), suggesting that CEVE homopropagation reactions preferentially occurred during copolymerization. To suppress CEVE homopropagation reactions, the initial concentration of the cyclic trimer was set twice that of CEVE. The <sup>1</sup>H NMR analysis of the obtained polymer indicated that the amount of the incorporated cyclic trimer increased. However, the result of the acid methanolysis of the obtained polymer indicated unsuccessful copolymerization. The peak top of the MWD curve did not shift to the lower-MW region after methanolysis (Figure 1A). If copolymerization is successful, acid-labile acetal structures would be generated in the main chain of a copolymer. The results revealed that CEVE homopolymer chains, which did not have acid-degradable units, were predominantly produced during copolymerization (Figure 1A). Furthermore, the cyclic trimers consisting of BzA and St derivatives did not copolymerize with CEVE likely because of the steric hindrance around the cyclic acetal structures, and instead, CEVE homopolymers were obtained (entries 3 and 4 in Table 2). These results indicated that cyclic trimers consisting of BzA and vinyl monomers would not be suitable for copolymerization with CEVE.



**Scheme 3.** Cationic copolymerization of CEVE with (A) various cyclic trimers and (B) cyclic trimers consisting of VEs and BzA or NNE.

**Table 2.** Cationic copolymerization of CEVE and various cyclic trimers<sup>a</sup>

entry	CEVE (M)	cyclic trimer	(M)	time	catalyst	conv. (%) <sup>b</sup>		units per block <sup>d</sup>			
						CEVE	cyclic trimer	$M_n \times 10^{-3}$ <sup>c</sup>	$M_w/M_n$ <sup>c</sup>	CEVE	cyclic trimer
1	0.50	IBVE-BzA	0.50	70 h	GaCl <sub>3</sub>	37	11	1.1	1.48	(25) <sup>e</sup>	(1.0) <sup>e</sup>
2	0.40	IBVE-BzA	0.80	24 h	GaCl <sub>3</sub>	72	7	2.1	1.51	(11) <sup>e</sup>	(1.0) <sup>e</sup>
3	0.20	pMeSt-BzA	0.20	30 sec	TiCl <sub>4</sub> /SnCl <sub>4</sub>	74	2	5.5	1.07	45	1.0
4	0.20	DPE-BzA	0.20	5 min	TiCl <sub>4</sub> /SnCl <sub>4</sub>	>99	0	4.2	1.09	n.d. <sup>f</sup>	n.d. <sup>f</sup>
5	0.39	IBVE-NNE	0.40	25 h	GaCl <sub>3</sub>	52	21	2.5	1.59	6.1	1.0

<sup>a</sup> [EtSO<sub>3</sub>H]<sub>0</sub> = 4.0 (entries 1, 2, and 5) or 0 (entries 3 and 4) mM, [IBEA]<sub>0</sub> = 0 (entries 1, 2, and 5) or 4.0 (entries 3 and 4) mM, [GaCl<sub>3</sub>]<sub>0</sub> = 4.0 (entry 1), 10 (entries 2 and 5), or 0 (entries 3 and 4) mM, [TiCl<sub>4</sub>]<sub>0</sub> = 0 (entries 1, 2, and 5) or 4.0 (entries 3 and 4) mM, [SnCl<sub>4</sub>]<sub>0</sub> = 0 (entries 1, 2, and 5) or 20 (entries 3 and 4) mM, [1,4-DO] = 1.0 (entries 1 and 2), 0 (entries 3 and 4), or 0.47 (entry 5) M, [EA] = 0 (entries 1, 2, and 5) or 20 (entries 3 and 4) mM, in toluene (entries 1, 2, and 5) or toluene/dichloromethane (9/1 v/v; entries 3 and 4) at -78 °C.

<sup>b</sup> Determined by <sup>1</sup>H NMR analysis of quenched reaction mixtures. <sup>c</sup> Determined by GPC (polystyrene standards). <sup>d</sup> Estimated by <sup>1</sup>H NMR analysis of the obtained products. <sup>e</sup> Estimated by the <sup>1</sup>H NMR spectrum of the obtained product. However, the MWD curve of the acid methanolysis product indicated that CEVE homopolymers were predominantly produced (Figure 1A). <sup>f</sup> Not determined due to negligible crossover reactions.

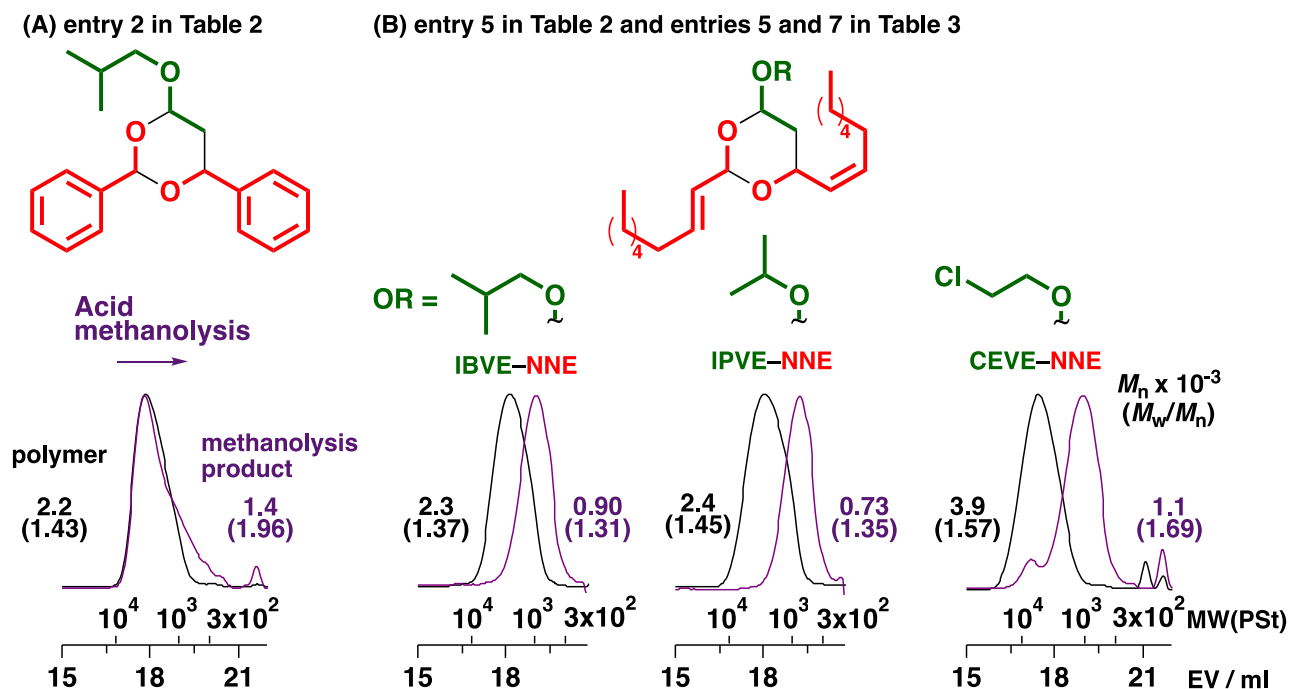


**Figure 1.** MWD curves of the polymers obtained by the cationic copolymerization of CEVE and various cyclic trimers (black line; after purification by preparative GPC; entries 2 and 5 in Table 2 and entries 5 and 7 in Table 3), and their acid methanolysis products (purple line).

Unlike BzA-containing cyclic trimers, NNE-containing cyclic trimers were highly effective for copolymerization with CEVE (Scheme 3B and entry 5 in Table 2). The concurrent cationic vinyl-addition and ring-opening copolymerization processes of CEVE and the cyclic trimer, which consisted of IBVE and NNE, were conducted under conditions similar to those used for the cationic copolymerizations of CEVE and the IBVE-BzA cyclic trimer, yielding a polymer of  $M_n = 2.5 \times 10^3$  (entry 5 in Table 2). The introduction of the cyclic trimer derived from crossover reactions was confirmed by  $^1\text{H}$  NMR analysis of the obtained polymer (Figure 2). The olefin structures derived from NNE were assigned to the peaks at 5.0–5.8 ppm (peaks 15 and 16). The peaks at 4.2–5.0 ppm (peaks 6, 9, 21, and 23) were attributed to the acetal structures generated by the crossover reaction from CEVE to the cyclic trimer. From the integral ratios of the olefin moiety and CEVE homosequences (peaks 2, 3, and 4), the average numbers of CEVE and the cyclic trimer units per block were estimated to be 6.1 and 1.0, respectively, indicating that the cyclic trimer consisting of IBVE and NNE underwent frequent crossover reactions with CEVE, differing from the IBVE-BzA cyclic trimer. The absence of cyclic trimer homopropagation was assumed from the result that the homopolymerization of the cyclic trimer did not proceed under the same conditions as those for copolymerization. In addition, the MWD curve obviously shifted to the lower-MW region after acid methanolysis (Figure 1B, left), indicating that acid-labile acetal moieties were incorporated into all the polymer chains by successful copolymerization. The  $M_n$  value of the acid methanolysis product was consistent with the average numbers of CEVE and cyclic trimer units per block, as shown above.



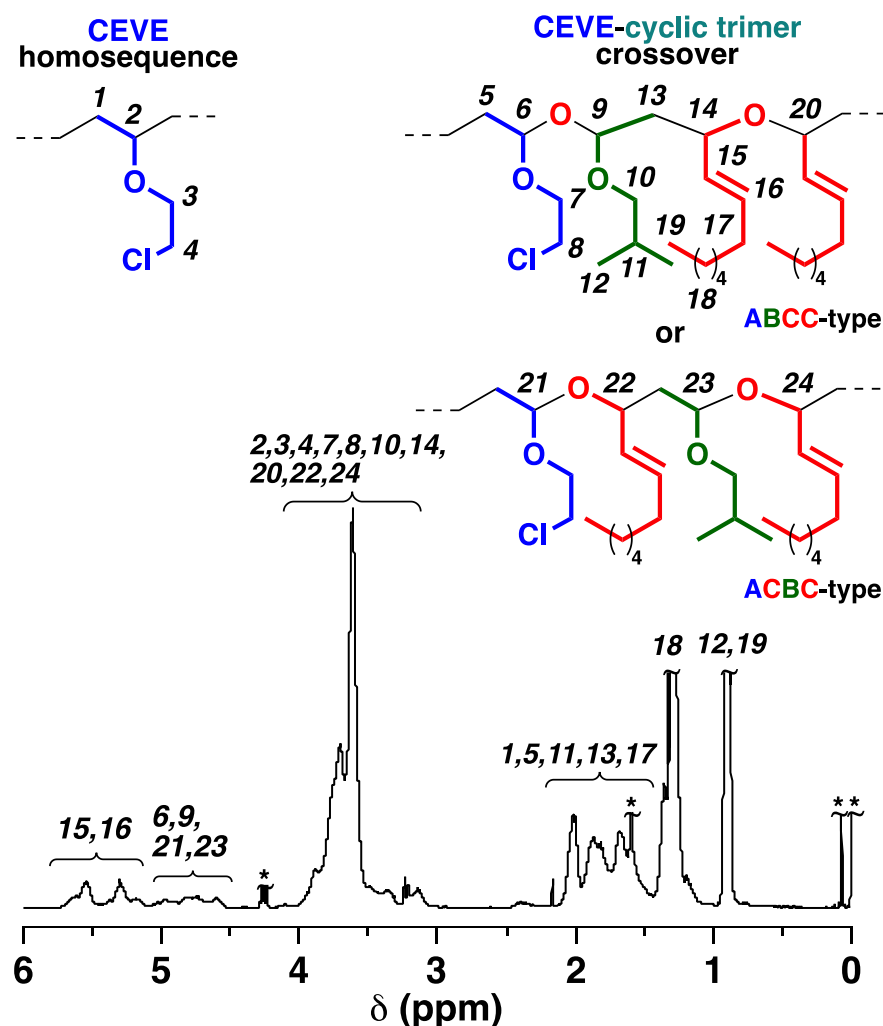


**Figure 2.**  $^1\text{H}$  NMR spectrum of the polymer obtained by the copolymerization of CEVE and the cyclic trimer consisting of IBVE and NNE [entry 5 in Table 2; after purification by preparative GPC; in  $\text{CDCl}_3$  at 30  $^\circ\text{C}$ ; \* water, grease, TMS, or others; the structures derived from crossover reactions were determined by  $^1\text{H}$  NMR and ESI-MS spectra of the methanolysis product of the alternating-like polymer of CEVE and the IBVE–NNE cyclic trimer (vide infra)].

Cationic copolymerizations of CEVE and cyclic trimers of VEs and NNE under various conditions

To achieve ABCC-, ACCB-, or ACBC-type periodic sequences by alternating copolymerizations of CEVE and the cyclic trimer, appropriate reaction conditions were investigated; there was a particular focus on solvents, VE units incorporated into cyclic trimers, and monomer concentrations. Initially, the cationic copolymerizations of CEVE and the IBVE–NNE cyclic trimer were conducted in a mixture of toluene/*n*-hexane (6/4 v/v; entry 1 in Table 3; Figure 3). The  $^1\text{H}$  NMR spectrum of the obtained polymer indicated that the average numbers of CEVE and cyclic trimer units per block were estimated to be 4.0 and 1.0; these results suggested that the crossover reactions occurred more frequently in the mixed solvent than in toluene alone (entry 5 in Table 2). The kinds of VEs incorporated into cyclic trimers affected copolymerization behaviors. The frequencies of crossover reactions increased when the cyclic trimer consisting of NNE and IPVE, a more reactive VE than IBVE, was used (entry 5 in Table 3). A polymer with shorter CEVE blocks (CEVE/cyclic trimer = 4.4/1.0; entry 5 in Table 3) than the IBVE–NNE counterpart (CEVE/cyclic trimer = 6.1/1.0; entry 5

in Table 2) was obtained. However, the use of the CEVE–NNE cyclic trimer resulted in copolymerization with less frequent crossover reactions (CEVE/cyclic trimer = 6.3/1.0; entry 7 in Table 3). These results indicated that the use of cyclic trimers containing more reactive VEs was suitable for crossover reactions with CEVE.

**Table 3.** Cationic copolymerization of CEVE and cyclic trimer consisting of VEs and NNE <sup>a</sup>

entry	CEVE (M)	cyclic trimer	(M)	additives	(mM)	toluene/ hexane (v/v)	time	conv. (%) <sup>b</sup>		$M_n \times 10^{-3} \text{ }^c$	$M_w/M_n \text{ }^c$	units per block <sup>d</sup>		ABCC/ ACBC ratio <sup>e</sup>
								CEVE	cyclic trimer			CEVE	cyclic trimer	
1	0.40	IBVE–NNE	0.40	1,4-DO	$2.0 \times 10^2$	6/4	144 h	92	27	3.7	1.51	4.0	1.0	–
2	0.20	IBVE–NNE	1.0	–	–	6/4	1 min	92	20	4.3	1.41	1.7	1.0	86/14
3	0.10	IBVE–NNE	1.0	–	–	6/4	10 min	>99	23	4.2	1.52	1.0 <sub>7</sub>	1.0	83/17
4	0.10	IBVE–NNE	1.0	EA	20	6/4	30 min	>99	23	3.0	1.50	1.0 <sub>3</sub>	1.0	74/26
5	0.40	IPVE–NNE	0.40	1,4-DO	$4.7 \times 10^2$	10/0	25 h	43	8	1.6	1.76	4.4	1.0	–
6	0.049	IPVE–NNE	0.50	–	–	6/4	5 min	61	7	2.0	1.61	1.0 <sub>4</sub>	1.0	40/60
7	0.41	CEVE–NNE	0.40	1,4-DO	$4.7 \times 10^2$	10/0	96 h	60	20	3.5	1.63	6.3	1.0	–

<sup>a</sup> [EtSO<sub>3</sub>H]<sub>0</sub> = 4.0 (entries 1–5 and 7) and 2.0 (entry 6) mM, [GaCl<sub>3</sub>]<sub>0</sub> = 10 mM, at –78 °C. <sup>b</sup> Determined by <sup>1</sup>H NMR analysis of quenched reaction mixtures. <sup>c</sup> Determined by GPC (polystyrene standards). <sup>d</sup> Estimated by <sup>1</sup>H NMR analysis of the obtained products after purification by preparative GPC. <sup>e</sup> Determined by <sup>1</sup>H NMR analysis of the acid methanolysis products.

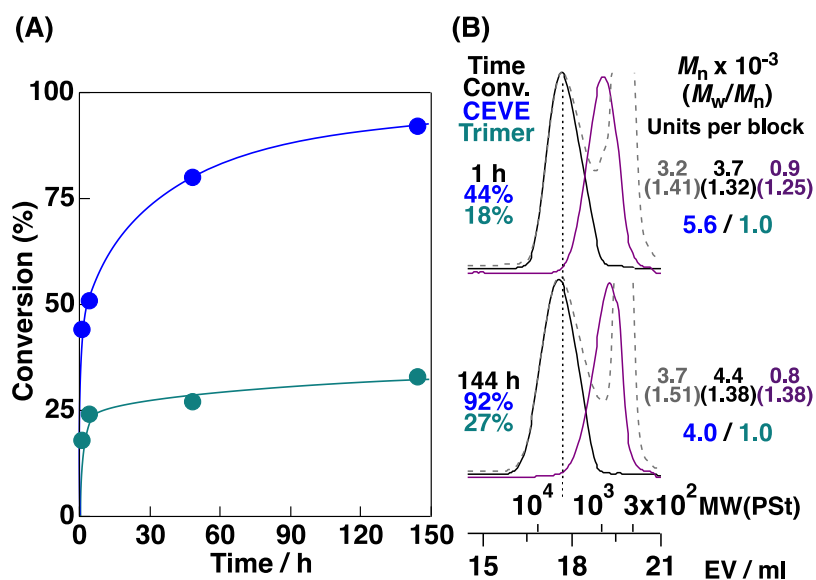


**Figure 3.** (A) Time-conversion curves of the cationic copolymerization of CEVE and the cyclic trimer consisting of IBVE and NNE and (B) MWD curves of the obtained polymers (dashed line), portions after purification by preparative GPC (solid line), and their acid methanolysis products (purple line) (entry 1 in Table 3).

For a cyclic trimer, the copolymerization at a higher initial concentration than that of a VE drastically promoted the crossover reactions. A polymer of  $M_n = 4.3 \times 10^3$  was obtained in the copolymerization at CEVE/IBVE–NNE cyclic trimer concentrations of 0.20 M/1.0 M (entry 2 in Table 3; black dashed line in Figure 4A). In the  $^1\text{H}$  NMR spectrum of the obtained polymer (Figure 5), the peak intensities of the structures derived from VE-to-cyclic trimer crossover reactions (peaks 2, 5, 17, and 19) were obviously larger than those obtained at equal concentrations of CEVE and the cyclic trimer (Figures 2 and 5). The integral ratio indicated that the average numbers of CEVE and cyclic trimer units per block were estimated to be 1.7 and 1.0, respectively. The acid methanolysis of this polymer produced a compound of  $M_n = 0.5 \times 10^3$  (the purple line in Figure 4A). The generation of the low-MW product after acid methanolysis indicated that acetal moieties were introduced into the main chain by frequent crossover reactions.

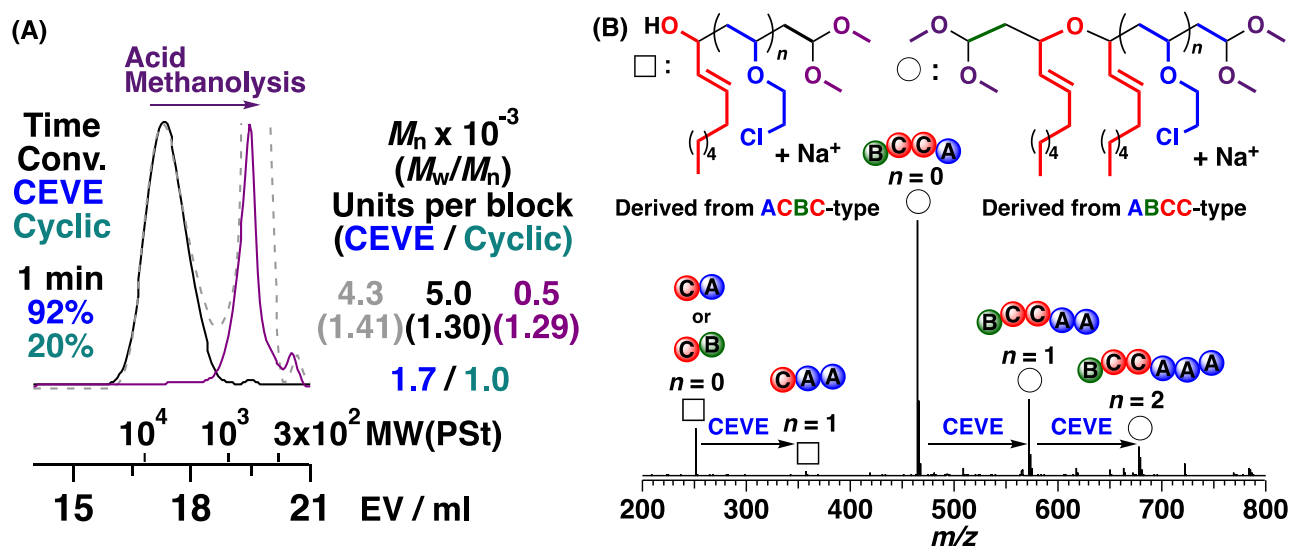


**Figure 4.** (A) MWD curves of the obtained polymer by the cationic copolymerization of CEVE and the cyclic trimer consisting of IBVE and NNE (dashed line), a portion after purification by preparative GPC (solid line), and its acid methanolysis product (purple line) and (B) the ESI-MS spectrum of the acid methanolysis product (entry 2 in Table 3).

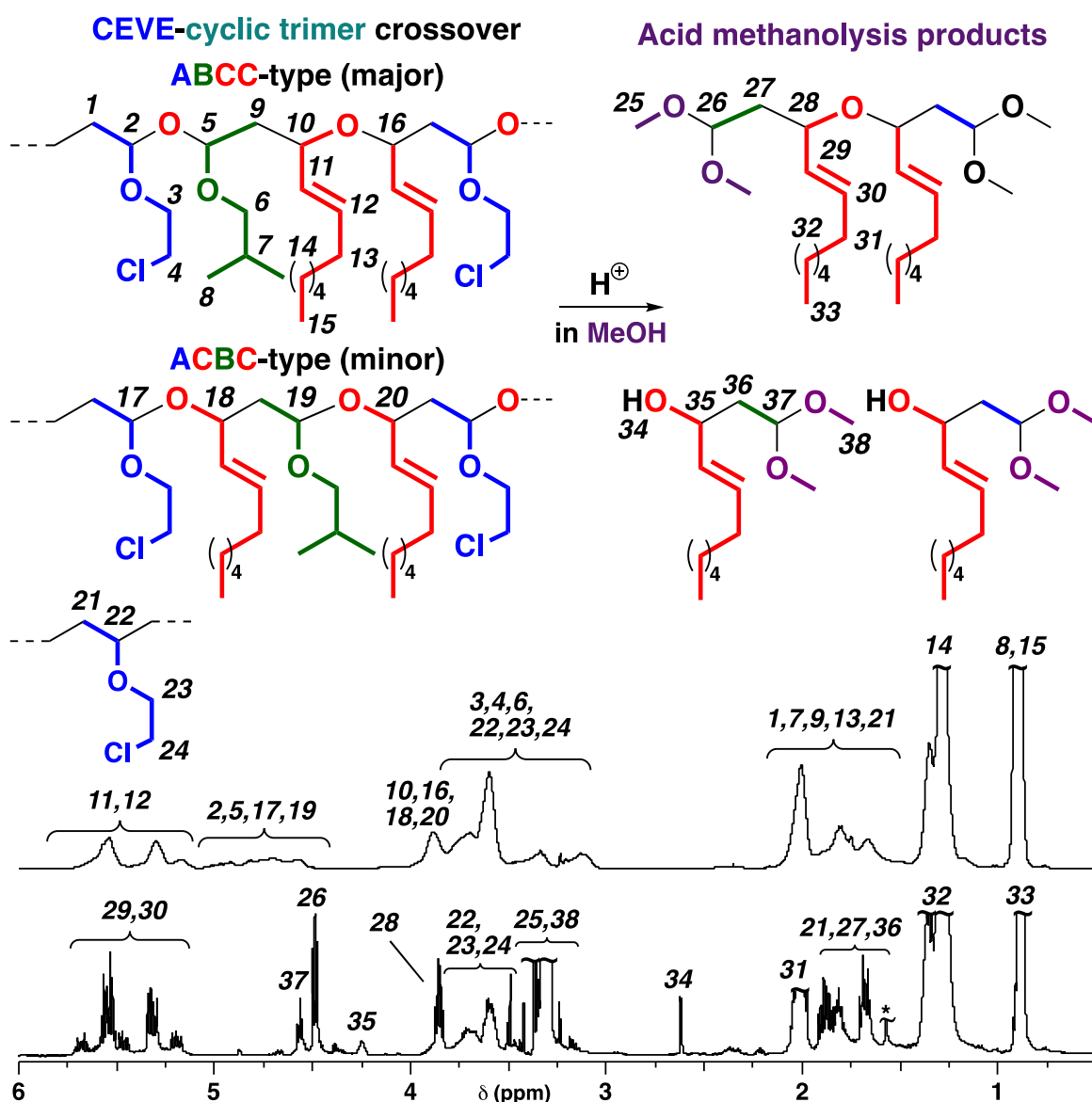
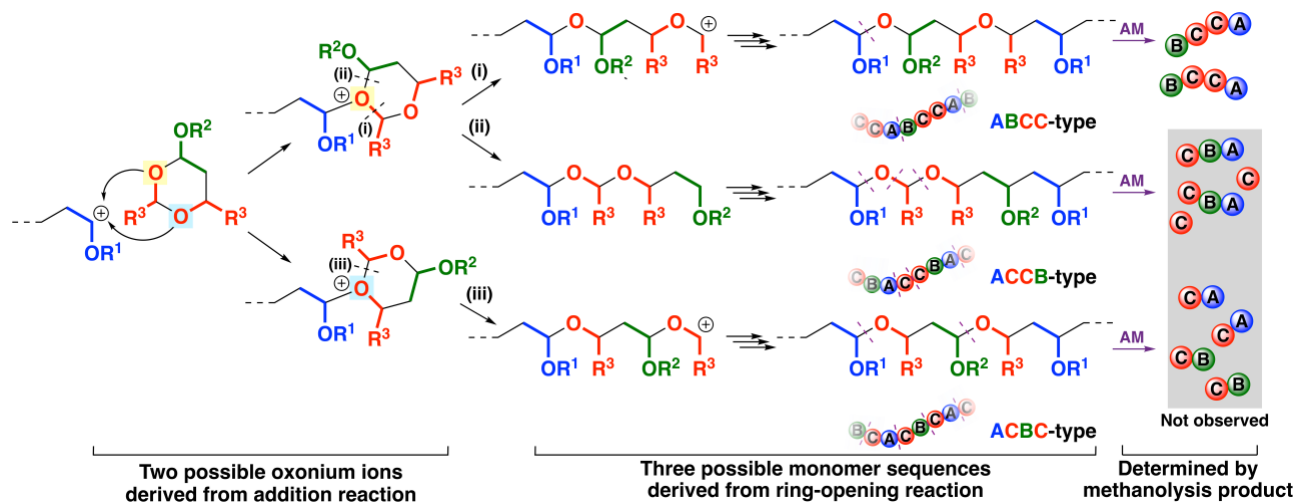


**Figure 5.** <sup>1</sup>H NMR spectra of the polymer obtained by the cationic copolymerization of CEVE and the cyclic trimer consisting of IBVE and NNE and its acid methanolysis product (entry 2 in Table 3; after purification by preparative GPC; in CDCl<sub>3</sub> at 30 °C; \* water; structures of ABCC- and ACBC-type sequences derived from alternating propagation reactions are shown. Non-periodic structures, such as AABCC- and AAABCC-type sequences, containing CEVE homosequences also exist (labels 21–24 are used for CEVE homosequences).

Structural analysis of the methanolysis product obtained above revealed the ring-opening mode of the cyclic trimer. The possible reaction mechanisms of the copolymerization are summarized in Scheme 4. Adding a cyclic acetal to the VE-derived carbocation formed an oxonium ion. Two possible oxonium ions were generated by the reaction of the oxygen atom at the 1-position or 3-position of the cyclic acetal. An oxonium ion was subsequently converted to a carbocation via a ring-opening reaction. The oxonium ion derived from the reaction of the oxygen atom at the 1-position had two acetal moieties; hence, two different carbocations were generated through paths (i) and (ii). The other possible oxonium ion afforded different carbocations through path (iii). Therefore, three different monomer sequences—ABCC-, ACCB-, and ACBC-type—were potentially generated through different addition and cleavage modes. Methanolysis products had

structures corresponding to the constitutional repeating units of the original polymers as a result of the cleavage of the acetal moieties; this phenomenon was very useful to reveal the ring-opening mode. Indeed, the ESI-MS analysis of the methanolysis product (Figure 4B) detected peaks assigned to the structures composed of four monomer units (CEVE/IBVE/NNE = 1/1/2; a circle symbol with  $n = 0$ ; two VE side chains were converted into methoxy moieties by transacetalization with methanol) or two monomer units (NNE/CEVE or IBVE = 1/1; a square symbol with  $n = 0$ ; a VE side chain was converted into a methoxy moiety). The other peaks (CEVE/IBVE/NNE = 2 or 3/1/2 (circle symbols with  $n = 1$  or 2) and NNE/CEVE = 1/2 (a square symbol with  $n = 1$ )) were derived from blocks with CEVE homosequences. The result suggested that the cyclic acetal underwent a ring-opening reaction by the modes shown by paths (i) and (iii) in Scheme 4. Possible products derived from the other mode (path (ii) in Scheme 4) were not observed in the ESI-MS analysis.

ABCC- and ACBC-type sequence generations were consistent with the  $^1\text{H}$  and  $^{13}\text{C}$  NMR spectra of the methanolysis product (Figure 5 lower and Figure S3). For example, peaks at 3.8 ppm (peak 28) and 4.5 ppm (peak 26) of the  $^1\text{H}$  NMR spectrum were assigned to the two allyl methine protons adjacent to the oxygen atom and the two acetal methine protons, respectively, of the methanolysis product from the ABCC-type monomer sequences. In addition, the hydroxy, hydroxy-adjacent methine, and acetal peaks assigned to the product from ACBC-type monomer sequences emerged at 2.6, 4.25, and 4.6 ppm (peaks 34, 35, and 37). These assignments were confirmed by analysis of the  $^1\text{H}$ - $^1\text{H}$  correlation spectroscopy (COSY) NMR spectrum (Figure S4). The ABCC-type/ACBC-type ratio was calculated to be 86/14 by the integral ratios of two allyl methine protons adjacent to the oxygen atom and hydroxy-adjacent methine proton of each methanolysis product (peaks 28 and 35).



**Scheme 4.** The reaction pathway of the generation of the different sequence-regulated polymers (AM: acid methanolysis).

Alternating-like cationic copolymerizations were found to proceed when the concentration of the cyclic trimer was set tenth that of CEVE due to the suppression of CEVE homopropagation (entries 3, 4, and 6 in Table 3). Moreover, the composition ratios of the ABCC-type to ACBC-type monomer sequences were tuned by the polymerization conditions. For example, the ACBC-type monomer sequences were preferentially generated with EA; hence the selectivity of generation of ABCC-type monomer sequences decreased (ABCC-type ratio = 74%; entry 4 in Table 3). An alternating polymer with comparable amounts of the ACBC- and

ABCC-type monomer sequences was obtained while copolymerizing CEVE and the IPVE–NNE cyclic trimer (entry 6 in Table 3). In addition, the alternating cationic copolymerization of CEVE and the IBVE–NNE cyclic trimer at  $-78\text{ }^{\circ}\text{C}$ , which was the most suitable polymerization temperature (Table S1), afforded a polymer with a relatively high ABCC-type ratio (ABCC-type ratio = 83%; entry 3 in Table 3;  $M_n = 4.2 \times 10^3$  (the black solid line in Figure 6A)), The average numbers of CEVE and the cyclic trimer units per block calculated by the  $^1\text{H}$  NMR spectrum of this polymer were 1.0<sub>5</sub> and 1.0, respectively, indicating the occurrence of alternating copolymerization. The unimodal MWD curve of the high-MW portion separated by preparative GPC shifted to the low-MW region after acid methanolysis (the purple line in Figure 6A). In the ESI–MS spectrum of the acid methanolysis product (Figure 6B), the major peak had an  $m/z$  value (465.3547) corresponding to the structure with four monomer units derived from the ABCC-type monomer sequences. Interestingly, the peaks derived from two or more CEVE units were extremely small; these results corroborated that ABCC-type periodic sequences were mainly generated.

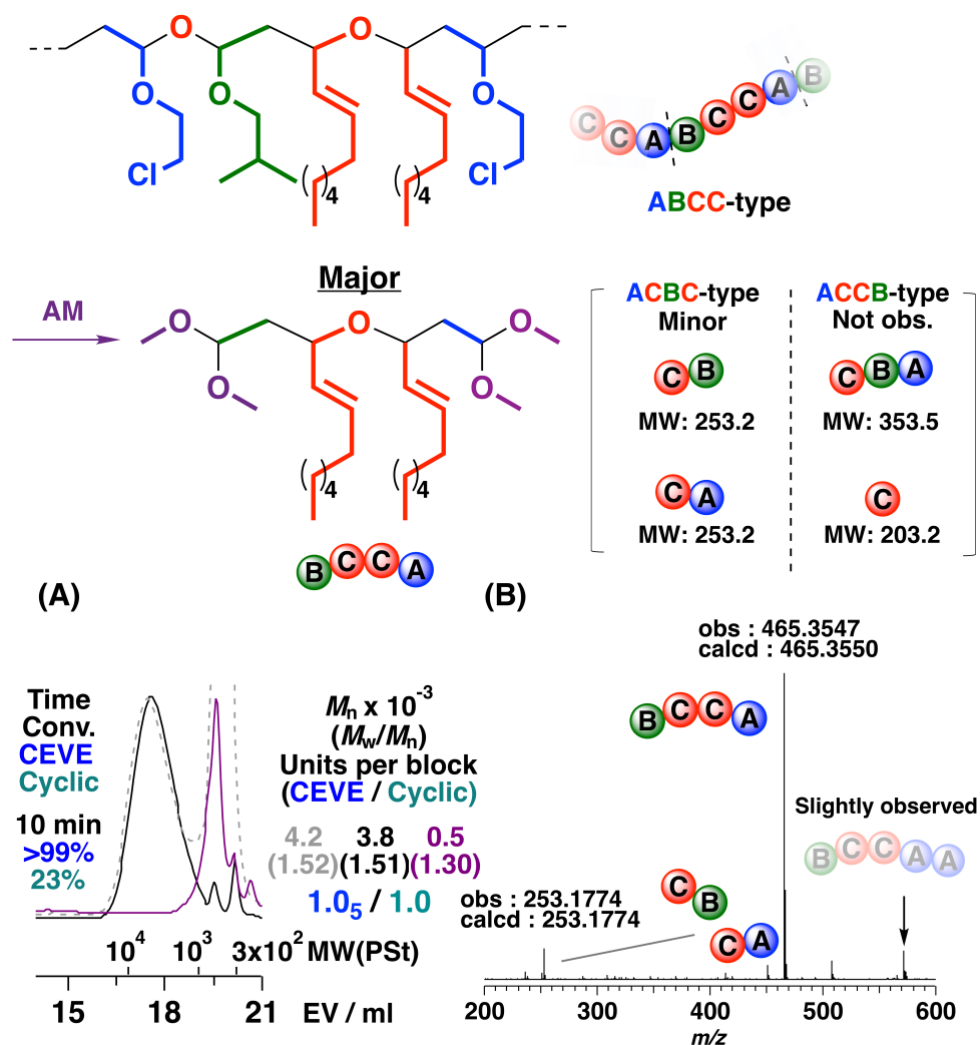


**Figure 6.** (A) MWD curves of the polymer obtained by the cationic copolymerization of CEVE and the cyclic trimer consisting of IBVE and NNE (dashed line), a portion after purification by preparative GPC (solid line), and its acid methanolysis product (purple line) and (B) the ESI-MS spectrum of the acid methanolysis product (entry 3 in Table 3).

## Conclusion

The alternating copolymerizations of CEVE and the NNE-containing cyclic trimer were demonstrated to proceed under optimized conditions. Among the three possible sequences—ABCC-, ACCB-, and ACBC-type—in the polymer chain, the ABCC- and ACBC-type sequences were selectively generated, which was revealed by the structural analysis of the acid methanolysis product of the obtained polymer. Moreover, the ABCC-type periodic sequences were preferentially generated during the copolymerizations of CEVE and a cyclic trimer consisting of IBVE and NNE without added bases (ABCC-type ratio = 83%).

## References

1. Nuyken, O.; Park, S. D. *Polymers* **2013**, *5*, 361–403.
2. Penczek, S.; Cypryk, M.; Duda, A.; Kubisa, P.; Stomkowski, S. *Prog. Polym. Sci.* **2007**, *32*, 247–282.
3. Xu, J.; Wang, X.; Liu, J.; Feng, X.; Gnanou, Y.; Hadjichristidis, N. *Prog. Polym. Sci.* **2022**, *125*, 101484.
4. Dechy-Cabaret, O.; Martin-Veca, B.; Bourissou, D. *Chem. Rev.* **2004**, *104*, 6147–6178.
5. Wu, J.; Yu, T.-L.; Chen, C.-T.; Liu, C.-C. *Coord. Chem. Rev.* **2006**, *250*, 602–626.
6. Marchildon, K. *Macromol. React. Eng.* **2011**, *5*, 22–54.
7. Rokicki, G.; Parzuchowski, P. G.; Mazurek, M. *Polym. Adv. Technol.* **2015**, *26*, 707–761.
8. Neffgen, S.; Keul, H.; Höcker, H. *Macromolecules* **1997**, *30*, 1289–1297.
9. Hill, J. W.; Carothers, W. H. *J. Am. Chem. Soc.* **1933**, *55*, 5031–5039.
10. Rokicki, G. *Prog. Polym. Sci.* **2000**, *25*, 259–342.
11. Tardy, A.; Nicolas, J.; Gigmas, D.; Lefay, C.; Guillaneuf, Y. *Chem. Rev.* **2017**, *117*, 1319–1406.
12. Jackson, A. W. *Polym. Chem.* **2020**, *11*, 3525–3545.
13. Pesenti, T.; Nicolas, J. *ACS Macro Lett.* **2020**, *9*, 1812–1835.
14. Pan, J.; Ai, X.; Ma, C.; Zhang, G. *Acc. Chem. Res.* **2022**, *55*, 1586–1598.
15. Endo, T.; Bailey, W. J. *Kobunshi* **1981**, *30*, 331–336.
16. Bailey, W. J.; Wu, S.-R.; Ni, Z. *Makromol. Chem.* **1982**, *183*, 1913–1920.
17. Ko, J. H.; Terashima, T.; Sawamoto, M.; Maynard, H. D. *Macromolecules* **2017**, *50*, 9222–9232.
18. Hill, M. R.; Kubo, T.; Goodrich, S. L.; Figg, C. A.; Sumerlin, B. S. *Macromolecules* **2018**, *51*, 5079–5084.
19. Tran, J.; Pasenti, T.; Cressonnier, J.; Lefay, C.; Gigmes, D.; Guillaneuf, Y.; Nicolas, J. *Biomacromolecules* **2019**, *20*, 305–317.
20. Yang, H.; Xu, J.; Pispas, S.; Zhang, G. *Macromolecules* **2012**, *45*, 3312–3317.
21. Kanazawa, A.; Kanaoka, S.; Aoshima, S. *Macromolecules* **2014**, *47*, 6635–6644.
22. Kanazawa, A.; Kanda, S.; Kanaoka, S.; Aoshima, S. *Macromolecules* **2014**, *47*, 8531–8540.
23. Kanazawa, A.; Aoshima, S. *Macromolecules* **2020**, *53*, 5255–5265.
24. Okada, M.; Yamashita, Y.; Ishii, Y. *Makromol. Chem.* **1966**, *94*, 181–193.
25. Okada, M.; Yamashita, Y. *Makromol. Chem.* **1969**, *126*, 266–275.
26. Shirouchi, T.; Kanazawa, A.; Kanaoka, S.; Aoshima, S. *Macromolecules* **2016**, *49*, 7184–7195.
27. Maruyama, K.; Kanazawa, A.; Aoshima, S. *Polym. Chem.* **2019**, *10*, 5304–5314.
28. Maruyama, K.; Kanazawa, A.; Aoshima, S. *Macromolecules* **2022**, *55*, 4034–4045.
29. Maruyama, K.; Kanazawa, A.; Aoshima, S. *Macromolecules* **2022**, *55*, 799–899.

30. Ishido, Y.; Aburaki, R.; Kanaoka, S.; Aoshima, S. *J. Polym. Sci., Part A: Polym. Chem.* **2010**, *48*, 1838–1843.
31. Ishido, Y.; Aburaki, R.; Kanaoka, S.; Aoshima, S. *Macromolecules* **2010**, *43*, 3141–3144.
32. Ishido, Y.; Kanazawa, A.; Kanaoka, S.; Aoshima, S. *Macromolecules* **2012**, *45*, 4060–4068.
33. Ishido, Y.; Kanazawa, A.; Kanaoka, S.; Aoshima, S. *J. Polym. Sci., Part A: Polym. Chem.* **2014**, *52*, 1334–1343.
34. Hurd, C. D. *J. Chem. Educ.* **1966**, *43*, 527–531.
35. Oon, S. M.; Kubler, D. G. *J. Org. Chem.* **1982**, *47*, 1166–1171.

### Supporting Information

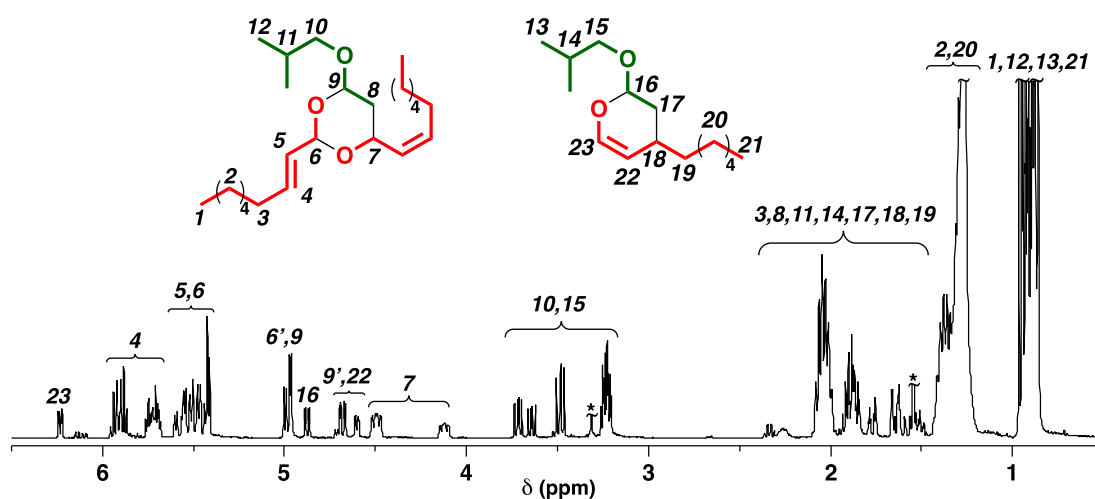


**Figure S1.**  $^1\text{H}$  NMR spectrum of the product obtained by the cyclotrimerization of IBVE and NNE (entry 2 in Table 1; in  $\text{CDCl}_3$  at 30  $^\circ\text{C}$ ; \* water or another).

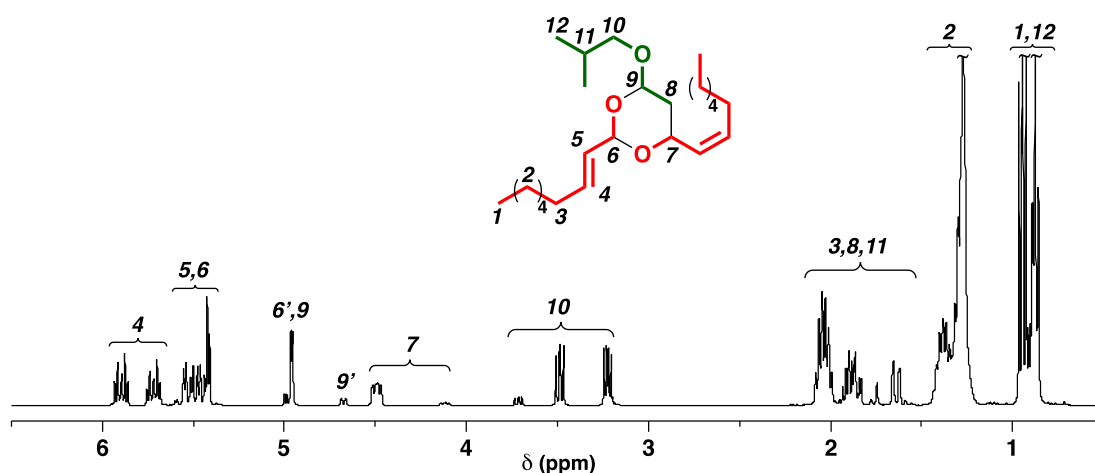


**Figure S2.**  $^1\text{H}$  NMR spectrum of the cyclic trimer consisting of IBVE and NNE after purification by column chromatography (in  $\text{CDCl}_3$  at 30  $^\circ\text{C}$ )



## DEPT 135

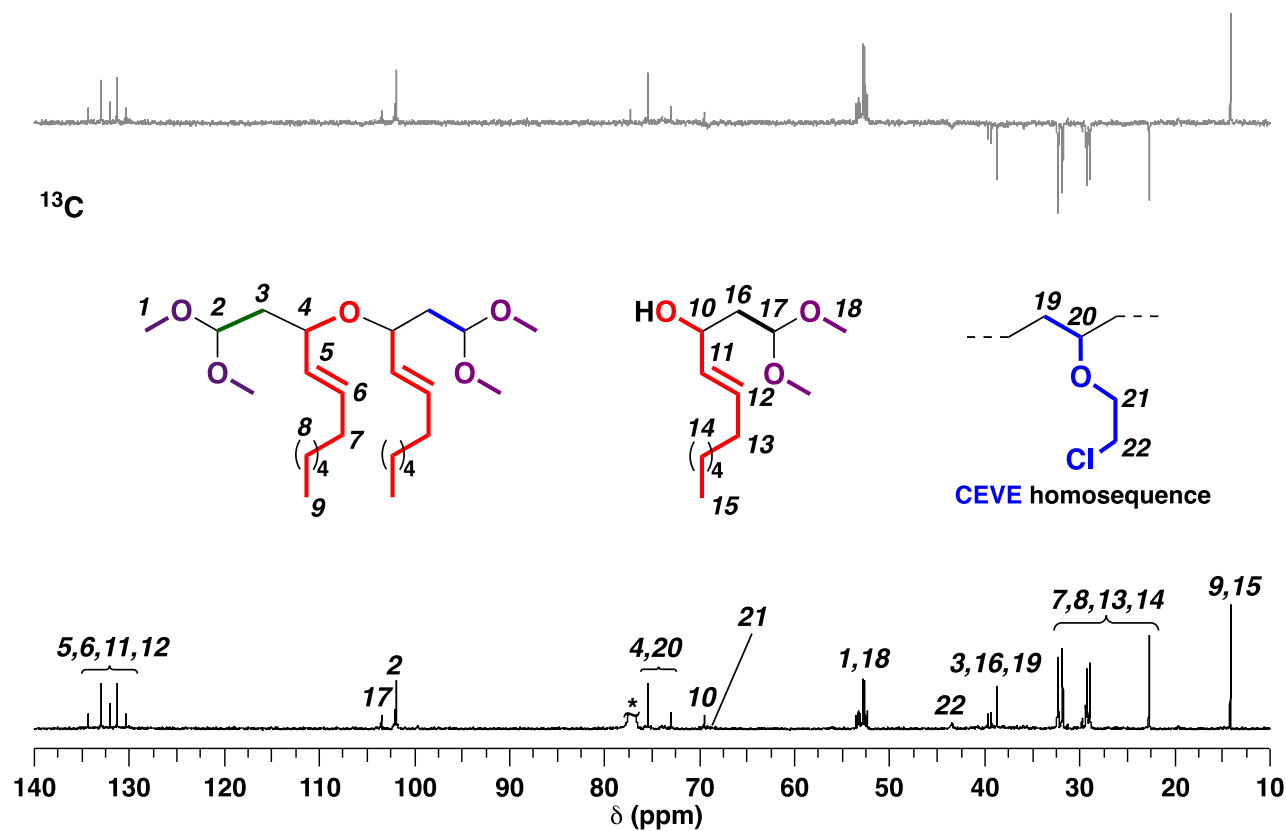


**Figure S3.**  $^{13}\text{C}$  and DEPT 135 NMR spectra of the acid methanolysis product of the polymer obtained by the copolymerization of CEVE and the cyclic trimer (IBVE–NNE) (entry 2 in Table 3; in  $\text{CDCl}_3$  at 30 °C; \*  $\text{CDCl}_3$ ).

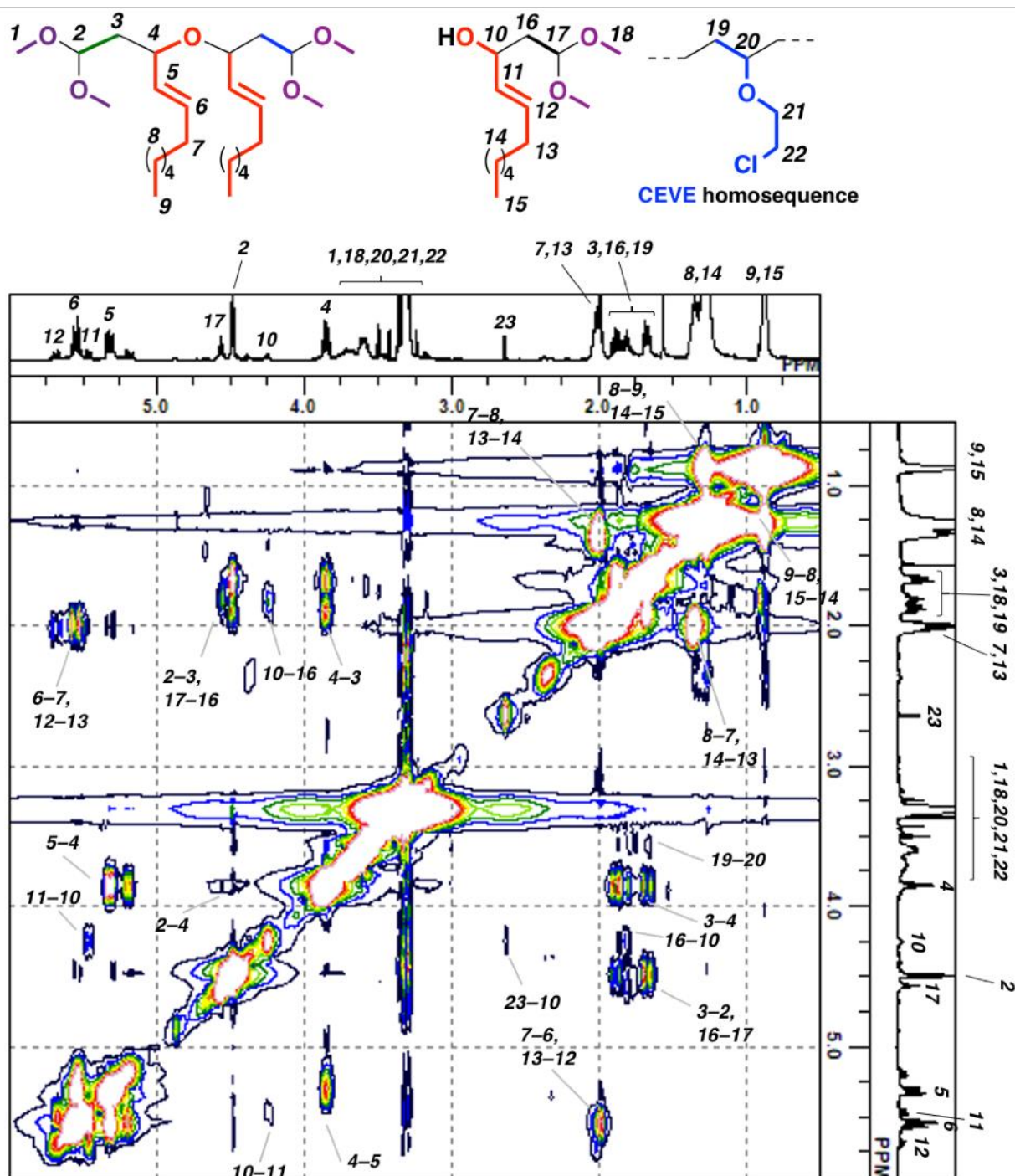


**Figure S4.**  $^1\text{H}$ - $^1\text{H}$  COSY spectrum of the acid methanolysis product of the obtained polymer by the copolymerization of CEVE and the cyclic trimer (IBVE-NNE) (entry 2 in Table 3; in  $\text{CDCl}_3$  at 30  $^\circ\text{C}$ ).

**Table S1.** Cationic copolymerization of CEVE and cyclic trimer consisting of IBVE and NNE <sup>a</sup>

entry	CEVE (M)	cyclic trimer	(M)	temp. (°C)	solvent (v/v) toluene/ hexane	time (min)	conv. (%) <sup>b</sup>		$M_n$ $\times 10^{-3}$ <sup>c</sup>	$M_w/M_n$ <sup>c</sup>	units per block <sup>d</sup>		ABCC/ ACBC ratio <sup>e</sup>
							CEVE	cyclic trimer			CEVE	cyclic trimer	
1	0.10	IBVE– NNE	1.0	–40	6/4	5	>99	19	1.3	1.41	1.0 <sub>0</sub>	1.0	67/33
2	0.10	IBVE– NNE	1.0	–60	6/4	5	>99	10	2.5	1.52	1.0 <sub>7</sub>	1.0	79/21
3	0.051	IBVE– NNE	0.51	–100	9/1	30	>99	15	3.6	1.68	1.0 <sub>0</sub>	1.0	67/33

<sup>a</sup> [EtSO<sub>3</sub>H]<sub>0</sub> = 4.0 (entries 1 and 2) or 2.0 (entry 3) mM, [GaCl<sub>3</sub>]<sub>0</sub> = 10 mM, at –78 °C. <sup>b</sup> Determined by <sup>1</sup>H NMR analysis of quenched reaction mixtures. <sup>c</sup> Determined by GPC (polystyrene standards). <sup>d</sup> Estimated by <sup>1</sup>H NMR analysis of the obtained products after purification by preparative GPC. <sup>e</sup> Determined by <sup>1</sup>H NMR analysis of the acid methanolysis products.

## Chapter 6

**Summary**

Introducing organic reactions into polymer chemistry potentially leads to novel polymerization systems. However, such polymerization systems are challenging to construct because of the requirement for the extremely high selectivity of organic reactions. The objective of this thesis was to develop strategies for the synthesis of polymers with specific structures and/or sequences in the main chain by selective organic reactions. The cyclotrimerization of one vinyl monomer and two aldehyde molecules, which had been reported as the side reaction in cationic alternating copolymerization of vinyl ethers (VEs) and conjugated aldehydes, was employed as the key reaction for both bond-forming reaction and sequence-programmed monomer synthesis.

Part I described the syntheses of copolymers containing specific structures in the main chain by polyaddition reactions based on the cyclotrimerization of vinyl monomers and dialdehydes. Poly(cyclic acetal)s and polymers with both cyclic acetal and ester structures in the main chain were synthesized via successive cyclotrimerization and tandem polymerization consisting of cyclotrimerization and the Tishchenko reaction, respectively.

In Chapter 2, model reactions using a series of Lewis acid catalysts and vinyl monomers were examined in the cyclotrimerization with benzaldehyde as a monofunctional conjugated aldehyde for the construction of appropriate reaction conditions. Based on these results of this model reactions, the polyaddition reactions of low reactive or nonhomopolymerizable vinyl monomers, such as 2-chloroethyl VE (CEVE), ethyl 2-methyl-1-propenyl ether, and 1,1-diphenylethylene (DPE), with dialdehydes were conducted to yield polymers with cyclic acetal structures in the main chain. The obtained polymers exhibited acid degradability due to the cyclic acetal structures in the main chain. In addition, the polymers obtained by the copolymerization of DPE and isophthalaldehyde or terephthalaldehyde had very high  $T_g$  due to the rigid structures.

Chapter 3 focused on the Tishchenko reaction, which is the reaction of two aldehydes into an ester, to establish a novel tandem polymerization system. First, model reactions of the tandem reaction consisting of cyclotrimerization and the Tishchenko reaction were conducted as in the case of Chapter 2. As a result of systematic investigation, the ratios and alkoxy ligand types of  $\text{EtAlCl}_2/\text{Al}(\text{OiPr})_3$  catalysts were found to be important for selective tandem reactions. Tandem polymerization consisting of cyclotrimerization and the Tishchenko reaction successfully proceeded under the optimized conditions, which resulted in acid- and alkali-degradable polymers with cyclic acetal and ester structures in the main chain. Furthermore, three-component tandem polymerization was demonstrated to proceed by adding diethyl fumarate as the third monomer that underwent transesterification reactions with Al-bonded alkoxy groups at polymer chain ends.

Part II dealt with the periodic polymer synthesis by sequential polymerization consisting of the sequence-programmed cyclic trimer formation and subsequent polymerization. ABAC- and ABCC-type

periodic sequences were attained by the successive cyclotrimerization and the cationic copolymerization, respectively, of the cyclic trimers and vinyl monomers.

In Chapter 4, ABAC-type periodic poly(cyclic acetal)s were synthesized via a combination of sequence-programmed cyclic trimer formation and the successive cyclotrimerization of the cyclic trimer with VEs. An ABA-type sequence-programmed cyclic trimer containing two unreacted aldehyde moieties was selectively generated in high yield using DPE (unit B) and dialdehyde (unit A) because the successive cyclotrimerization and other reactions were suppressed due to the steric hindrance of DPE. This cyclic trimer underwent the successive cyclotrimerization with other VEs (unit C). As a result, ABAC-type periodic poly(cyclic acetal)s with alternately arranged two phenyl rings and VE-derived side chains were obtained. ABAC-type periodic polymers underwent two-step degradation under acidic conditions. In the first step, the VE-derived cyclic acetal structures were selectively hydrolyzed. The remained cyclic trimer consisting of DPE and dialdehydes was further degraded for a prolonged reaction time. Furthermore, the obtained polymer exhibited good thermal properties, which were derived from the cyclic acetal structures and the two phenyl rings.

In Chapter 5, concurrent cationic vinyl-addition and ring-opening copolymerization of CEVE and BCC-type sequence-programmed cyclic trimers were examined. Alternating copolymers were obtained under the optimized conditions. Furthermore, the control of three different monomer sequences—ABCC-, ACCB-, and ACBC-type—due to three possible ring-opening modes was examined. Among the three types, the ABCC-type periodic sequence was preferentially generated in the copolymerization of CEVE and the cyclic trimer consisting of isobutyl VE and 2-nonenal (ABCC-type ratio = 83%), which was revealed by the structural analysis of the acid methanolysis product of the obtained polymer.

In conclusion, the author developed novel approaches for the synthesis of polymers with specific main chain structures and/or monomer sequences based on cyclotrimerization of one VE and two aldehyde molecules. The monomer sequences and functional group in the main chain were demonstrated to affect the degradation behavior and thermal properties. The results obtained in this thesis will contribute to the development of polyaddition reactions and periodic polymer synthesis based on highly selective organic reactions. The author believes that the research in this thesis will be a clue for precise control of primary structures of synthetic polymers by introducing novel organic reactions into polymer chemistry.

## List of publications

1. Tadashi Naito, Arihiro Kanazawa and Sadahito Aoshima  
“Polyaddition of vinyl ethers and phthalaldehydes via successive cyclotrimerization reactions: selective model reactions and synthesis of acid-degradable linear poly(cyclic acetal)s”  
*Polym. Chem.*, 2019, **10**, 1377–1385.  
(Corresponding to Chapter 2)
2. Tadashi Naito, Arihiro Kanazawa and Sadahito Aoshima  
“Tandem polymerization consisting of cyclotrimerization and the Tishchenko reaction: synthesis of acid- and alkali-degradable polymers with cyclic acetal and ester structures in the main chain”  
*Polym. Chem.*, 2022, **13**, 5757–5768.  
(Corresponding to Chapter 3)
3. Tadashi Naito, Arihiro Kanazawa and Sadahito Aoshima  
“Two-step degradable ABAC-type periodic poly(cyclic acetal)s synthesized by sequence-programmed monomer formation and subsequent polyaddition based on cyclotrimerization of one vinyl monomer and two aldehydes”  
*to be submitted.*  
(Corresponding to Chapter 4)